# Anatomical and physiological investigation of pathways mediating the effects of electrical stimulation of the external auricle of the ear on autonomic nervous system activity in rats

Mohd Kaisan Bin Mahadi

Submitted in accordance with the requirements for the degree of
Doctor of Philosophy

The University of Leeds
School of Biomedical Sciences

April, 2017

The candidate confirms that the work submitted is his/her own and that appropriate credit has been given where reference has been made to the work of others.

# Acknowledgements

# Abstract

The Auricular Branch of the Vagus Nerve (ABVN) is a sensory nerve that innervates select areas of the external auricular dermatome. Electrical stimulation of the auricular region innervated by the ABVN influences the autonomic nervous system, observed by changes in control of the heart in humans and animals. However, the pathways and mechanisms for these effects are unknown.

This thesis investigated in rats the pathways mediating the effects of electrical stimulation of the external auricle, comparing an ABVN innervated site of the external ear (the tragus) to an area not reported to receive ABVN innervation, the earlobe. Injection of the neuronal tracer cholera toxin B chain (CTB) into the right tragus (n=4) and right earlobe (n=4) revealed a large degree of similarity in sensory afferent termination sites. Afferent terminals were predominantly labelled ipsilateral to the injection site, with the densest labelling within laminae III-IV of the dorsal horn of the upper cervical spinal cord. In the medulla oblongata, CTB labelled afferents were observed in the paratrigeminal nucleus, cuneate nucleus, and to a minor extent in the nucleus tractus solitarius. Efforts were made to identify the targets of labelled afferents using immunofluorescence for choline acetyltransferase, calbindin, parvalbumin, glutamate decarboxylase 67 and neurokinin receptor 1 expressing cells, but inputs to each cell type were rare.

Physiological recordings of the responses to ear stimulation were made in an anaesthetic free Working Heart Brainstem Preparation (WHBP) of the rat. Autonomic profiles of WHBP rats were first examined. Recordings made from rats at night time, revealed more robust sympathetic activity in comparison to day time rats, thus subsequent experiments were conducted in rats at night time. Electrical stimulation (100 Hz, 2.5 mA) was delivered for 5 minutes into the auricular stimulation sites in the WHBP. Direct recording from the sympathetic chain revealed a central sympathoinhibition from both tragus and earlobe stimulation. Sectioning of upper cervical afferent nerve roots silenced the sympathoinhibitory effects of tragus stimulation.

Considering the predominance of afferent labelling in the cervical spinal cord dorsal horn and that cervical afferent nerve section reduced the sympathoinhibition evoked by tragus stimulation, this suggests that the autonomic effects of auricular stimulation are conveyed through somatosensory afferents rather than the ABVN.

# Table of Contents

# List of Tables

# List of Figures

# List of Abbreviations

| | |
|---|---|
| Abd | Abdominal |
| ABVN | Auricular Branch of the Vagus Nerve |
| AF | Atrial fibrillation |
| ANS | Autonomic nervous system |
| AP | Area postrema |
| ATN | Auriculotemporal nerve |
| Bmal | Brain and muscle ARNT like protein 1 – bmal |
| BP | Blood pressure |
| Calbindin | Calbindin-D28K |
| cAMP | Cyclic adenosine monophosphate |
| cf | Cuneate fasciculus |
| ChAT | Cholinergic Acetyl Transferase |
| Clock | Circadian locomotor output cycles kaput (clock) |
| CN | Cranial nerve |
| CNS | Central nervous system |
| CT | Cholera Toxin |
| CTB | Cholera Toxin B |
| Cu | Cuneate nucleus |
| CVLM | Caudal ventro lateral medulla |
| dmnX | Dorsal motor nucleus of the vagus nerve |
| DVN | Dorsal vagal nuclei |
| E | Expiratory |
| ECG | Electrocardiogram |
| EEG | Electroencephalographic |
| FDA | Federal drug administration |

| | |
|---|---|
| GAN | Great Auricular Nerve |
| GVA | General visceral afferent |
| GVE | General visceral efferent |
| HF | Heart failure |
| HR | Heart rate |
| HRP | Horseradish peroxidase |
| HRV | Heart rate variability |
| I | Inspiratory |
| IML | Intermediolateral nucleus |
| IML | Intermediolateral nucleus |
| IX | Glossopharyngeal nerve |
| LF | Low frequency |
| LLTS | Low level tragus stimulation |
| LVEF | Low ventricular ejection fraction |
| mSNA | Muscle sympathetic nerve activity |
| NA | Nucleus ambiguus |
| NEPS | Non-epileptic psychogenic seizures |
| NKR1 | Neurokinin-1 Receptor |
| NO | Nitric oxide |
| non-REM | Non- rapid eye movement |
| NTS | Nucleus tractus solitarius |
| NYHA | New York Heart Association |
| Pa5 | Paratrigeminal nucleus |
| Parv | Parvalbumin |
| PBS | Phosphate buffer saline |
| PHA-L | Phaseolus vulgaris-luecoagglutini |

| | |
|---|---|
| Ph-X | Pharyngeal branch of the vagus |
| PI | Post inspiratory |
| PND | Phrenic nerve discharge |
| PP | Perfusion pressure |
| PVN | Hypothalamic paraventricular nucleus |
| RLN | Recurrent laryngeal nerve |
| RSA | Respiratory sinus arrhythmia |
| RSG | Right stellate ganglion |
| RPM | Respiratory per minute |
| RVLM | Rostro ventro lateral medulla |
| SCN | Suprachiasmatic nucleus |
| SCS | Spinal cord stimulation |
| SLN | Superior laryngeal nerve |
| SND | Sympathetic nerve discharge |
| Sp5 | Spinal trigeminal tract |
| SPECT | Single photon emission computed tomography |
| SDSD | Successive differences R-R intervals |
| SVA | Special visceral afferent |
| SVE | Special visceral efferent |
| $T_E$ | Expiratory period |
| $T_I$ | Inspiratory period |
| $T_{TOT}$ | Total respiratory period |
| TWA | T wave alternans |
| VII | Facial nerve |
| VNS | Vagus nerve stimulation |
| WHBP | Working heart brainstem preparation |

# Chapter 1 General Introduction

## 1.1 Autonomic nervous system

Physiological homeostasis in the body is highly regulated by the central nervous system (CNS). The central command from the CNS reaches the tissues of effector organs through the peripheral nervous system (PNS). The afferent neurons in the PNS provides sensory input into the CNS, while output from the CNS into effector neurons is commonly referred as efferent. Modulation of the vital internal organs (e.g.: viscera and blood vessels) is conducted without the need of conscious inputs. As such, the autonomic (Greek *auto* = self, *nomos* = rule) nervous system (ANS) is appropriately named for its capability of coordinating physiological outputs to regulate internal visceral functions and homeostasis.

The ANS organization is divided into three different sub-divisions; the sympathetic, parasympathetic and enteric. The sympathetic and parasympathetic sub-divisions are complementary in nature where visceral organs receive dual input from sympathetic and parasympathetic nerve fibres (Sherwood, 2008). Under normal circumstances both nervous systems are partially active. The ongoing tonic sympathetic/parasympathetic activities will, however, be influenced from external stimuli (e.g. threats), causing activity of one division to dominate the other. The activation of sympathetic is commonly referred to as a "fight-or-flight" response while the parasympathetic activation often considered as "rest-and-digest" state. Hence, the shifting of autonomic predominance balances physiological demands of the body without the need of reaching consciousness. However, the dual reciprocal actions of the autonomic nervous system divisions are not applicable in some visceral organs. One of the examples would be blood vessels (except in parotid gland) which have sole innervation by the sympathetic nerve fibres. Vasoconstriction or vasodilation is achieved by regulating the firing rate of the sympathetic nerve fibres alone.

## 1.1.1 The sympathetic nervous system

Sympathetic nerve fibres have long been thought to originate from the thoracic and lumbar regions of the spinal cord to supply sympathetic transmission into various organs such as lungs, heart, blood vessels, eyes, sweat glands, kidneys and digestive tracts. However, recently sacral preganglionic neurons commonly considered as parasympathetic were reported to exhibit properties (anatomical, physiological, and pharmacological) more like sympathetic thoracolumbar than brainstem parasympathetic preganglionic neurons, suggesting that all spinal autonomic outflow is sympathetic (Espinosa-Medina *et al.*, 2016) **(Figure 1.1)**. At all levels, sympathetic preganglionic cell bodies form the intermediolateral column in the lateral horn of mammals. The preganglionic sympathetic fibres with myelinated axons leave the ventral nerve roots of the spinal segments through the white rami communicantes. The sympathetic preganglionic axons are commonly short and synapse with cell bodies of postganglionic neurons within the ganglia in the sympathetic trunk that lies on each sides of the spinal cord. Non-myelinated postganglionic sympathetic fibres exit the sympathetic trunk through the grey rami communicantes and travel to the effector organs. Some preganglionic fibres pass through the sympathetic chain without synapsing and later synapse with the postganglionic neurons in the collateral ganglia, about halfway between the designated organs and the CNS. Projections from the postganglionic neurons of the collateral ganglia are commonly to the pelvic visceral organs. A direct projection from the CNS to the adrenal gland has also been documented, where the cells are "modified" sympathetic ganglion neurons and have the ability to secrete epinephrine and norepinephrine upon activation (Sherwood, 2008).

The neurotransmitter released from the sympathetic preganglionic fibres is acetylcholine (Ach), hence all sympathetic pre-ganglionic fibres are cholinergic, acting on nicotinic receptors on the post-ganglionic neurons.

3

Postganglionic cells release norepinephrine and hence are called adrenergic fibres. Adrenergic receptors are heterogeneous ($\alpha_1$, $\alpha_2$, $\beta_1$, $\beta_2$) depending on anatomical location, showing different sensitivities to allow specific physiological responses during sympathetic activation. As such, the release of norepinephrine during the fight-or-flight condition binds to $\beta_1/\beta_2$-adrenoreceptors in the heart to induce myocardial contraction and increase in heart rate (McCorry, 2007) . The $\alpha_1$-adrenoreceptors are mainly involved in smooth muscle contraction which includes vasoconstriction of blood vessels during heightened sympathetic nerve activity. Conversely, the $\alpha_2$-adrenoreceptor activation causes negative feedback on the presynaptic norepinephrine release in the CNS. Unlike other postganglionic sympathetic neurons mentioned above, Ach is released from the postganglionic sympathetic fibres into sweat glands and binds onto muscarinic receptors. This promotes sweating, in anticipation of the heat production due to extreme physical exertions (Sherwood, 2008).
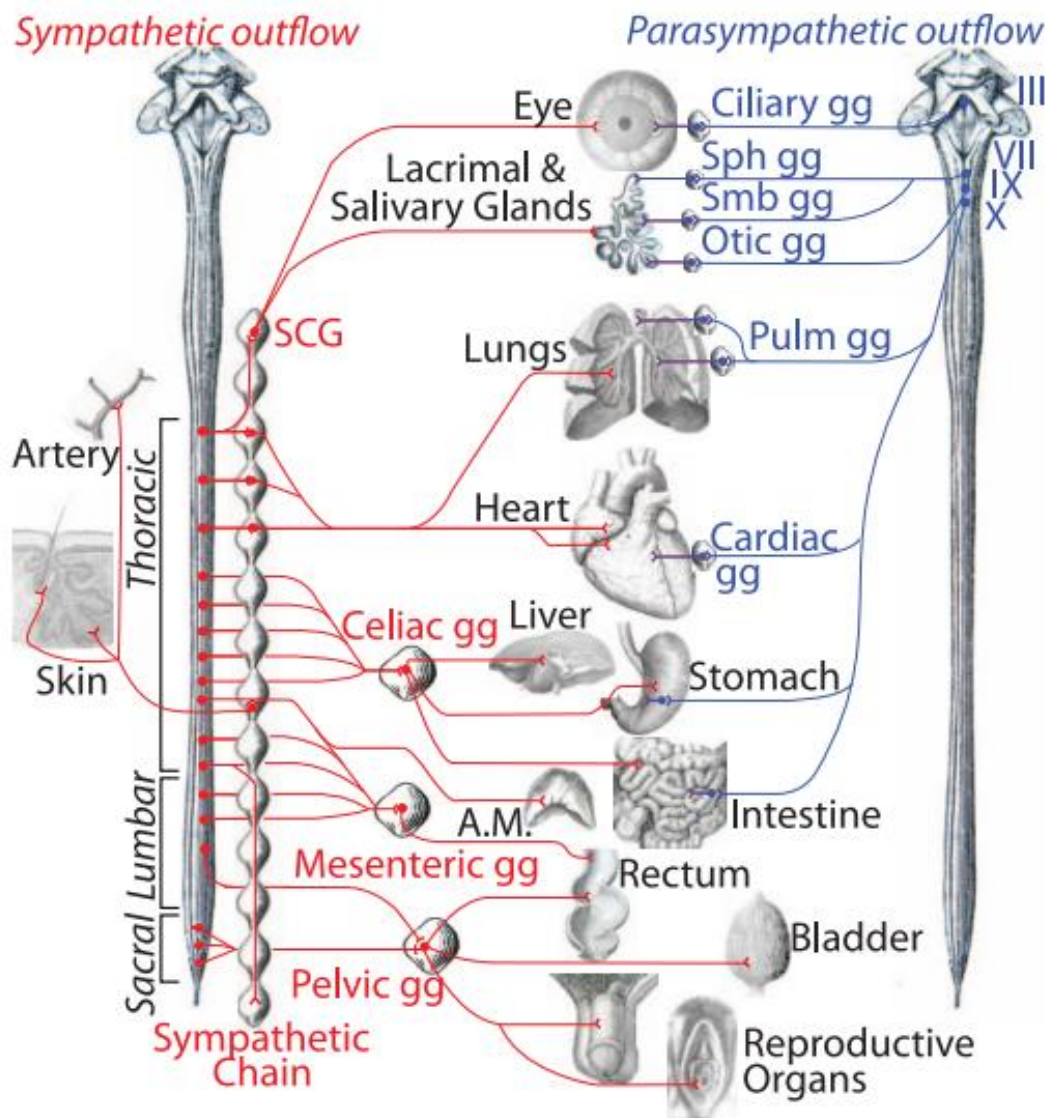
**Figure 1.1 Central efferent distribution from the autonomic nervous system**

The sympathetic efferent projection (red) originates from the intermediolateral cell column and targets various vital organs. The complementary actions from the parasympathetic nerve originates from the cranial structures (blue). Majority of the vital organs received dual innervations from the autonomic sub-division. III-oculomotor nerve, VII-facial nerve, IX-glossopharyngeal nerve, X-vagus nerve, A.M.-adrenal medulla, gg-ganglion, pulm-pulmonary, SCG-superior cervical ganglion, Sph-sphenopalatine, Smb-submandibular. Image source: Espinosa-Medina et al. (2016).

## 1.1.2 The parasympathetic nervous system

The efferent parasympathetic ANS has a cranial outflow. The cranial parasympathetic nerves arise from specific nuclei in the brainstem and synapse at one of the parasympathetic ganglia near to, or within, end organs. The cranial nerves (CN) that arise from parasympathetic nuclei in the brainstem include the CN III – oculomotor nerve, which innervates ciliary and pupillary constrictor smooth muscles, CN VII – facial nerve, innervating lacrimal, nasal, sublingual and mandibular gland, CN IX – glossopharyngeal nerve to the zygomatic and parotid glands. The CN X – vagus nerve which has extensive innervation in the body regarded as the main parasympathetic transmission medium into the cardiorespiratory system, which will be covered in more detail later in **Section 1.2**. Both the preganglionic and postganglionic fibres in parasympathetic pathways are cholinergic, acting on nicotinic and muscarinic receptors respectively. The activation of parasympathetic nervous system dominates during quiet, relaxed and non- threatening situations. This is normally referred as a "rest and digest" state where the body can be concerned with general housekeeping activities.

## 1.1.3 Reflex control of cardiovascular autonomic functions

The body's blood pressure (BP) fluctuates in everyday life, triggered by various factors such as exercise (Kelley & Kelley, 2000), drugs (Law *et al.*, 2009), postural changes (Borst *et al.*, 1984) and even time of day (Pickering *et al.*, 1982). The control of BP is through a negative feedback mechanism that influences the heart and blood vessels to adjust cardiac output and total peripheral resistance in order to keep BP with certain limits (Wehrwein & Joyner, 2013). This rapid autonomic response is known as the baroreceptor reflex. The baroreceptors lie strategically in the carotid sinus to provide critical information about arterial blood pressure in the vessels leading to the brain, and also the aortic arch to monitor the pressure in the major arterial trunk

before branching off to the rest of the body. The baroreceptors continuously fire action potentials to provide constant information of the ongoing pressure within the arteries. Accumulation of pressure within the blood vessels above the normal level stretches the mechanoreceptors, increasing action potential firing to propagate the signals to the autonomic integration circuits in the brainstem (Andresen & Kunze, 1994). The resulting efferent signals decrease heart rate, decrease stroke volume, cause arteriolar and venous vasodilation, causing a decrease in cardiac output and total peripheral resistance. Ultimately the rise in blood pressure will be restored back to normal. In contrast, the falls of BP below normal causes a decrease in the baro-mechanoreceptor signals into the brainstem, leading to an increase in heart rate and stroke volume coupled with vasoconstriction of the arteriolar and venous vasculature. As a result, both cardiac output and total peripheral resistance elevates blood pressure back to normal.

Another negative feedback mechanism that is important in maintaining the physiological homeostasis of the body is the chemoreflex. In this homeostatic control mechanism, the changes in $O_2$/$CO_2$ content in the body are initiated by sensors located either centrally and/or peripherally. The central chemoreceptors are groups of cells sensitive to the changes of pH that located on the ventrolateral medullary surface. These cells also referred to as the retrotrapezoid nucleus, sensitive to pH changes that originated from increased carbon dioxide (Guyenet & Bayliss, 2015). The peripheral chemoreceptors detect arterial $PO_2$ within carotid (Prabhakar & Semenza, 2015) and aortic (Brophy *et al.*, 1999; Piskuric & Nurse, 2013) bodies. Activation of both central and peripheral chemoreceptors causes elevation in respiration, where the excess $CO_2$ will be exhaled.

## 1.1.4 Fundamentals of central circuitry underlying cardio-autonomic reflexes

Cardiovascular afferent signals (e.g.: baro/chemoreceptors) are integrated in the CNS primarily in the nucleus tractus solitarius (NTS), an aggregate of neuronal cell bodies in the dorsomedial medulla oblongata. The neural pathways underlying the processing of such signals to alter efferent outputs have been determined to some extent (Guyenet, 2006; Wehrwein & Joyner, 2013). In brief, transganglionic neuronal tracing from aortic and carotid sinus nerves that carry signals from major baroreceptor sites has revealed major labelled afferent projections into the ipsilateral interstitial nucleus and dorsolateral aspect of the of the NTS (Ciriello *et al.*, 1981; Ciriello, 1983). Striking differences between projections of the baroreceptor and chemoreceptor fibres were demonstrated with the antidromic mapping technique (opposite axonal impulse) in anaesthetized cats (Donoghue *et al.*, 1984). Using this technique, barosensitive and chemosensitive neurons in the petrosal ganglia were identified during different physiological interventions (e.g.: baroreflex activation by controlled haemorrhage and re-infusion of blood; chemoreflex activation by changing the inspired $O_2/CO_2$ content). Whilst all baroreceptor afferents showed dense projections to the lateral aspects of the NTS, the afferents from chemoreceptors consistently projected to the medial regions of the NTS. Cardiovascular signals from the baroreceptors and chemoreceptors into the specified NTS regions are propagated through myelinated and non-myelinated axons (determined via differences in conduction velocity) (Donoghue *et al.*, 1984). Nevertheless, lesioning of the NTS in various animal models results in acute and extreme blood pressure and respiratory lability, indicating a major role of NTS in autonomic modulation of baro and chemo reflexes (Nathan & Reis, 1977; Laubie & Schmitt, 1979; Sato *et al.*, 1999).

Autonomic responses from peripheral chemoreceptor and baroreceptor activation are dependent on convergence of inputs from the NTS into sympathetic related circuitry in the ventrolateral medulla structure (Guyenet,

2006). Elevated blood pressure activates the baroreflex, the increase of firing in the NTS transmits glutamate modulated signals to the caudal ventrolateral medulla (CVLM). This was evident in anaesthetized rabbits, as bilateral glutamate injection into the CVLM inhibited the renal sympathetic discharge associated with decreases in arterial pressure (Masuda *et al.*, 1991). Acute stimulation of rabbit CVLM neurons silences presympathetic rostral ventrolateral medulla (RVLM) firing to reduce renal sympathetic tone and arterial pressure (Terui *et al.*, 1990). In contrast, inhibition of glutamatergic inputs into the CVLM of anaesthetized rats with kynurenic acid increases RVLM neuronal activity, heart rate and arterial pressure (Agarwal *et al.*, 1990). The CVLM contains GABAergic neurons which project to the pressor RVLM, resulting in suppression of sympathetic preganglionic neuron firing in the intermediolateral nucleus (IML). This results in reduction of the tonic activity of the sympathetic nerves (Guyenet, 2006).

It has been postulated that carotid chemoreceptor inputs in the NTS arborize in the RVLM. Single unit recording of anaesthetized rats revealed presence of chemosensitive neurons in the NTS that were tonically activated by peripheral chemoreceptor stimulation and did not fire in synchrony with the phrenic nerve discharge (Koshiya & Guyenet, 1996). Antidromic stimulation of the RVLM resulted in activation of a population of chemosensitive neurons in the NTS, suggesting neuronal connection between these two regions. Indeed, a mapping study in awake rabbits exposed to hypoxia for a period of 60 minutes, increased cFos expression (indirect measurement for neuronal activity) largely in the ventrolateral medulla as well as the NTS (Hirooka *et al.*, 1997). The chemoreflex activated neurons also showed immunoreactivity towards tyrosine hydroxylase, a neuronal marker of pre-sympathetic neurons. In addition,, electrophysiological recording in the rat brainstem spinal-cord preparation showed sympathetic preganglionic neurons received sympathoexcitatory drive from the RVLM (Deuchars *et al.*, 1995a). Taken together, activation of the carotid chemoreceptors during hypoxia results in increase of the central sympathetic outflow that is coupled with breathing rate.

The central circuitry of vagal activity is also coordinated in cardiovascular autonomic reflexes. Injection of retrograde tracer into the myocardium in the region of the sinoatrial node of rats labelled neurons predominantly in the ventral, external formation of the nucleus ambiguus (NA), the lateral dorsal vagal nucleus (DVN) and an area between the two that is known as the intermediate zone (Izzo *et al.*, 1993). These projections have been confirmed by the converse experiments of injection of anterograde neuronal tracer into the DVN (Cheng *et al.*, 1999) or NA (Cheng & Powley, 2000) with visualisation of fibres in the myocardium, sinoatrial and atrioventricular plexi. Investigation on firing pattern of these vagal preganglionic motoneurons activation in cats, revealed 2 distinct populations of motoneurons that are either cardioinhibitory or bronchoconstrictor (McAllen & Spyer, 1978). The cardioinhibitory motoneurons showed a parallel discharge with the cardiac rhythm and caused slowing of heart rate when activated. In contrast, the bronchoconstrictor motoneurons were spontaneously active and had an inspiratory-firing pattern. The bronchoconstrictor motoneurons discharges were independent of cardiac rhythm and did not inhibit the heartbeat (McAllen & Spyer, 1978).

The summary of cardio-autonomic reflexes neural pathway is shown in **Figure 1.2** below.
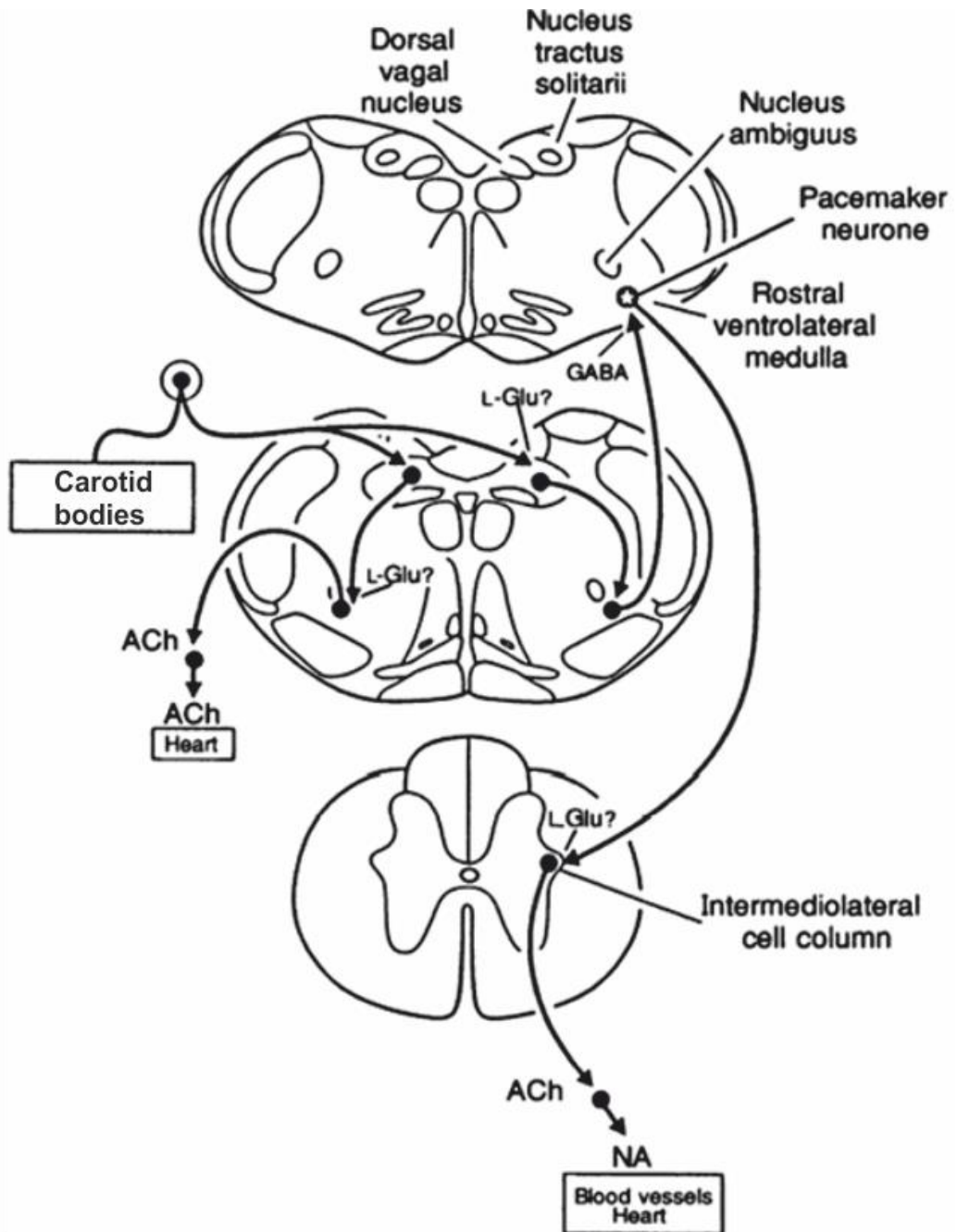
**Figure 1.2 The summary of cardiac autonomic regulation involved in baroreflex and potentially in chemoreflex**

Incoming baroreceptor and chemoreceptor afferents from carotid bodies terminate in the autonomic relay centre in the NTS. Autonomic signals from the NTS either projects to the cardiac vagal preganglionic neurons in the NA, or GABA-containing neurons in the CVLM. The latter further send inhibitory signals to the pacemaker neuron in the RVLM which may project directly to the sympathetic preganglionic neurons in the IML. NTS – nucleus tractus solitarius, NA – nucleus ambiguus, CVLM - caudal ventral lateral medulla, RVLM – rostro ventral lateral medulla, Image acquired from Spyer (1994).

11

## 1.2   The vagus nerve

*Vagus* in Latin can be translated to English as wandering; hence the vagus nerve is appropriately named due to its widespread projections throughout the body. The vagus nerve originates as the 10th cranial nerve, leaves the medulla as a series of rootlets in the groove between the olive and the inferior cerebellar peduncle, crosses through the posterior cranial fossa and exits the cranium through the jugular foramen **(Figure 1.3).** Upon its exit from the brain, the upper and lower vagal ganglionic swellings can be identified. The upper swelling is known as the superior/jugular ganglion, whereas the distal swelling is commonly identified as the inferior/nodose ganglion. The accessory nerve essentially join with the vagal ganglia and extend to most organs in the neck, thorax and abdomen**.** Later, the vagus nerve travels vertically in the neck within the carotid sheath between the internal carotid artery and the internal jugular vein. Histological silver staining of the vagus from adult cats revealed that it had a composition of 20% of myelinated efferent fibres (identified with osmic acid preparation) and 80% unmyelinated afferent fibres (the difference between the total and myelinated fibres) (Foley & DuBois, 1937). This suggests the vagus also has a major role in relaying sensory information from visceral organs to the CNS.

The vagal afferents can be classified into three different categories depending on their neuroanatomical functions; general visceral afferent (GVA), special visceral afferent (SVA) and the general somatic afferent (GSA). The GVA plays a vital role in conducting sensory impulses (e.g.: referred pain) from thoracic and internal organs such as the larynx, trachea, lungs, heart and gastrointestinal tract. This type of afferent also may carry baroreceptor and chemoreceptor information from the aortic arch into the autonomic relay centre in the brainstem (Berthoud & Neuhuber, 2000)**.** The SVA fibres have a specific function carrying taste information from taste buds on the epiglottis, larynx and pharynx. The cell bodies of visceral afferent fibres (GVA and SVA) reside within the nodose ganglion of the vagus nerve and are involved in the

modulation of respiration, cardiovascular system, swallowing and digestion (Ruffoli *et al.*, 2011)**.** The vagus nerve GSA relays sensory impulses from the lower pharynx, larynx, trachea, oesophagus, and posterior dura mater. The GSA also carries somatic sensory information of pain, touch and temperature rises from select regions of the surface of the body, including the external ear. Intriguingly, bringing sensation from the external ear results in various somatovisceral reflexes **(will be discussed further in Subsection 1.3.2)** highlighting the complexity of the vagus nerve neuroanatomy and prompting this present investigation.

Although a smaller proportion of the vagus, the functions of the vagal efferent component is as equally important as the afferent. The vagal efferent fibres leave the cranial structure and provide vagal input into effector organs in the form of General Visceral Efferent (GVE) or Special Visceral Efferent (SVE). The GVE has preganglionic parasympathetic fibres projecting into smooth muscle in the thoracic and abdominal cavities, cardiac muscle and glands . This type of efferent neuron mainly originates from the dorsal vagal nucleus (DVN), as well as the nucleus ambiguus (NA) (Izzo *et al.*, 1993). The SVE neurons also originates from the NA and supplies vagal innervation into the striated muscle of the palate, larynx, pharynx and also upper oesophagus (Bieger & Hopkins, 1987; Kitamura *et al.*, 1991).
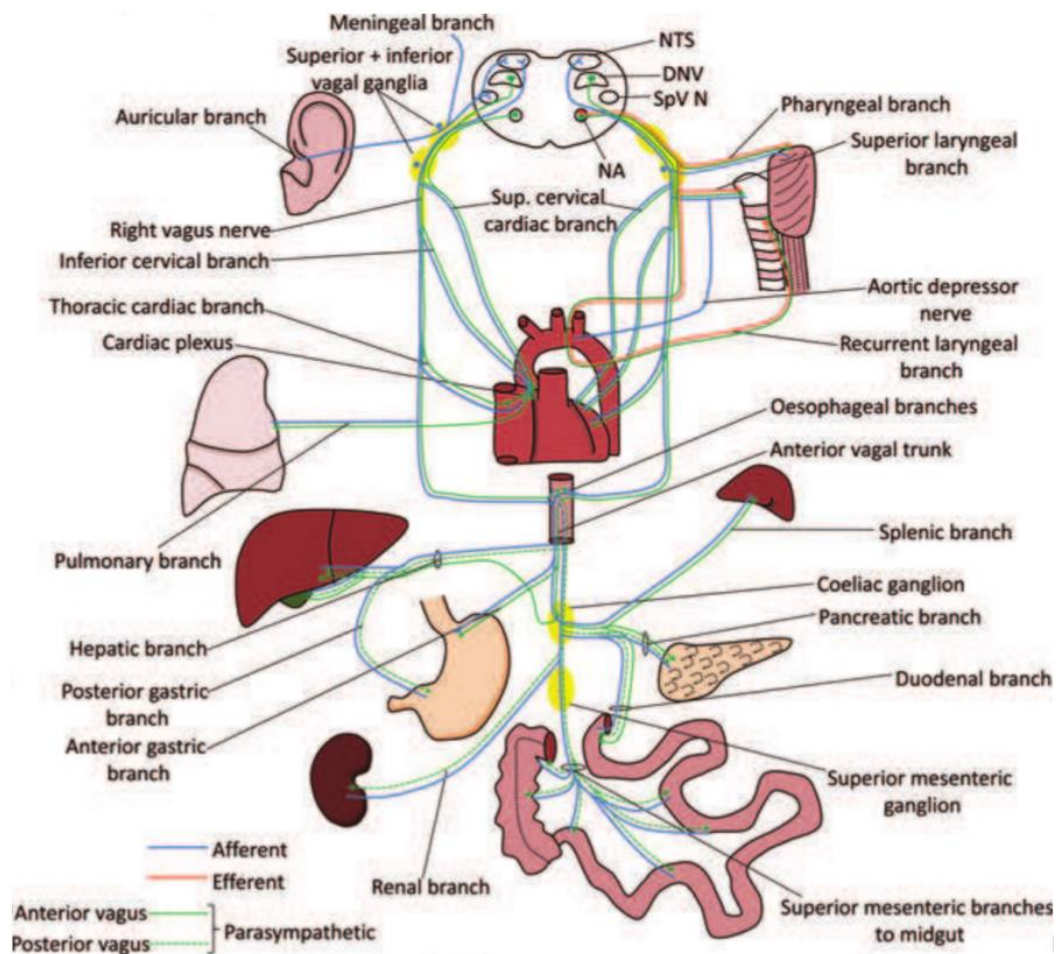
**Figure 1.3 Distribution of the vagus nerve into visceral organs**

The vagus nerve acts as a main parasympathetic innervation of the body with the preganglionic neurons located in the DVN and also the NA. The vagus leaves the brainstem at the 10th cranial nerve and supplies the efferent and afferent parasympathetic innervation of various organs throughout the body. A sensory branch arises from the superior ganglia to the external auricle, thus named the Auricular Branch of the Vagus Nerve (ABVN). The vagus nerve distributions are bilateral and have been omitted for clarity. NTS – nucleus tractus solitaries; DVN – dorsal vagal nucleus; SpVN – spinal trigeminal nucleus; NA – nucleus ambiguus. Image source: Clancy *et al.* (2013).

### 1.2.1 History of Vagal Nerve Stimulation

Vagus nerve stimulation (VNS) has become a target for therapy for many potential disorders, including epilepsy, heart failure, tinnitus (Clancy *et al.*, 2013). Of such disorders, VNS is most commonly applied as a treatment for epilepsy. Epilepsy is a common disorder that affects patients at all ages and ethnicity, with an estimated 50 million people in all nationalities (WHO, 2017). Epilepsy is a neurological disorder where large numbers of brain cells fire signals at the same time, leading to episodic seizures. This phenomenon can re-occur overtime without any known causes. In the early 1880s, the seizure attacks were believed to be a result from cerebral hyperaemia. Thus the medical strategies at that time involved carotid artery compression or ligation to reduce the recurrent seizures. A New York physician James Leonard Corning developed a two-pronged, fork like instrument to temporarily compress blood flow of the carotid artery, which successfully reduced the duration of the epilepsy events **(Figure 1.4).** Several years later, Corning combined the carotid artery compressor with a cervical vagal nerve stimulator to further decrease the cerebral blood flow. The underlying concept was that the vagal efferent stimulation would slow down heart rate and reduce cardiac output, so reducing the proposed hyperaemia causing epilepsy. Despite various claims on the success of reducing seizure events, vagus stimulation caused unintended side effects such as dizziness, bradycardia, general weakness and occasionally syncope. With a lack of clear theoretical frameworks and inadvertent complications, Corning's innovation was then left overlooked until a century later (Lanska, 2002).

The use of an implantable VNS device was approved by the USA Federal Drug Administration (FDA) as an adjunct treatment for epilepsy in 1997. In the UK, clinical guidelines the VNS in epilepsy is 'for use as an adjunctive therapy in reducing the frequency of seizures in adults (and children) who are refractory to antiepileptic medication but who are not suitable for respective surgery'. It is also specifically indicated that the VNS therapy is for patients in whom focal or generalised seizures predominate (NICE, 2004).

The programmable VNS pulse generator is implanted under a subcutaneous pocket in the chest just below the clavicle; the electrical stimuli propagate through a lead connected to the electrode. Unlike the traditional conceptual framework of VNS to reduce the global blood flow through vagal efferent fibres to the heart as proposed by Corning, the modern VNS device stimulates vagal afferent fibres to the brain while circumventing the vital vagal-cardiac alterations.
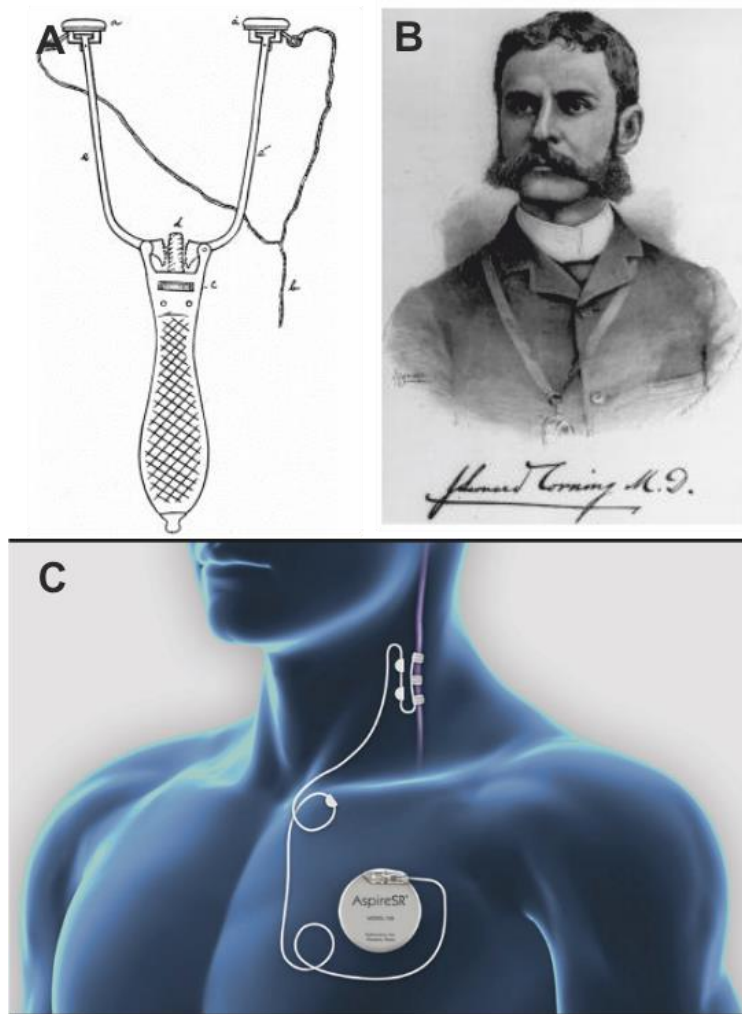
**Figure 1.4 Vagus nerve stimulating (VNS) devices**

A) The initial vagus nerve 'electrocompressor' device was developed by (B) J.L. Corning (image courtesy of the National Library of Medicine) combining the simultaneous bilateral compression of the carotid arteries and transcutaneous cervical vagus nerve stimulation. Corning's 'electrocompressor' components device comprises of insulated sponge electrodes (a and a'), connecting wire (b), adjusting wheel (c) of a simple screw (d) for flexible armatures width (e). C) A modern VNS stimulator is implanted under the skin on the chest with a lead wire connects to the left cervical vagus nerve. Source of image: A) Corning (1884) C) www.epilepsysociety.uk.

The heterogeneity of vagal afferent activation thresholds determines the specificity of VNS activation. Vagal afferents contain three different fibres, myelinated A and B and also unmyelinated C. These 3 fibres can easily be identified in mammals (cats and dogs) since the A fibres are the biggest (5 – 20 μm diameter), followed by B fibres (<5 μm diameter). The smallest and unmyelinated are regarded as C fibres (Blair & Erlanger, 1933). In cats, comparing these elements using light and electron microscopy revealed more non-myelinated than myelinated nerves, with the ratio of myelinated to non-myelinated total averaging approximately 1:4 (Mei *et al.*, 1980). Each fibre type also possesses a different activation threshold, inversely proportional to the square of fibre diameter. As such, the A fibres have the lowest threshold activation activated at 0.02 – 0.2 mA, the B fibres at 0.4 – 0.6 mA, and C fibres with the highest activation threshold at more than 2 mA (Blair & Erlanger, 1933). Selective activation of vagal C fibres (from maximal stimulation) at 4 Hz, 0.2 – 0.5 mA/mm$^2$ reduces incidence of seizures that were induced by chemical or electrical stimuli in rats, suggesting the antiepileptic potency is mainly due to stimulation of vagal C fibres (Woodbury & Woodbury, 1990). Woodbury's finding was rebutted in later years as following selective destruction of vagal C fibres with systemic capsaicin injection, electrical stimulation of the vagus still suppressed induced seizures in rats (Krahl *et al.*, 2001). Furthermore, clinical evidence showed the stimulation parameter of VNS is clinically effective below the specific C-fibre threshold (DeGiorgio *et al.*, 2000; Koo *et al.*, 2001). Also, continuous stimulation of the peroneal/sciatic nerve of cats at high parameters (>50 Hz, 2.5 mA) resulted in irreversible axonal injury (Agnew & McCreery, 1990). On these bases, the stimulation parameters for clinical use of VNS approved by the FDA are below activation threshold for vagal C fibres ranging between 20 and 30 Hz (DeGiorgio *et al.*, 2000).

Despite success of the VNS as a refractory seizures therapy, the underlying mechanism of the VNS antiepileptic effect is still not fully understood. Since the NTS is the major CNS region receiving vagal afferent signals, it has been suggested to play a major role in altering the uncontrolled cortical excitability

seen in epileptic seizures (Krahl & Clark, 2012). Indeed, the activated myelinated vagal afferent fibres primarily originated from neurons in the nodose ganglion and send projections into the nucleus of the solitary tract (Kalia & Sullivan, 1982; Nomura & Mizuno, 1984). Changing the synaptic transmission profile of the NTS proved to be beneficial in regulating induced seizures in rats since seizure responses were attenuated with muscimol (GABAergic agonist injection) or kynurenate (glutamate receptor antagonist) injections into the medial caudal subnuclei of the NTS, but not adjacent sub-nuclei. (Walker *et al.*, 1999). This suggests, contrary to the obvious explanation, that VNS could work via inhibition of the NTS output - such inhibition has been suggested to be the outcome of high frequency VNS (Walker *et al.*, 1999).

The effects of long-term VNS treatment on GABA receptor density was then studied using single photon emission computed tomography (SPECT) to identify binding of the iodinated benzodiazepine receptor inverse agonist iomazenil to GABA receptors in patients with drug resistant partial epilepsy. It was found after 1 year of VNS treatment that GABA receptor binding was increased in cortical regions where the GABA cortical inhibition was absent in the control group (Marrosu *et al.*, 2003). As a relay centre, activation of the NTS from VNS therapy may send signals to the hypothalamus, the amygdala nucleus, the dorsal raphe, the NA, the parabrachial nucleus, the thalamus which further projects to the insular cortex (Rutecki, 1990). The wide neuronal projection from the NTS may provide an antiepileptic platform through induction of cortical changes as seen in the electroencephalographic (EEG) activity and sleep states. Normal EEG recording is indicated by a clear visible alpha (7.5-13 Hz) and beta rhythm (>14 Hz), while abrupt increase in various band peak observed in the epileptic EEG periodogram (Dash, 2014). In an effort to understand the influence of NTS activation from the VNS, direct electrical stimuli applied to the NTS produced a long lasting increase in theta and beta bands (12 hours) of the EEG in unrestricted cats. This EEG band synchronization was coupled to increases in the total time of wakefulness (up to 6 hours) and also rapid eye movement (REM) sleep (Martínez-Vargas *et*

*al.*, 2016). However, the synchronization or desynchronization of the EEG activity may be dependent on the stimulus parameters applied. Low frequency electrical stimulation (1-16Hz) in the NTS produced EEG synchronization in cats, while these effects were reversed with higher stimulation frequency (>30Hz) (Rutecki, 1990).

Autonomic dysregulation has been linked with epilepsy during ictal and interictal periods. Ictal refers to a physiological condition during seizure, while interictal is a state between the seizure attacks. In most epilepsy cases, the seizure attack coincides with an increase in heart rate >120 bpm, with the frequency potentially reaching 201 bpm (Leutmezer *et al.*, 2003). Tachycardia events precede the onset of EEG abnormality in epilepsy by several seconds, highlighting manifestation of the ANS sympathoexcitation rather than secondary effects of motor control dysregulation (Baumgartner *et al.*, 2001; Leutmezer *et al.*, 2003). Examining the sympathetic responses in epileptic patients with isometric hand grip test and vagal tone with Valsalva manoeuvre revealed a diminished cardiovascular responses (HR and BP responses) , reflecting a blunted ANS associated with epilepsy during the interictal period (Isojärvi *et al.*, 1998). Similar interictal autonomic evaluation in groups of subjects with different types of epilepsy (partial vs general) indicated a prominent sympathetic dysfunction in partial epilepsy while parasympathetic dysfunction is recorded in patients with the general epilepsy (Berilgen *et al.*, 2004). The seizure attack that was not accompanied by abnormal electrical activity in the brain is known as non-epileptic psychogenic seizures (NEPS). Unlike epilepsy, ANS evaluation during interictal and postictal in NEPS displayed normal ANS functions highlighting the ANS disability was associated with epilepsy central pathogenesis not seizure (Müngen *et al.*, 2010).

While the link between ANS dysfunction and epilepsy is beginning to be appreciated, the effect of VNS on autonomic function in epilepsy still remains controversial. A periodic beat to beat variation in the amplitude of the ST segments in an electrocardiogram (ECG) is known as a T wave alternans (TWA), provides a non-invasive predicting marker for cardiac arrest. Six

months of VNS therapy in the drug-resistant focal epilepsy had significantly reduced the number of TWA, where the reduction was correlated with the VNS intensity. Also, the HRV analysis showed a reduction in the low-to high-frequency showing the parasympathetic predominance (Schomer *et al.*, 2014). Similarly, a HRV analysis in epilepsy patients who had the VNS treatment for 4.5 month showed increases in the HF power, which is associated with increase in vagal tone. There was also a slight increase in the baroreflex index during the VNS indicating the cardiovascular stability where adequate sympathetic and parasympathetic supply to adjust the cardiovascular in response to the BP (Stemper *et al.*, 2008). These HRV observations in epilepsy patients however have been reported to be inconsistent either in short term VNS therapy (<3 months) (Barone *et al.*, 2008) or long term therapy (over than a year) (Ronkainen *et al.*, 2006).

## 1.2.2 VNS and Heart Failure

Despite conflicting evidence from VNS on the cardiovascular protection among the epilepsy patients, the therapeutic potential of VNS among the heart failure (HF) patients is being tested. Stimulation at the right cervical vagus in healed myocardial infarction (MI) dogs successfully reduced the incidence of atrial fibrillation from 100% to 10% of cases. When the same VNS group underwent exercise without VNS stimulation, the incidence of atrial fibrillation increased to 89% (Vanoli *et al.*, 1991), suggesting that VNS is protective on the heart. In a later study, 6 weeks of VNS on HF rats showed improvement in survival rate (86% versus 50%), lower left ventricular end diastolic pressure (17.1±5.9 versus 23.5±4.2 mm Hg, P<0.05) and lower normalized biventricular weight (2.75±0.25 versus 3.14±0.22 g/kg, P<0.01) compared to the control. This suggests VNS treatment improved haemodynamic properties in the failing heart of the rat (Li *et al.*, 2004). This finding is in agreement with another study on burn induced HF rats that demonstrated significantly

improved end diastolic pressure in VNS treated animals compared to control groups (Niederbichler *et al.*, 2010).

Activation of the vagus nerve has also been documented to provide cardiac protection against myocardium remodelling in HF. Signal decay rate of nitroxyl probe in HF mice revealed elevated redox status compared to controls. The application of VNS on HF mice normalized the redox status ($0.13 \pm 0.01$ min$^{-1}$) indicating the reversal effect of VNS on oxidative stress in cardiomyocytes (Tsutsumi *et al.*, 2007). A study on microembolized induced chronic HF dogs , found that 6 months of VNS caused a significant reduction in proinflammatory factors such as CRP protein, TNF$\alpha$ and IL6. In addition, cardiac pumping efficiency significantly improved as there was a reduction in end systolic volume compared to an increase in controls (Hamann *et al.*, 2013).

Clinical trials of the VNS reported contradictory cardio autonomic endpoints. A 6 month pilot study of VNS application (CardioFit™) on ventricular dysfunction patients (n=8) found significant reductions in cardiac end systolic volume as well as New York Heart Association (NYHA) class function (Schwartz *et al.*, 2008). The continuation of this study was performed by De Ferrari et al into a multicentre trial, two staged study (n=32) where a similar series of data collection completed with an optional 1 year follow-up. VNS successfully improved patients NYHA class quality of life, exercise ability, left ventricular systolic volume as well as ejection fraction. Intriguingly, these effects were maintained at 1 year follow-up (De Ferrari *et al.*, 2011). The Autonomic Neural regulation Therapy to Enhance Myocardial Function in Heart Failure (ANTHEM-HF) study assessed the effects of therapy on LV structure and function in patients with chronic stable HF. Stimulating either left or right side of the vagus nerve in HF patients significantly improved the cardiac contractility function as measured from low ventricular ejection fraction (LVEF), HRV, and also plasma HF marker (Pro-BNP) (Premchand *et al.*, 2016). A randomized sham control trial in The Neural Cardiac Therapy for Heart Failure (NECTAR-HF) however failed to demonstrate any significant effect on the aforementioned endpoint measures after 6 months of right vagal stimulation (Zannad *et al.*, 2015). A multinational randomized trial of The

Increase of Vagal Tone in Heart Failure (INOVATE-HF) showed the risk of death or events among HF patients was not improved in VNS treated group (Gold *et al.*, 2016). Despite conflicting cardiac functions as primary endpoints of VNS, these trials mutually agreed on an improved overall quality of patient's life after long term therapy.

Whilst VNS may be effective at improving quality of life in HF patients, there are several implications involving surgical implantation of the device. This includes technical difficulties such as electrode malfunction, cardiac arrhythmia during test stimulation as well as post-surgery wound infection (Spuck *et al.*, 2010). It was also reported that patients experienced side effects such as hoarseness, dysphagia, cough and also pain which potentially due to undifferentiated glossopharyngeal stimulation (Smyth *et al.*, 2003). Finding alternative to VNS with a less invasive method therefore would provide a valuable therapeutic option to treatment of HF and indeed epilepsy.

### 1.2.3 Various medical applications of VNS

In addition to epilepsy, there have been many interesting studies on the application of VNS in treating various medical conditions. These conditions can either be associated with autonomic or non-autonomic imbalance. Since our main interest in this project was autonomic function, the other applications of VNS are summarized in **Table 1.1.**

**Table 1.1 Examples of other medical applications tested for VNS**

| Chronic medical conditions | Approval from the US Food Drug Administration (FDA) | | Clinical evidence | | |
|---|---|---|---|---|---|
| | Status | Year of approval | Author | Aims | Results |
| Depression | Yes | 2005 | Christmas and Matthews (2015) | Investigate response rate in chronic depression patients after 12 months of VNS therapy. | Reduction in the depression symptom score |
| Crohn's Disease | No | No | Bonaz et al. (2016) | Evaluate the effect of 6 month VNS therapy by looking at clinical, biological and also vagal tone. | The long-term effect of VNS on vagal tone depends on the basal level. Biological parameters relating to Crohn's disease improved after VNS. |
| Tinnitus | No | No | De Ridder et al. (2014) | Evaluate the effect of VNS on tinnitus patients | The medication-free patients reported a positive improvement in quantified tinnitus. |
| Obesity | No | No | Bodenlos et al. (2014) | Examine calories consumption when VNS device is on or off in lean and obese subjects | The VNS significantly reduced calories intake where this is dependent on subjects BMI |

| Migraine | No | No | Pintea et al. (2016) | Assessed the long term effect of VNS on headache severity and associated functional comorbidities. | The VNS treated group a lower headache related pain severity score and anxiety scale. The score for migraine wasn't significantly affected by the VNS. |
|---|---|---|---|---|---|
| Alzheimer's | No | No | Merrill et al. (2006) | Long-term effect (6 months) of VNS on patients with Alzheimer's disease was studied | Majority patients (70.6%) improved or did not decline the cognitive functions from baseline. Significant decrease in CSF biomarkers for Alzheimer's disease. |

## 1.3 The auricular branch of the vagus nerve

### 1.3.1 Anatomical structure of the auricle

The auricle is a visible and paired external ear structure that resides on the lateral aspect of the head. Generally, the auricle structure of rats is similar to that in humans but it is mostly referred to as pinnae. The concave shaped arrangement of the auricle reflects its main function to capture sounds from various directions and amplify via resonance to the external acoustic meatus/ear canal where the sound is transmitted to the tympanic membrane. The human auricle is largely made of a flexible elastic cartilaginous framework to support the external ear shape while allowing its flexibility. The outer curvature of the ear is referred to as the helix and the presence of another curved elevation parallel to the helix is called anti-helix. Moving inwards, in middle of the auricle an upper region is referred as cymba concha and the lower region is the cavity conchae. Just before entrance of the external acoustic meatus, the elevation of cartilage tissue is identified as tragus. Unlike any other auricle structures, the absence of cartilage in the bottom ear structure (lobule) results in less elasticity in this region (**Figure 1.5).** Similar auricular anatomy is denoted in rats.
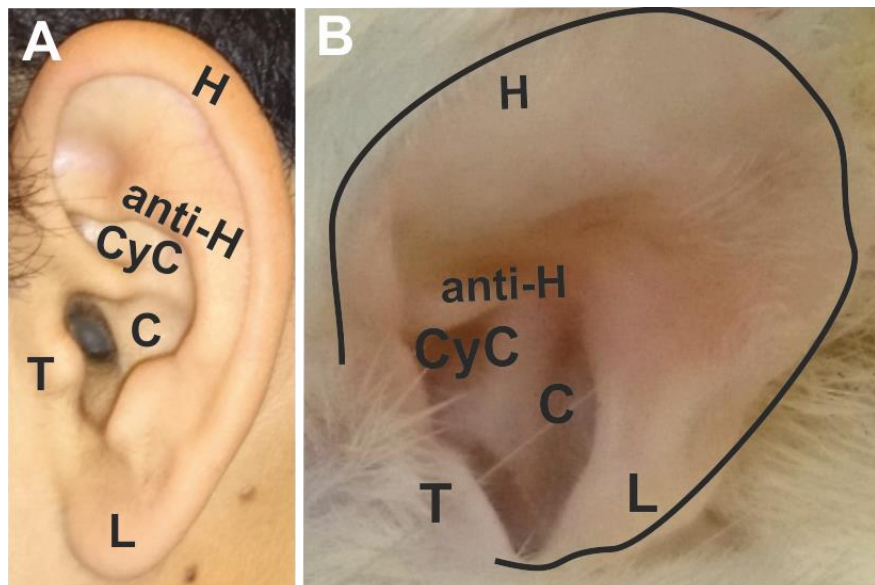
**Figure 1.5 Anatomical representation of human and rat external ear**

Similar external ear structure denoted in A) humans and B) rats. H- helix, Anti-H- anti-helix, C- concha, CyC- Cymba concha, T- tragus, L- ear lobe.

## 1.3.2 Ear somatovisceral reflexes

In addition to acting as a sound amplifier, the auricle has been reported to produce various somatovisceral reflexes. The gastro-auricular phenomenon was described as intense itching comparable to a scratch with a toothpick or a hairpin in the left external auditory meatus that corresponded with severe heartburn. This medical observation was commonly reported in gastro-surgical ward where the physicians were left puzzled since medical examinations found no dermatological or neurological abnormalities (Malherbe, 1958; Engel, 1979).

In lung tuberculosis patients, hypersensitivity of the auricle region has been reported on the side with more advanced tubercular progression. This clinical observation was then referred to as the pulmonary-auriculo phenomenon (Engel, 1979). Activation of the pulmonary-auriculo pathway potentially

explains the radiating unilateral facial pain experienced among patients with lung cancer that can be initially felt deep within the ear (Bindoff & Heseltine, 1988; Abraham *et al.*, 2003; Palmieri, 2006).

Manual stimulation of the external auditory meatus, for example through cleaning of the ears, elicits an ear cough reflex, in 2.3% to 4.2% of the general population (Gupta *et al.*, 1986; Tekdemir *et al.*, 1998). Vagal sensory hyperactivity in the ear-cough reflex has been linked to refractory chronic cough since patients experienced neuropathic features such as throat irritation and cough upon exposure to non-tussive triggers such as cold air.

The auriculogenital reflex has also been described previously in cats where introducing manual stimulation into the external auditory canal of the ear caused gross contraction of the musculature around the vaginal orifice. Electrical stimulation on the external ear of decerebrated cats with specific nerves transected (e.g. cervical, trigeminal, facial) preserved the auriculogenital responses. However, this reflex was absent when the vagus nerve (at jugular foramen) was cut (Bradford, 1938).

A connection between the ear and the heart has been reported in a recurrent syncopal attack and bradycardia due to light stimulation of the external ear canal. Targeted baseline autonomic function test (e.g.: cold face test and HRV) confirmed hyperactivity of vagal response as the pathophysiological mechanism rather than autonomic neuropathy complication (Thakar *et al.*, 2008). The ear-cardiac modulation however was reported to be rare, potentially due to the variability in the nerve innervation of the external ear in humans. Extra precaution was advised in patients undergoing ear manipulation (e.g.: myringotomy and ear tube insertion) during surgery due to incidence of dysrhythmias (Moorthy *et al.*, 1985). The cardiac-auriculo connectivity might be associated with referred facial pain which happens together with angina and myocardial infarction (Rothwell, 1993; Amirhaeri & Spencer, 2010).

### 1.3.3 Neuroanatomy of the auricular branch of vagus nerve (ABVN) and the vagus nerve

The auricular branch of the vagus nerve is given off from the vagal trunk at the jugular ganglion. In rats, the ABVN nerve passes behind the external jugular vein, enters the mastoid canaliculus on the lateral wall of the jugular fossa, and runs towards the external acoustic meatus. Continuing on its lateral direction, it traverses the temporal bone and crosses the facial canal and receives communication from the facial nerve(Weijnen *et al.*, 2000). The interconnection between the ABVN and facial nerve is however, reviewed to be inconsistent in humans (Mitchell, 1954). These interconnections may be more constant in rats as identified by retrograde tracer injections into the wall of the auditory canal and examination of the ganglia of the aforementioned nerves (Folan-Curran *et al.*, 1994). The ABVN further traverses the tympanomastoid fissure and gives off two rami; one to the floor and another to the posterior wall of the external ear (Weijnen *et al.*, 2000). The highest density of fibres of the ABVN in human external ear could be found surrounding the cymba conchae (Peuker & Filler, 2002). Details of the findings from humans ABVN innervation is included in **Table 1.2 and Figure 1.6**. The anatomical knowledge of the ABVN innervation of the rat ear however still needs to be examined.

**Table 1.2 Nerve innervation pattern on lateral surface of human auricle as outlined by Peuker and Filler (2002)**

| | ABVN | GAN | ATN |
|---|---|---|---|
| **Crus of helix** | 20% | | 80% |
| **Spine of helix** | | 9% | 91% |
| **Tail of helix** | | 100% | |
| **Scapha** | | 100% | |
| **Crura of antihelix** | 9% | 91% | |
| **Antihelix** | 73% | 9% | 18% |
| **Antitragus** | | 100% | |
| **Tragus** | 45% | 46% | 9% |
| **Cymba conchae** | 100% | | |
| **Cavity of conchae** | 45% | 55% | |
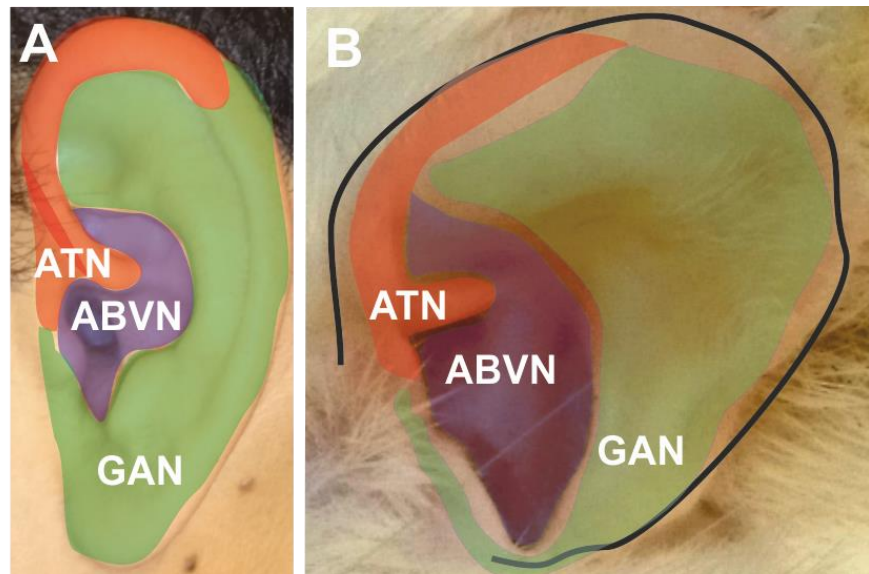


**Figure 1.6 The nerve innervation pattern of the external auricle**

A) Lateral aspect of the humans' ear has distribution of the ATN, ABVN and GAN where the main distribution is colour coded (extrapolated from Peuker and Filler (2002)). B) Similar auricular nerve distribution proposed from similar structures observed in rats. ATN- Auriculotemporal Nerve, ABVN – Auricular Branch of the Vagus Nerve, GAN- Great Auricular Nerve.

## 1.3.4 Central projections from the auricle/pinna

Although there have been several gross examinations of nerve innervation of the pinna in humans, the central projection studies utilizing transganglionic tracing techniques have necessarily been performed on animals.

Central projections of the Great Auricular Nerve (GAN) in animals have been examined only in rabbit. The application of HRP on the GAN nerve revealed afferent cell bodies in the ipsilateral dorsal root ganglion (C2-C3) and the superior cervical ganglion. Nerve fibres were detected in the dorsal column of the upper cervical spinal cord and strongly stained in laminae I-V at the C2 level. The afferent GAN projection also has intense labelling in the cranial nerve nuclei in the medulla, accounting for caudal subnuclei of the spinal trigeminal nerve, the solitary nucleus, and also medial and lateral cuneate nuclei (Liu & Hu, 1988). Unlike for GAN, studies on central termination of the Auriculotemporal Nerve (ATN) have been explored in rodents (Jacquin *et al.*, 1982; Takemura *et al.*, 1987). Horseradish Peroxidase (HRP) labelled primary afferent fibres of the ATN were confined to the ipsilateral brainstem. The nerve terminals projected to the caudal medulla; specifically staining the dorsolateral border of the mandibular division of the trigeminal principal nucleus, cuneate nucleus and also paratrigeminal nucleus (Pa5). Travelling further caudally until the 3$^{rd}$ cervical level, a termination of the ATN was also found in the dorsolateral spinal dorsal horn complex at laminae I-V but more intensely in III-IV (Takemura *et al.*, 1987).

Understanding patterns of the main vagus nerve projections is important before studying its branch projections. Central projections of the sensory vagus nerve in rats have been shown by use of HRP histochemistry (Kalia & Sullivan, 1982). It was found that the vagus entered the medulla in fascicles on the lateral side, travelled dorsolaterally and projected to the tractus solitaries. Vagal projections could also be observed on the caudal aspect of the tractus solitarius in laminae V of the upper cervical cord (C1 and C2). The sensory fibres of the vagus terminated bilaterally in the nucleus tractus

solitarius (NTS); area postrema (AP); as well as dorsal motor nucleus of the vagus nerve (dmnX). The ipsilateral projection onto the NTS and dmnX was found to be heavier than that onto the contralateral side. The projection onto the AP however, was found to be equally distributed on both sides (Kalia & Sullivan, 1982). The central projection study of ABVN showed slight differences in the termination pattern than that of the main vagus nerve. HRP applied to the ABVN of cats showed cell bodies stained in the superior ganglion of the vagus nerve confirming its connection with the main trunk of the vagal nerve, but not on the nodose ganglion (Nomura & Mizuno, 1984). The sensory labelling could be seen on the solitary nucleus covering interstitial, dorsal, dorsolateral as well as commissural subnuclei. Other terminal labelling was detected on the ventral aspect of the principal sensory trigeminal nucleus, the ventrolateral of the cuneate nucleus as well as in the dorsal horn of C1-C3 cervical spinal (laminae I-IV) (Nomura & Mizuno, 1984). Injection of 1% CTB into the junction of cavity of the auricular concha and postero-inferior wall of the external acoustic meatus (presumed to be ABVN innervated) of rats showed ipsilateral staining with the fibres terminating in the caudal part of the lateral NTS, dorsomedial edge of the spinal trigeminal nucleus, rostro-lateral cuneate nucleus, and also spinal dorsal horn of upper cervical (He *et al.*, 2013).

It is important to note that the afferent from the external ear exhibited some degree of overlap in each of the neurotracing studies performed previously **Figure 1.7.** For example all the auricular nerve tracing studies (GAN, ATN, and ABVN) ipsilaterally labelled laminae III and IV of the dorsal horn (Nomura & Mizuno, 1984; Takemura *et al.*, 1987; Liu & Hu, 1988). Intriguingly, this wasn't the case when the vagal tracing was performed directly from the vagal trunk. HRP injection into the rats' vagus nodose ganglion resulted in afferent terminal labelling of the laminae V only in the C1 and C2 region (Kalia & Sullivan, 1982). Similarly, when the middle portion of cervical trunk of the vagus nerve in cats was injected with HRP, it labelled the nucleus ambiguus and labelling extended into the basolateral portions of the ventral horn (border of laminae V) of the C1 and C2 cord segments (Nomura & Mizuno, 1983).

Furthermore, both of the vagal tracing studies showed no afferent terminations within the trigeminal structures such as the paratrigeminal and also trigeminal nucleus (Kalia & Sullivan, 1982; Nomura & Mizuno, 1983). This raises caveats of the previous auricular nerve tracing studies (particularly the ABVN) since the neuronal tracers were injected subcutaneously, causing non-selective nerve detection (Chien *et al.*, 1996; He *et al.*, 2013). The comparison between respective auricular nerve studies and the cervical vagal studies are summarised in **Table 1.3**.
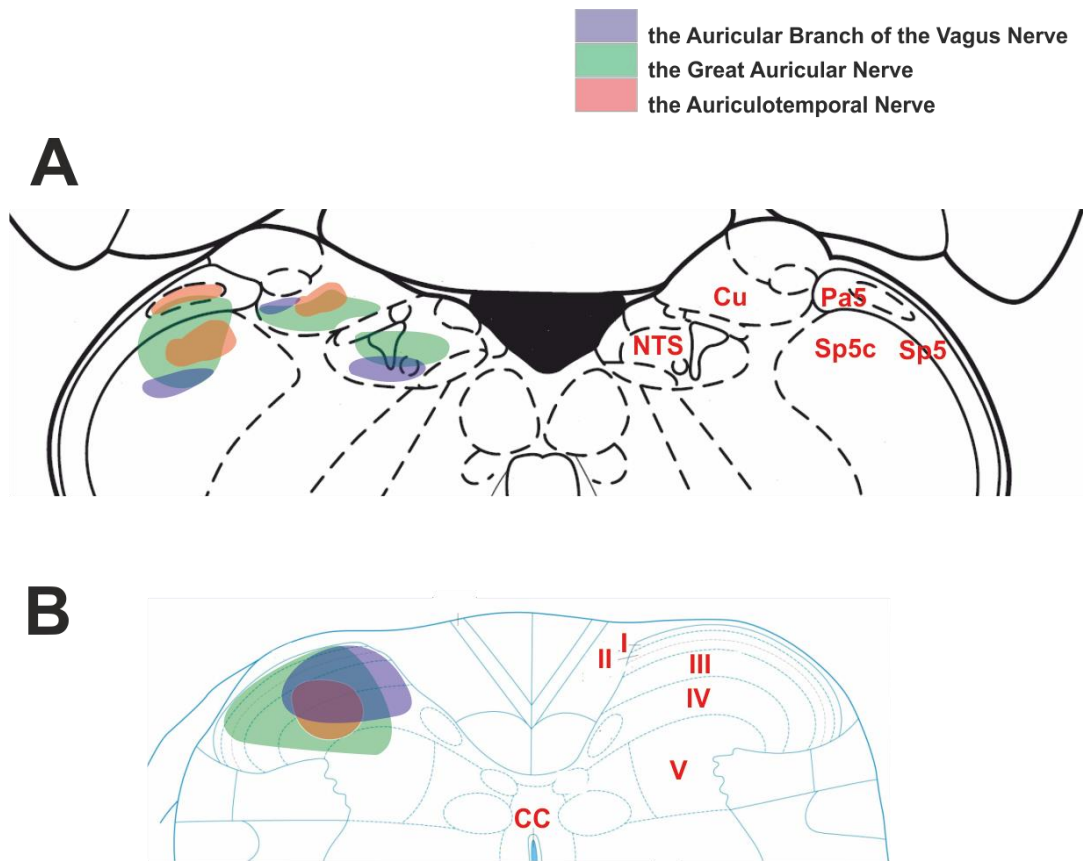
**Figure 1.7 Summary of external auricle afferent projections to brainstem and upper cervical spinal cord**

A) In the brainstem, the GAN (green) projects into the Sp5, Cu and a little in the NTS. The ATN (red) terminates into the Sp5, Sp5c and Cu. The ABVN (blue) has projection into the NTS, Cu, and Sp5c. B) Projection of the GAN into upper cervical cord has wide coverage from laminae I to laminae V, and smaller coverage by the ATN concentrated in the laminae III-IV. The ABVN afferents terminates into the laminae I-IV. The level central nervous axis was omitted for clarity. GAN- Great Auricular Nerve, ATN- Auriculotemporal Nerve, ABVN- Auricular Branch of the Vagus Nerve, CC- Central Canal, DVN- Dorsal Vagal Nucleus, NTS- Nucleus Tractus Solitarius, Cu-cuneate nucleus, Pa5- Paratrigeminal Nucleus, Sp5- Trigeminal tract, Sp5c- Caudal Trigeminal Nucleus.

**Table 1.3 Comparison between neuronal tracing studies of the auricular nerves and the cervical vagal trunk**

| | | | | | NTS | | | | | | | Vagal | | | trigeminal | | | cervical | | |
|---|---|---|---|---|---|---|---|---|---|---|---|---|---|---|---|---|---|---|---|---|
| Study | Author | Site of injection | Tracer | Species | l | dl | comm | m | d | i | v | DVN | AP | Cu | Pa5 | SP5n | SP5 | C1 | C2 | C3 |
| Non-isolated ABVN | Chien *et al.* (1996) | Middle & Caudal auricular | HRP | Dogs | + | ■ | ■ | ■ | + | ■ | ■ | ■ | | + | + | + | + | + | + | + |
| | He *et al.* (2013) | Auricular conchae | CTB | Rats | + | ■ | ■ | ■ | ■ | ■ | ■ | ■ | | + | ■ | + | ■ | ■ | + | + |
| Isolated ABVN | Nomura and Mizuno (1984) | ABVN | HRP | Cats | ■ | + | + | ■ | + | ■ | + | + | ■ | + | ■ | + | + | + | + | + |
| Vagal Nerve | Kalia and Sullivan (1982) | Cervical trunk | HRP | Rats | + | + | + | + | + | + | + | + | + | ■ | ■ | ■ | ■ | + | + | ■ |
| | (Nomura & Mizuno, 1983) | Cervical trunk | HRP | Cats | + | + | + | + | + | + | + | + | ■ | ■ | ■ | ■ | ■ | + | + | ■ |

35

| Isolated GAN | (Liu & Hu, 1988) | GAN root | HRP | Rabbit | | | | | + | | | + | | + | + | + | + | + |
| Isolated ATN | (Takemura *et al.*, 1987) | ATN branch | HRP | Rats | | | | | | | | + | + | + | + | + | + | + |

l – lateral, dl – dorsolateral, comm – commissural, m- medial, d – dorsal, I – intermediate, v – ventral, SP5n – trigeminal nucleus, SP5 – trigeminal tract

## 1.3.5 NTS as a mediator site for cardio-auriculo reflexes

The NTS lies in the dorsomedial medulla oblongata and runs from the caudal end of the pyramidal decussation to the caudal end of the facial motor neurons. As noted earlier, the NTS receives numerous primary afferent inputs, processes this information and projects the output to several other brain regions to influence autonomic control. There are three major NTS subregions: rostral, medial and caudal NTS. The caudal NTS nuclei are part of the respiratory and swallowing generators while the rostral nucleus is involved in somatosensation and taste (Chen, 2006).

ABVN stimulation in rats activates baroreceptor sensitive neurons in the NTS (Gao *et al.*, 2011). The barosensitive neurons were identified by possession of a rhythmic discharge that fluctuated more than 15% in response to administration of the vasodilator sodium nitroprusside. The changes in neuronal firing were compared for ABVN stimulation at the auricular point Heart and a somatic acupuncture point of the lower leg near to the tibia. Activated NTS neurons were mostly detected in subnuclei located at the dorsolateral, medial and solitary tract of the intermediate and caudal NTS **(Figure 1.8)** (Gao *et al.*, 2011). The dorsal and commissural subnuclei of the NTS of rats were reported to have vagal innervations originating from the carotid sinus where baroreceptors lie (Ciriello & Calaresu, 1981). Hence, it is evident that the central termination of the ABVN in NTS suggests its involvement in controlling the cardiorespiratory reflexes and this hypothesized pathway is known as the Auriculovagal Afferent Pathway (He *et al.*, 2013).
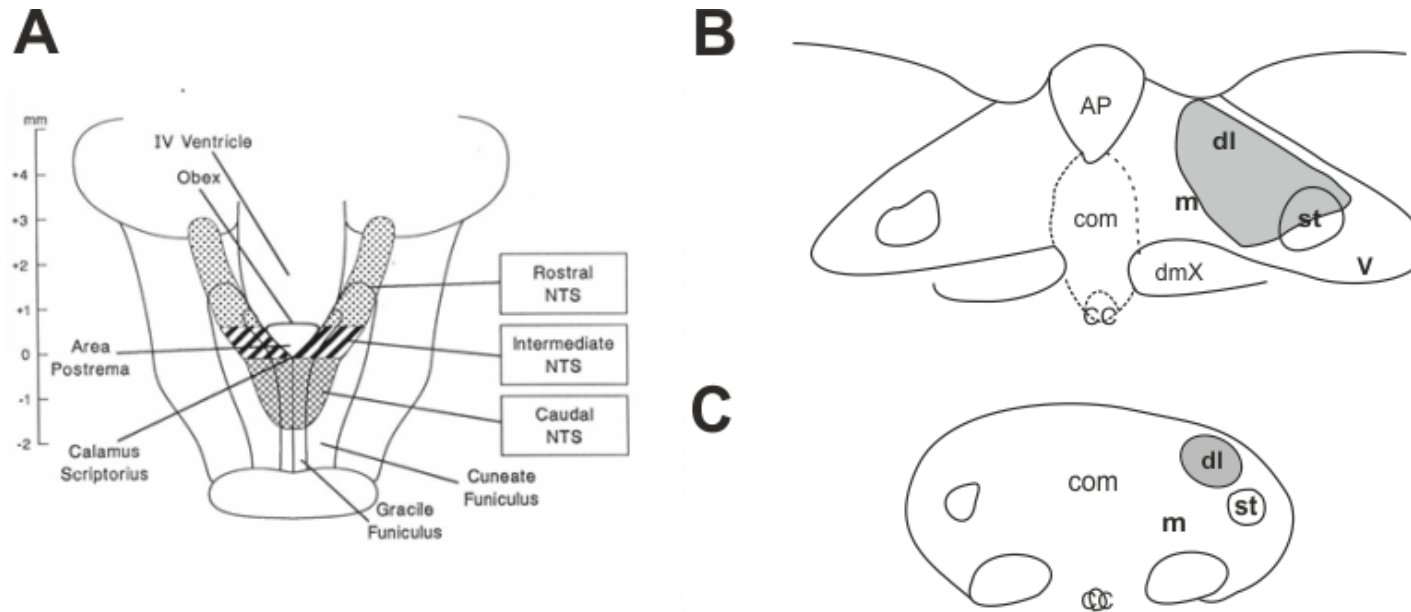
**Figure 1.8 The brainstem region with active barosensitive neurons**

Diagram illustrates the A) Posterior view of the brainstem showing three NTS regions; rostral, intermediate, and caudal as outlined by Loewy and Spyer (1990) from cat brainstem. The sub nuclei from B) intermediate and caudal NTS were illustrated with a coronal section of the brainstem. The circled grey are areas with active barosensitive neurons as identified by Gao *et al.* (2011). Abbreviations Com= commissural subnuclei, dl = dorsolateral subnucleus, m = medial subnuclei, v = ventral subnucleus.

### 1.3.6 History of ABVN stimulation

The idea for ABVN stimulation has been around for thousands of years in a form of acupuncture, which has even been suggested to have arisen during pre-historic period and have been inherited by various parts of the world today (Gori & Firenzuoli, 2007). During pre-historic periods, the rudimentary form of acupuncture revolved from sharp stones, bamboo, substituted by fish bones, bamboo clips and later various shapes of needles made of metal. The use of acupuncture as a way of healing in wounded primeval warriors is supported by scars on the skin of the mummified body of Similaun Iceman, Italy. The auricular acupuncture had been reported in the healing practice of ancient Egypt, Greek and Chinese civilization. The women in ancient Egypt were documented to have their external ear prickled with a hot needle to induce contraception, while gold earrings worn by the Mediterranean sailors was meant to improve vision. The father of Greek medicine, Hippocrates, who was also a paragon in modern medicine, reported that the cutting veins behind the ear improved male sexual functions (Gori & Firenzuoli, 2007). In ancient Chinese medicine, auricular acupuncture was developed from the concept of life force energy (qi) that flowed through channels (Nozdrachev, 2002). In much later periods, the inclusion of this ancient healing practice into the modern western medicine was first documented, to the best of our knowledge, by a French neurologist and trained acupuncturist Dr Paul Nogier in 1950 (Nogier, 2014). Dr Nogier realized a small burn scar on parts of his patient's ear, arose from a sciatic pain treatment by a local lady. He tested and later improvised the treatment strategy with simple needle jabs on underlying cartilage of the pinna. He discovered that auricular acupuncture may result in radial pulse shift (slowing or acceleration of heart rate).

## 1.3.7 Current clinical studies/applications of the ABVN stimulation and its effects on autonomic control

The auriculo-medicine theory developed by Dr Nogier was not scientifically recognized due to lack of structural evidence (Nogier, 2014). One pilot study specifically developed a method to register pulsatory surface changes using microscopy to quantify the Nogier pulse reflex. This method revealed the reflex-based changes on blood flow velocity but more evidence is required to provide conclusive perspective on auricular acupuncture medicine (Litscher *et al.*, 2015).

Studies on assessing the effects of ABVN stimulation on ANS activity in healthy volunteers are rather conflicting. The responses of cardiac autonomic influence from ABVN stimulation were analysed non-invasively using heart rate variability (HRV), which was derived from R-R intervals of ECG recording. Power spectral analysis of the R-R interval produces measures which reflect the sympathetic activity (High Frequency; HF) and parasympathetic activity (Low Frequency – sympathetic). Earlier evidence with 25 minutes cavum conchae stimulation using manual acupuncture has shown a significant increase in the HF of the HRV, suggesting elevation in cardiac parasympathetic activity (Haker *et al.*, 2000). The significant increase in the cardiac vagal tone was seen at the ear stimulation period, as well as for 60 minutes post-stimulation. However, no changes were seen either in the sympathetic activity as measured by the low frequency (LF) of the HRV, blood pressure or heart rate (Haker *et al.*, 2000). Similar work to stimulate the tragus for 15 minutes in healthy volunteers showed increases in HRV towards parasympathetic predominance, accompanied by decrease in muscle sympathetic nerve activity (MSNA) recorded from the common peroneal nerve (Clancy *et al.*, 2014). This does not align with what was reported by Haker's study where no sympathoinhibition was seen, at least in the heart. In a recent study, randomisation of healthy participants into left or right conchae stimulation increased the HRV vagal tone only from right-sided stimulation (De Couck *et al.*, 2017). Further, the confounding factors contributing to ANS

changes from prolonged right conchae stimulation was analysed. The significant increase in cardiac vagal activity was only observed in women and not a total sample of participants. In addition the stimulation time and gender interaction were more consistent after 30 minutes of stimulation, suggesting moderate modulation effects of prolonged ABVN stimulation only in women (De Couck *et al.,* 2017).

Despite conflicting ideas on ABVN stimulation on cardiac ANS, the tVNS has been proposed as an inexpensive alternative to treat autonomic imbalance in heart failure (Clancy *et al.,* 2013; Murray *et al.,* 2016). Pioneering studies in this niche were performed on coronary artery disease and angina pectoris patients who underwent surgery for coronary bypass grafting (Zamotrinsky *et al.,* 2001). Acupuncture needles were attached bilaterally on the "heart acupoint" in the inferior conchae, where the ABVN was stimulated for 15 minutes for 10 days. This resulted in improved clinical presentation including a reduction in cardiac incidence of angina pectoris, and a decrease in the reliance on vasodilator usage (Zamotrinsky *et al.,* 1997; Zamotrinsky *et al.,* 2001). In addition, the tVNS also resulted in a reduction of atrial noradrenergic plexus, suggesting cardiac sympathoinhibition effects (Zamotrinsky *et al.,* 2001). A further study that examined the HRV in coronary artery disease patients using similar tVNS protocols (15 minutes for 10 days) showed alleviation of the cardiac angina signs, and more importantly the non-invasive autonomic measurement (LF/HF index) converted to healthy normal values among the responders (Popov *et al.,* 2013). The effects of low level electrical stimulation on tragus in patients with paroxysmal atrial fibrillation (AF) were studied (Stavrakis *et al.,* 2015). It was found after an hour of tVNS, the vicious cycle of AF induction was inhibited by reducing the AF duration and the AF cycle length. The level of inflammatory cytokines was also reduced, highlighting activation of the vagal cholinergic anti-inflammatory pathway (Stavrakis *et al.,* 2015).

Beneficial evidence of the transcutaneous vagal activation has been tested in various HF animal studies. Applying low-level tragus stimulation in dogs with healed MI for 90 days attenuated the ventricular remodelling which recognised

by smaller infarct size, and better cardiac contractile and diastolic functions. In post-MI, the cardiac tissue started to develop scars and the level of fibrosis is influenced by enhanced sympathetic nerve activity. However, the low-level tragus stimulated group exhibited reduction in plasma NE level thus indicated that the central sympathoinhibition was responsible for the amelioration of the post-MI remodelling (Wang *et al.*, 2014).

Neuromodulation of the cardiac ANS from the low-level tragus stimulation has also been reported in an arrhythmia model in dogs. In this HF model, the sympathoactivation was induced with electrical stimulation on the right stellate ganglion and resulted in cardiac sinus node acceleration. The irregularity of the sinus nodal activity was nevertheless attenuated after 3 hours of tragus stimulation (20 Hz, 2ms), in conjunction with reduction in the expression of neural synaptic proteins (cFos and NGF) from the right stellate ganglion (Zhou *et al.*, 2016). The low level tragus stimulation is also effective in suppressing intrinsic cardiac ANS in AF dogs. Neural hyper activation of the cardiac ganglionated plexus (intrinsic cardiac autonomic nervous system) has been suggested to trigger AF events. In AF model dogs using rapid atrial pacing, the low level tragus stimulation (20 Hz, 1ms) elicited an antiarrhythmic effect coupled with a suppression of the neural firing in the cardiac ganglionated plexus (Yu *et al.*, 2012). When the low level stimulation was applied to the vagotomised dogs, the antiarrhythmic effects were eliminated indicating the vagal efferent activation in inhibiting the intrinsic cardiac ANS (Yu *et al.*, 2013).

**Table 1.4 Studies of cardiac neuromodulation by tVNS**

| Paper | Species | n | Sampling group | Stimulation site | Stimulation parameters | Main outcomes |
|---|---|---|---|---|---|---|
| Haker *et al.* (2000) | H | 12 | Healthy | Right cavum conchae | Manual acupuncture | Increased the HF of the HRV during and after stimulation. The LF, BP and HR not significantly changed |
| Clancy *et al.* (2014) | H | 14 | Healthy | Right tragus | 10 – 50 mA, 30 Hz | Reduced the LF/HF ratio and decreased the mSNA |
| Stavrakis *et al.* (2015) | H | 40 | AF | Right tragus | 1ms duration, 20 Hz | The AF was suppressed seen from total AF duration and cycle length. Inflammatory marker levels decreased significantly |
| Wang *et al.* (2014) | D | 30 | MI | Right tragus | 1ms, 20 Hz | The contractility of the left ventricular functions improved, smaller infarct size, lower plasma remodelling factors, lower plasma NA. |
| Zhou *et al.* (2016) | D | 16 | Tachycardia | Right tragus | 2ms, 20 Hz | The acceleration of the sinus nodal attenuated where lower neural activation in the stellate ganglion of the tVNS group |

| Paper | Species | n | Sampling group | Stimulation site | Stimulation parameters | Main outcomes |
|---|---|---|---|---|---|---|
| Yu *et al.* (2013) | D | 16 | AF | Right tragus | 1 ms, 20 Hz | The atrial remodelling from induced AF was reversed in the tVNS group where bivagal transection inhibited the reversal. |
| Zamotrinsky *et al.* (1997) | H | 10 | Preoperative coronary artery disease patients | Bilateral cymba concha | 0.2-1.5 mA, 1.5 ms, 3 Hz | Relieve anginal symptoms, improved biochemical properties of myocardium, and increased heart's tolerance of operative reperfusion damage. |
| Zamotrinsky *et al.* (2001) | H | 16 | Preoperative coronary artery disease patients | Bilateral cymba concha | 0.2-1.5 mA, 1.5 ms, 3 Hz | In tVNS groups, the noradrenergic nerves in the atrial tissues are significantly lower. Better cardiac functions reported in tVNS. |
| Popov *et al.* (2013) | H | 48 | Coronary artery disease patients | Bilateral cymba concha | 0.05-0.15 mA | The effects of tVNS in responders showed improvement in health and the LF/HF index approached normal values. |
| De Couck *et al.* (2017) | H | 60 | Healthy | Left or right conchae | 0.7 mA, 250 µs, 25 Hz | No consistent changes in HRV. The tVNS effect is more prominent on the right tVNS, and in women. |

## 1.4    Research Gap

Previous studies suggested that tVNS restores brings the autonomic balance in HF subjects presumably by augmenting parasympathetic actions and reducing sympathetic activity However, there are several areas of investigations identified for study:

a) Determine the sensory afferent nerves from the site of transcutaneous stimulation to the brain

b) Develop an ear stimulation model in an anaesthetic free preparation

c) Examine the acute effect of tVNS on heart rate, respiration and sympathetic activity

d) Investigate the effect of stimulation on different parts of the external ear in the anaesthetic free model.

## 1.5    General Hypothesis

Stimulation of the ABVN in the ear effectively alters the autonomic function of the rats as previously shown in humans. The physiological changes elicited from the ABVN stimulation in WHBP is mediated through afferent projection to the NTS.

## 1.6    Aims and objectives

1) To reveal the afferent projections from the stimulation sites (e.g.: tragus, lobe) into the CNS using neuronal tracing,

2) To study the differences in autonomic profile of the rats in different circadian phases (dark/light) to determine the appropriate time of day for the ear stimulation,

3) To study the effects of auricular stimulation through direct recordings of the sympathetic and phrenic nerve activity, along with heart rate,

4) To determine the effect of stimulating different regions in the ear.

# Chapter 2 Methods

## 2.1 Transganglionic labelling of afferents from auricular stimulation sites

In an effort to understand the pathways through which transcutaneous ear stimulation could influence autonomic function, the central projections of the afferents innervating the stimulations sites were studied. For this reason, afferent projections from the external auricle were traced using the retrograde neuronal tracer Cholera Toxin B (CTB).

### 2.1.1 Introduction

**Cholera toxin as a neuronal tracer**

Cholera toxin (CT) is produced by *Vibrio cholera, the* family of bacteria which is responsible for the intoxication of intestinal cells after ingestion. *V. cholera* was first isolated by Robert Koch (1843 - 1910) from a stool sample that originated in Egypt where he noted the physical appearance of the bacteria - "a little bent, like a comma"; different from any other common bacillus. Despite Koch's discovery, the pathogenesis of cholera only came to be understood years later by Sambhu Nath De (1915-1985). De's findings involved ligated loops of rabbit small intestine injected with filtrates that originated from several strains of *V. cholera* (De *et al.*, 1960). De noted that the immunoreactive peptides are naturally secreted by the *V. cholera* during bacterial growth as the isolated intestinal loops weren't affected by filtrate from the washed bacterial bodies broken with ultrasonic vibrations (De *et al.*, 1960).

## Cholera toxin structure and actions

This immunoreactive protein became later known as CT and it presents a hexameric protein structure consisting of 2 major domains **(Figure 2.1)**. The A subunit domain (240 amino acids; MW 28 kD) has a central location and is surrounded by 5 B subunits (103 amino acids; MW 11 kD each). The release of CT from *V. cholera* to the infected intestine causes pentameric B subunit binding with the GM1 ganglioside receptor on enterocytes (epithelial cells). This is followed by cleavage of the $A_1$ domain from the $A_2$, where the $A_1$ fragment enters the cytosol to initiate the enzymatic cascades of enterotoxicity. The $A_1$ subunit catalyses an activation of adenylate cyclase to produce cyclic adenosine monophosphate (cAMP) within the host cells and causes internal electrolytic imbalance. Ultimately, there is massive water efflux in the intestinal cells and this result in watery diarrhoea and vomiting, the clinical symptoms of cholera. Unlike the A domain, the B pentamer is non-toxic. Isolated cholera toxin B subunit is suggested to be essential as a tool for the design of drugs/vaccines due to great interactions involving GM1 mediated signal transduction (Thiagarajah & Verkman, 2005). In fact, neuronal projection studies have been facilitated by this technology where central nerve projections can be labelled either anterogradely or retrogradely.
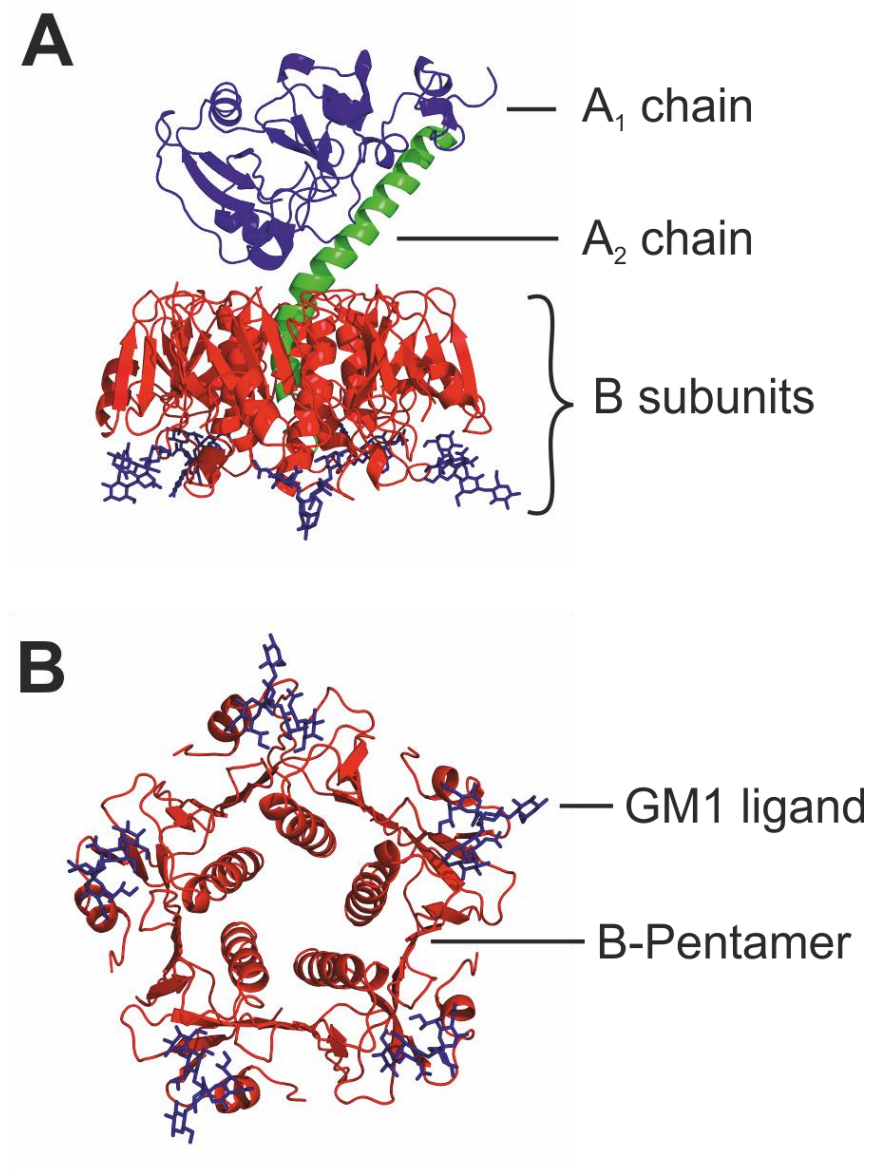
**Figure 2.1: The structure of cholera toxin (composite of PDB 1S5E and 3CHB)**

A) Cholera toxin complex consists of 2 major domains; A and B subunits. The A subunit is made up of 2 protein chains. $A_1$ is the catalytic domain joined to $A_2$ via a disulphide bond. $A_2$ is a linker protein, that joins $A_1$ to B pentamer by protuding through the central pore. B) The B pentamer of the cholera toxin provides specific binding interaction with the host cells via GM1 ganglioside before enterotoxicity cascades are initiated. Image acquired from the NCBI Protein Database website: https://www.ncbi.nlm.nih.gov/

The neuronal membrane is generally rich with gangliosides (Sonnino *et al.*, 2007). The gangliosides play a passive role in reducing fluidity of the membrane by maintaining the membrane lipid domains as well as an active role in modulating membrane biological signalling. Abundant presence of gangliosides on the neuronal membranes provides affinity for binding interaction between the cholera toxin pentamer and $GM_1$ pentasaccharide (Stoeckel *et al.*, 1977). The binding of each B subunit to high affinity monosialoganglioside GM1 receptors initiates endocytosis and delivers the A subunit to the endoplasmic reticulum in a retrograde fashion (Merritt *et al.*, 1994). The retrograde axonal transport of cholera toxin in rats was completely abolished by pre-incubated cholera toxin with bovine brain $GM_1$ gangliosides, indicating that it is the GM1 binding sites on the CT that mediate its uptake (Stoeckel *et al.*, 1977). The conventional retrograde neuronal tracing technique by Stoekel nevertheless didn't permit a characterization of the identified pathway as it was visualized by radioactive materials (Stoeckel *et al.*, 1977). Later on, a new tracing technique was introduced by Luppi *et al.* (1987) where the CTB subunit was isolated and detected with immunoreactivity. The combination of CTB tracer with immunohistochemistry has not only allowed visualization of neuronal projections, but also identification of specific pathways involved through double/triple labelling (Luppi *et al.*, 1987; Fort & Jouvet, 1990). In the present study CTB has been used to trace the projections from the external auricle to the CNS.

## 2.1.2 Materials and Methods

### Injection Procedure

Young male Wistar rats (65-85g, to match the age used for WHBP) were deeply anaesthetised with a 4% mixture of isoflurane in oxygen. Absence of the paw withdrawal reflex confirmed the depth of anaesthesia. For each animal, a total of 5 µl of 20 mg/ml CTB in 0.1 M phosphate buffer saline (PBS) was injected on right tragus (n=4) and right ear lobe (n=4) at using a glass microelectrode (inner diameter 0.84 mm, outer diameter 1.5 mm, World Precise Instrument, UK) attached via rubber tubing to a 10 µl Hamilton syringe (Sigma Aldrich, UK). The animals were allowed to recover for 3-4 days prior to being humanely sacrificed as below.

### Isolation of the brainstem and spinal cord

Animals were deeply anaesthetized with 60-80 ml/kg of intraperitoneal sodium pentobarbitone. Appropriate anaesthesia was confirmed by the absence of the paw withdrawal reflex. The abdomen was first transected transversely. Without cutting any other internal organs, the heart was exposed by a thoracotomy. The left ventricle was pierced and a blunt needle inserted and clipped into place. A small cut was made on the right atrium and the animals were flushed with 0.1 M phosphate buffer. Finally, transcardial perfusion was performed with approximately 200 ml of 4% paraformaldehyde (PFA) fixative.

The posterior part of the vertebra column and skulls were carefully removed to allow the spinal cords and the brainstem to be collected and post-fixed overnight.

## Serial sectioning of the brainstem and upper cervical spinal cord

Transverse sections at 50 µm were made from the upper cervical C4 to rostral brainstem (4th Ventricle) with a vibrating microtome (Leica, UK).Serially sectioned brain slices were collected and sequentially placed into a 6- well plate with free-floating sections in 0.1M phosphate buffer (PB). The process was repeated until all brain tissues were sectioned, such that groups of section subsequently processed from any well included representative sections from across the brainstem and upper cervical cord. This method allowed a systematic sampling coverage of the brain sections.

## Immunofluorescence

Tissue sections were washed three times for 10 minutes each in 0.1 M PBS followed by incubation in 10% donkey serum for 30 minutes. The incubation with donkey serum aimed to inhibit non-specific binding on tissues. After several washes, sections were incubated overnight in primary antibody (**Table 2.1)** in PBS with 0.3% Triton X-100 (Row & Haas, UK) added to facilitate antibody penetration across cellular membranes. Sections were left on a shaker at 4°C overnight.

Following overnight incubation (exception was 3-4 nights for ChAT), sections were rinsed 3 times with PBS. The sections were incubated in secondary antibody **(Table 2.2)** for 2-3 hours at room temperature. Tissue was then rinsed for 3 times for 10 minutes before being dried and mounted on glass slides with Vectashield mounting medium (Vector Laboratories, USA) and sealed.

**Table 2.1: Primary antibodies used on free floating tissue sections**

| Primary antibody | Abbreviation | Raised in | Dilution | Source | Catalogue |
|---|---|---|---|---|---|
| Cholera toxin b subunit | CTB | Chicken Rabbit | 1:10000 1:10000 | Abcam Sigma | AB19106 C3062 |
| Choline acetyltransferase | ChAT | Goat | 1:500 | Chemicon | AB144 |
| Parvalbumin | Parv | Mouse | 1:2500 | Swant | PV235 |
| Calbindin-D28K | Calbindin | Mouse | 1:1000 | Swant | CB300 |
| Neurokinin-1 Receptor | NKR1 | Guinea pig | 1:500 | Biomol | NA 4200 |

**Table 2.2: Secondary antibodies used to visualize the primary antigens**

| Secondary antibody | Raised in | Antigen | Concentration | Source |
|---|---|---|---|---|
| Alexa Fluor 488 | Donkey | Mouse | 1:1000 | Invitrogen |
| Alexa Fluor 488 | Donkey | Goat | 1:1000 | Invitrogen |
| Alexa Fluor 488 | Donkey | Guinea Pig | 1:1000 | Invitrogen |
| Alexa Fluor 488 | Nil | Nil | 1:1000 | Invitrogen |
| Alexa Fluor 555 | Donkey | Rabbit | 1:1000 | Invitrogen |
| Alexa Fluor 555 | Donkey | Chicken | 1:1000 | Invitrogen |

**Fluorescence Microscopy**

Images were visualized with an epifluorescence microscope (Eclipse E600; Nikon, UK). Sections with staining were marked for later image processing with a confocal microscope. Images for double staining were captured by Zeiss LSM 880 with AiryScan. To see the projection of the nerve terminals, Tile Scan and Z stacks processes were chosen under x20 magnification. Any close apposition between CTB staining and potential contact cells was then

scanned under higher magnification with x40 and x63 oil immersion Plan-neofluar lenses. The images were captured with ZEN Digital Imaging for Light Microscopy Black Edition. The analysis of the figures was done with ZEN Digital Imaging for Light Microscopy Blue Edition. Z stacks images were compressed and maximum intensity projection of the nerve terminations were visualized. These images were exported in TIFF format and final image editing (eg: labelling) was processed with CorelDRAW® software (X8 Edition).

**Anatomical location of termination**

The localisation of the neuronal tracer terminations were examined and clarified in reference to the Allen Brain Atlas (http://www.brain-map.org).

## 2.2 Physiological Study using Working Heart Brainstem Preparation

### 2.2.1 Introduction

The physiological effects of ear stimulation were studied in the Working Heart Brainstem Preparation (WHBP). To the best of my knowledge, this is the first study that ever performed ear stimulation in the WHBP. This is an ideal method in determining the central mechanism of the cardiovascular autonomic response to the stimulation since it allows direct nerve recording and isolation of nerve pathways (eg:vagotomy), all without the use of anaesthetic agents.

**History of Development of the Working Heart Brainstem Preparation**

An *in vitro* brain stem spinal cord preparation was developed by Suzue where the isolated brain stem and the spinal cord of the neonatal rat was placed in a bath and superfused with a modified Krebs solution (Suzue, 1984). Viability for up to 7 hours was suggested by the presence of periodic discharges from respiratory nerves corresponding to a respiratory rhythm. Compared to *in vivo* models, this preparation provided easy access to the extracellular environment and also exhibited smaller movement artefacts. These properties facilitated pharmacological studies on functionally intact respiratory neurons and networks (Smith *et al.*, 1991; Dong *et al.*, 1996; Mellen *et al.*, 2003) as well as circuitry controlling sympathetic preganglionic neurons (Deuchars *et al.*, 1995b; Deuchars *et al.*, 1997) and dorsal column nuclei neurons (Deuchars *et al.*, 2000). However, from a respiratory function perspective, the respiratory rhythmogenesis in this *in vitro* preparation is now considered to be less reflective of the adult scenario, limiting its benefits (Johnson *et al.*, 2012). In addition, another limitation was that it instead of being arterially perfused,

these *in vitro* preparations were commonly superfused, thus causing heterogeneity in the $PO_2$, $K^+$, and $H^+$ gradients within the tissue (Brockhaus *et al.*, 1993; Okada *et al.*, 1993). Inadequate oxygenation of the brainstem raised a question if the medullary breathing circuitry was functioning normally (Richter, 2003; St-John & Paton, 2003). This claim was supported by an earlier report that the breathing pattern from the *in vitro* preparation was markedly different from eupnoea, but instead was identical with gasping (Wang *et al.*, 1996). Thus, a better preparation was required.

Some of the technical limitations of the reduced brainstem-spinal cord preparation were circumvented by Hayashi et al in 1991 through an arterially perfused *in situ* rat brainstem–spinal cord preparation (Hayashi *et al.*, 1991).This preparation was characterized by its eupneic-like phrenic nerve activity suggesting adequate oxygenation of the brainstem. Hayashi claimed a rhythmic activity of the phrenic nerve recorded from his *in situ* model could be maintained up to 11 hours, longer than any reduced brainstem preparation. However, limited numbers of studies employed this technique in investigating the medullary respiratory rhythm generator in rats (Hayashi & Lipski, 1992). The fact that the whole heart was removed due to continuous artefact produced by the heartbeat activity during intracellular recording required a better *in situ* model with preserved cardiorespiratory coupling.

A working heart brainstem preparation (WHBP) was introduced by Julian Paton to study the underlying mechanisms of medullary cardiovascular and respiratory modulation in an *in vitro* milieu (Paton, 1996a, b). The central autonomic motor output was shown to be present in the preparation as blockade of parasympathetic muscarinic receptors by atropine application caused an elevation in HR while sympathetic blockade with propranolol produced a bradycardia (Paton, 1996b). A strong cardiac vagal modulation was also evident in the WHBP as central respiratory activity displayed an abrupt and pronounced bradycardia concomitant with the respiratory phases (respiratory sinus arrhythmia) which was attenuated by bilateral vagotomy.

The WHBP also preserves integrity of the peripheral synaptic input into the autonomic central circuits such as the NTS in response to various

stimulations. This preserved coupling enabled WHBP as a scientific tool to study medullary cardio-respiratory neuron interactions with various afferent inputs (Potts *et al.*, 2000; Smith *et al.*, 2001; Braga *et al.*, 2007). Activation of nociceptors, baroreceptors or chemoreceptors immediately caused cardiovascular and respiratory responses which could be abolished by pharmacological NTS blockade (Paton & Butcher, 1998; Potts *et al.*, 2000; Boscan *et al.*, 2001; Smith *et al.*, 2001). For example, peripheral chemoreceptor reflex with sodium cyanide increased breathing frequency while baroreceptor vagal reflex activation decreased the breathing frequency in mice and musk shrews (Paton & Butcher, 1998; Smith *et al.*, 2001). The central coupling between the central respiratory drive and cardiac motor neurons seems well preserved since each reflex pattern in the WHBP was qualitatively identical to the urethane anesthetised *in vivo* mice (Paton & Butcher, 1998). Hence the synaptic interactions and the central medullary tonic responses from peripheral cardio-respiratory receptors can be studied in the WHBP due to its preserved neuronal network (Potts *et al.*, 2000).

Since the WHBP is skinned and perfusion means that muscles can be removed without bleeding compromising the preparation, there is easy access to various autonomic and peripheral nerve bundles. Such easy access allows direct extracellular nerve recordings to be made by using simple suction electrodes. Numerous extracellular recordings that have been recorded from the WHBP are phrenic (Paton, 1996a, b; Pickering *et al.*, 2002), sympathetic (Zoccal *et al.*, 2008; Lall *et al.*, 2012), hypoglossal (Edwards *et al.*, 2015) and vagus (Paton, 1996b). Cardiovascular variables such as aortic pressure (in this case perfusion pressure) and ECG can also be derived and analysed. Over the years, the utilization of WHBP in the laboratory has been rapidly advanced where it is now commonly used in studying the peripheral and central control of the autonomic nervous system.

**Identifying eupnoea in the WHBP is a key indicator of preparation viability**

A key advance of the WHBP over previous *in situ* preparations is the generation of a breathing pattern that closely resembles eupneic, normal breathing. The maintenance of the eupneic motor generation is vital to WHBP preparation as the non-eupneic breathing is an indicator of inadequate ventilation and thus poor viability of the preparation (Paton, 1996b).

Respiration is a fundamental physiological process in mammals that involves oxygen inhalation and carbon dioxide exhalation from the lungs to sustain cellular metabolism by providing enough energy. These two respiratory processes are controlled by specific groups of muscles including the diaphragm and intercostal muscles. The muscle activity is coordinated by three rhythmically active motor neural phases which is commonly monitored by extracellular recording of nerves containing axons of rhythmically active motor neurons (Smith & Feldman, 1987). Clear visualization can be obtained through recordings of activity of the phrenic nerve which innervates the diaphragm. In such recordings, inspiration is seen as a ramp like augmentation of discharge (I), post-inspiration (PI) – a ramp rapid decline, followed by expiration (E) as a silent phase **(Figure 2.2)** (Richter, 1982). The presence of all three breathing phases is the main characteristic for eupneic breathing at rest (St John & Bartlett, 1985; St-John & Paton, 2003).
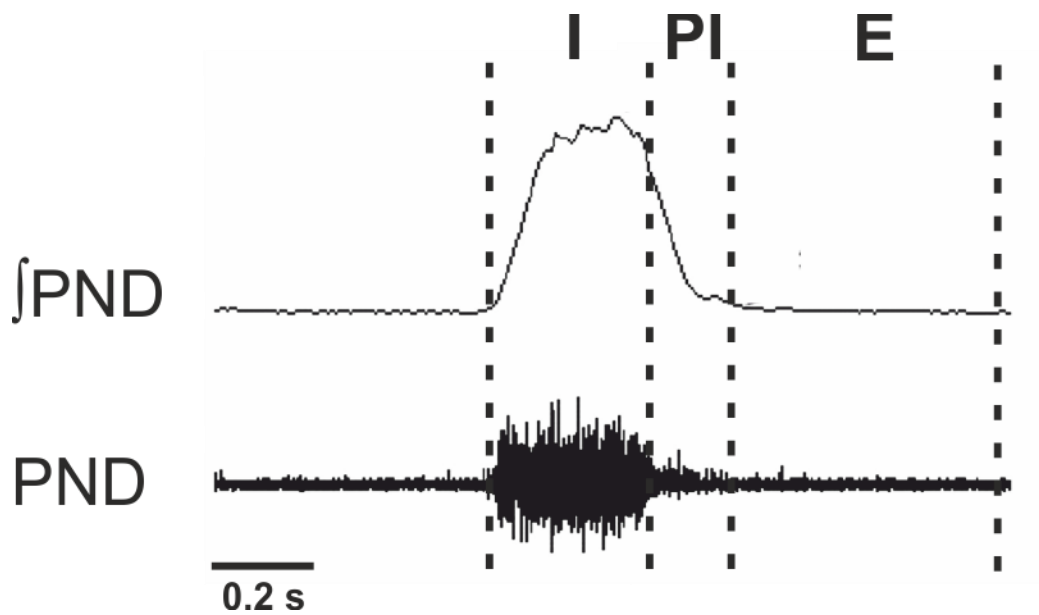
**Figure 2.2: The example of oscillatory breathing phases in raw and integrated phrenic nerve activity recorded from a WHBP rat**

The 3 phases of respiration begin with I phase, ramp-like augmentation; quickly followed by PI phase- rapid decline from I, and E- silent phase. The integrated phrenic nerve activity is shown at the bottom. I- inspiratory, PI- post inspiratory, E- expiratory. Diagram adapted from St-John and Leiter (2003).

Each phase has its own physiological importance in allowing the respiratory muscles to work to alternately fill the lungs with air and empty them. In eupnea, the diaphragm and external intercostal muscles contract during the inspiratory phase, causing enlargement of the thoracic cavity volume which drives atmospheric air into the lungs. Negative pressure generated by the inspiratory muscles contraction however, needs to be preceded by dilating the upper airway muscles to maintain open airspace for effective breathing to prevent the risk of obstructive apnoea (Bianchi & Gestreau, 2009). The glossopharyngeal nerve that is responsible for pharyngeal dilatation is activated during inspiration; while the pharyngeal branch of the vagus nerve that is responsible for pharyngeal constriction is triggered in expiration. The abdominal muscles and internal intercostal muscles are activated during late expiratory phase to drive the carbon dioxide out of the lungs. During resting

59

breathing however these muscles tend to remain silent thus no discharge is observed from these motor outputs **(Figure 2.3)** (Bianchi & Gestreau, 2009).
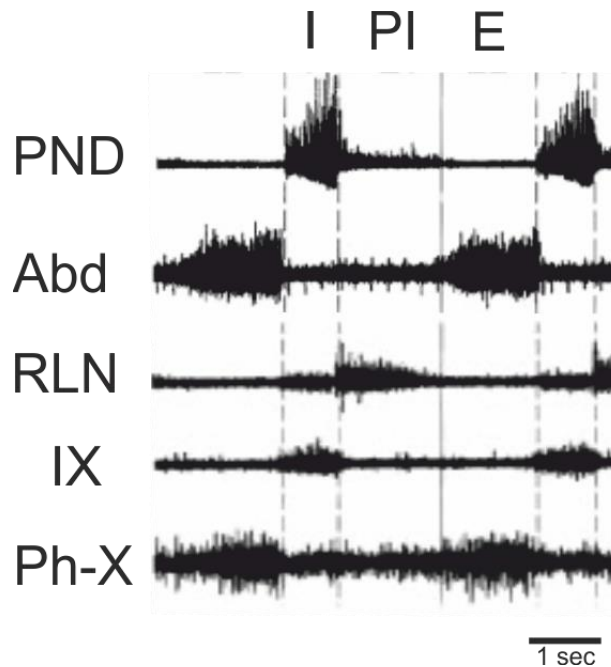


**Figure 2.3: The example of oscillatory motor nerve pattern during respiration of a cat**

The respiratory motor nerves are involved in: creating air aspiration and air expulsion (pump muscles), or regulating air flow (valve muscles). The coordination of discharge from cranial outputs and spinal respiratory inputs assist in creating an effective breathing activity. PND- phrenic nerve discharge, Abd- Abdominal (L1 Lumbar nerve branch), RLN- recurrent laryngeal nerve, SLN- superior laryngeal nerve, VII- facial nerve, IX- glossopharyngeal nerve, Ph-X; pharyngeal branch of the vagus. Figure adapted from Bianchi and Gestreau (2009).

**Identifying gasping**

Unlike eupnea, gasping is a resuscitative mechanism due to accumulation of cellular carbonic acid to initiate breathing following a period of apnoea (Lumsden, 1923). It is characterized by slowing of respiration with increased depth and prolongation of inspiration. Induced gasping in decerebrated cats

showed a significant higher peak in integrated phrenic activity than that of eupnea (St John & Knuth, 1981). This is accompanied by an increase in total ($T_{TOT}$) and expiratory period ($T_E$), shorter inspiratory period ($T_I$) and lower mean arterial pressure **(Figure 2.4)**. The need to identify differences between eupneic and gasping is vital in order to study the physiology of the breathing and ultimately determining viability of the preparation.

Gasping and eupnea in rat WHBP has been documented indicating its fully functioning respiratory circuit similar to *in vivo* mammals (John & Paton, 2000; St-John & Paton, 2002). It is common to observe a classical "gasping" activity quickly after reperfusion. The hypoxic state in the WHBP began once the animal was deeply anaesthetized with isoflurane and time taken for dissection, nerve isolation and cannulation of the descending aorta which would take 5 minutes altogether. The ventilatory pattern between gasping and eupnea is remarkably distinctive. In eupnea, the phrenic nerve discharge reaches its peak close to the end of the burst, but in gasping its peak is close to the beginning of the burst. In other words, this gasping inspiratory activity is identified by its extremely rapid rise of phrenic nerve burst followed by a rapid cut off. Thus instead of incrementing inspiratory activity in eupnea, the gasping is fundamentally decrementing (John & Paton, 2000). Prolonged gasping activity in the WHBP may become pathological. Since the source of oxygen in the preparation comes solely from the Ringer's solution, the pump fed into the preparation was carefully increased so that more oxygenated perfusate will be supplied into the respiratory networks in the brainstem. Once the initial decrementing phrenic burst transformed into augmenting bursts, the preparation was left for at least 20 minutes for the strong eupneic pattern to settle in before any other experiments were undertaken.
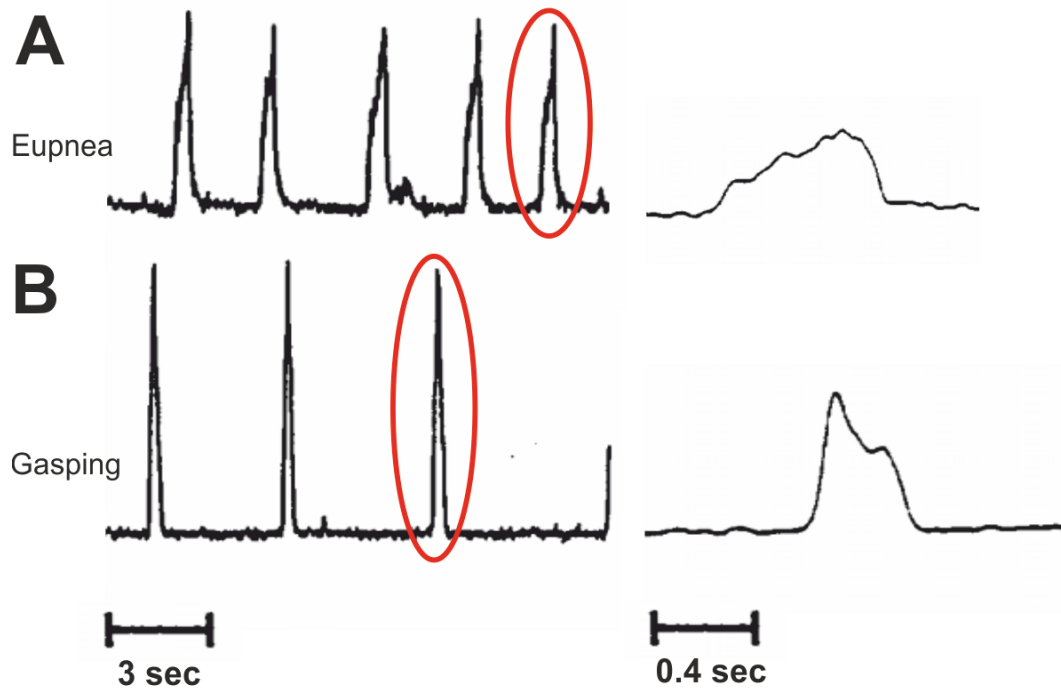
**Figure 2.4: Integrated activities of phrenic nerve in eupnea (A) and gasping (B) of adult rat in the Working Heart Brainstem Preparation**

A) The phrenic nerve activity in the eupneic preparation is identified by a regular breathing frequency with an incrementing nerve discharge. B) Gasping is identified by irregular breathing frequency where there is an increase in the expiratory period and decrease in inspiratory duration. Note that phrenic nerve activity has a decrementing pattern of the phrenic discharge which is the hallmark of gasping. Source of image: John and Paton (2000).

## 2.2.2 Materials and methods

Animals were obtained internally from the Central Biomedical Services, University of Leeds, United Kingdom. All experiments were performed under UK Home Office License and in accordance with the regulations of the UK animals (Scientific Procedures) Act, 1986. Efforts were made to adhere with the 3R's principle: Replacement, Reduction and Refinement.

### Surgical procedures

Pre weaned rats ranging between 18 – 21 days of either sex were deeply anaesthetized through 4% isoflurane (Abbott, UK) inhalation. The depth of anaesthesia was tested by a pinch paw test. Once animals ceased to respond to the noxious pinch of the tail or hind paw they were bisected sub diaphragmatically. The rostral half (head, forelimbs and thorax) was submerged immediately in ice-cold Ringer's solution to slow down the cellular metabolism, bubbled with 95% $O_2$ – 5% $CO_2$ gas mixture in an effort to preserve the viability. Animals were decerebrated at pre-collicular level, and skinned while keeping the body submerged in the ice-cold water. The frontal portion of the thorax was removed exposing chest cavity internal organs. The lungs were removed to prevent inflation due to breathing activity during the preparation. The descending aorta was isolated from the front of vertebral column, extending from the thoracic aorta into the abdominal aorta just below the diaphragm. The phrenic nerve was cut distally to leave sufficient length for placement of a suction electrode to monitor the viability of the preparation. The lumbar sympathetic chain was identified as a chain of ganglia lying in a vertical row on both sides of the spinal cord and a distal cut was made at the inferior mesenteric ganglia that gives rise to renal sympathetic innervation. The preparation was moved to the recording chamber where the descending aorta was cut caudally and cleaned of any excess fat that could cause blockage. The aorta was then cannulated by pulling the cut end of the aorta over the cannula to allow retrograde perfusion to be initiated using a roller

pump at a constant flowrate (15-21 ml/min) (Watson-Marlow, 520Du) (**Figure 2.5**). These procedures took approximately 10 minutes before perfusion was initiated.

## Additional procedures

Additional considerations were included in the preparation to maximize preparation viability. Constant perfusion pressure (pp) recording allowed a suitable perfusate inflow and therefore allowed the brainstem to be physiologically stable. Previous literature indicated that the pp recorded in pre-weaned rats ranged between 50 and 75 mmHg, consistent with our observation (Potts *et al.*, 2000; Lall *et al.*, 2012). This was achieved by titrated vasopressin (final concentration 200-400 pM, Abcam, Cambridge, UK) directly into the perfusate within 5 minutes of cannulation of the aorta. Aortic pp was measured by a MEMSCAP SP844 physiological sensor that measured the intravascular pressure of a double lumen catheter. Perfusate temperature as measured from the outflow of the cannula was recorded and maintained at $31^0C$ using a heat exchanger.

Any possible blockage in the capillary beds by fungal hyphae, blood clots and cellular debris, was avoided by utilising a propylene screen filter (Millipore, pore size: 0.45 µm) in the perfusion circuit. Air bubbles in the perfusion circuit were trapped to prevent air embolism. In addition, the presence of the bubble trap also dampened the roller pump and cardiac pulse pressure waves superimposing on the perfusion pressure recording.

It is important to have a suitable oncotic pressure in providing sufficient oxygen to the brainstem (Paton, 1996b). Thus the carbogenated Ringer's solution (95% $O_2$ and 5% $CO_2$) was modified with an oncotic agent, Poly(ethylene glycol) BioUltra 20 000 (Sigma Aldrich), to prevent oedema. The oncotic agent added was 2.5 mg for each 200 ml perfusate.

To maintain a constant homeostatic temperature and prevent the loss of washed-out essential amino acids, the perfusate was recycled after reoxygenation.
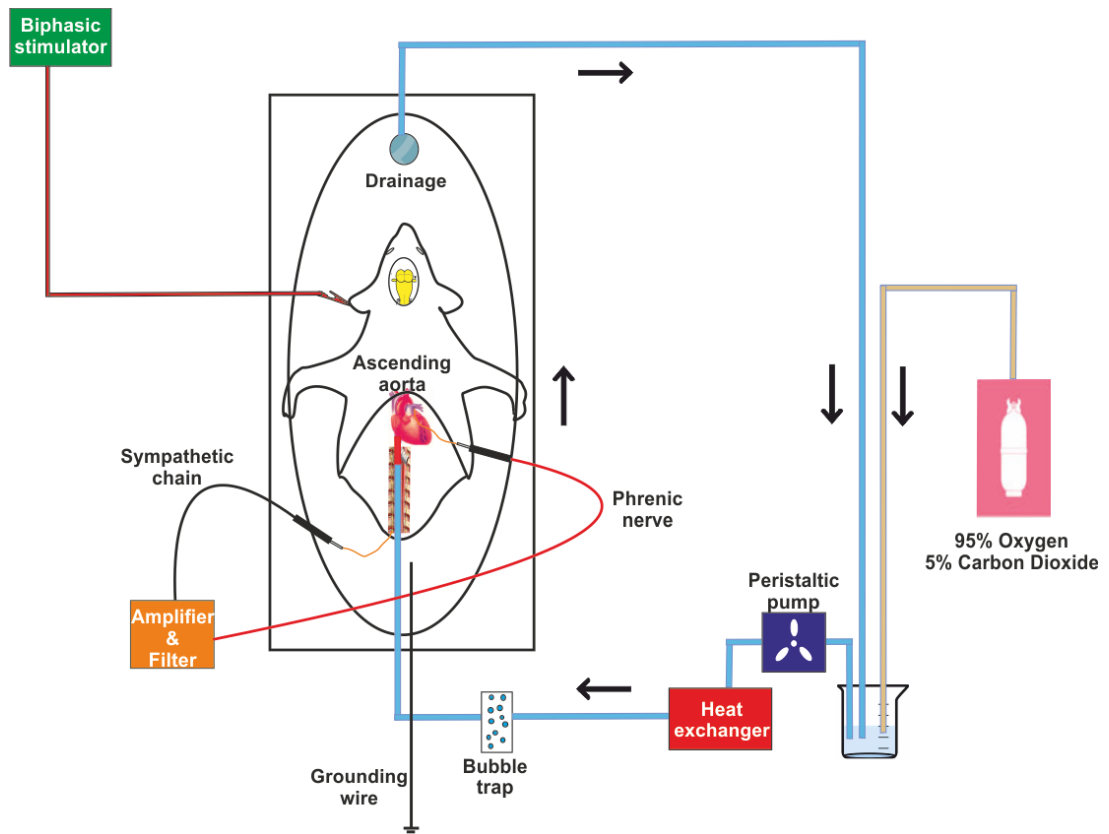


**Figure 2.5: Representation of the ear stimulation in a working heart brainstem preparation experimental set up**

The decerebrated animals were placed in the recording chamber. The descending aorta was cannulated with a double lumen catheter that perfused with modified Ringer's solution containing 95% $O_2$ and 5% $CO_2$ mixture. The perfusate was drawn from the reservoir by a peristaltic pump and fed into a heat exchanger, bubble trap and filtered to remove cellular debris. The perfusate was recycled to prevent from any proteins or nutrient loss. The ear stimulation was achieved with a biphasic stimulator delivered via a metal clip. An autonomic effect of the stimulation was measured from the ECG tracer and respiratory activity taken from the phrenic nerve, sympathetic nerve discharge from the lower thoracic sympathetic chain was also measured.

**Modified Ringer's Solutions**

The Ringer's solution contained in mM: NaCl, 125; NaHCO$_3$, 25; KCl, 4; CaCl$_2$.2H$_2$O, 2.5; MgSO$_4$, 1.25; KH$_2$PO$_4$ 1.25 and D-Glucose, 10. A high molecular weight oncotic agent, Polyethylene glycol was added to the perfusate (Paton, 1996b). Vecuronium bromide (2-4 µg/ml, Organon Teknica, Cambridge, UK) was added during initial stages of the preparations to block neuromuscular transmission (Potts *et al.*, 2000).

**Tuning in the prep**

The intra-arterial perfusion in the WHBP allows generation of robust respiratory bursts that are comparable to *in vivo* conditions (Paton, 1996b). To achieve this physiological respiratory activity the perfusion rate needs to be correctly "tuned" without over perfusion. The pump flow was finely adjusted in order to supply sufficient oxygen in restoring the brain stem function to control cardiorespiratory responses to produce a eupneic motor pattern, and has a core that is neither hypoxic nor anoxic. Ideally, eupnic respiratory motor pattern was targeted from the phrenic nerve discharge (PND) recording where a "ramp-like rise" followed by a rapid cut off indicates an inspiration phase. As shown from previous studies, breathing frequency targeted in all preparations ranged from 16-40 phrenic bursts per minute (Potts *et al.*, 2000; Baekey *et al.*, 2008; Dutschmann *et al.*, 2009). When tuning the preparation, over perfusion needed to be avoided as it will minimize the brainstem neuronal CO$_2$ content. Removing CO$_2$ from WHBP perfusate without changing its arterial pH reduced the respiratory activity, indicating that PCO$_2$ is a necessary chemostimulant for eupnogenesis (Wilson *et al.*, 2001). Thus, respiratory activity requires the presence of CO$_2$ and will be silent without it (Phillipson *et al.*, 1981). Commonly, poor perfusion would be characterised by augmented or "gasp" rather than eupneic breathing as CO$_2$ is cleared to which the drive to breathe

66

is eliminated. Upon reaching the eupnic breathing state, the constant perfusion pump rate attained a range between 20- 25 ml/min.

## 2.2.3 Defining Variables

**Cardiovascular variables**

Mean Heart rate (HR), perfusion pressure (PP) and respiratory sinus arrhythmia (RSA) are the indirect measures of sympathovagal balance in the WHBP.

Average perfusion pressure recorded from distal end of the common artery in the WHBP ranged between 50 – 80 mm Hg.

Cardiac activity returned seconds after reperfusion with electrocardiogram (ECG) traces from the beating heart and picked up by the phrenic nerve recording electrode. The ECG displayed a complete P wave and also QRS. The heart rate was derived offline by measuring the frequency of R peaks within one minute. A stable cardiac rate (after 30 minutes of initial reperfusion), normally ranged around 300 bpm.

The cardiac rate was often modulated by central respiratory activity (e.g. respiratory sinus arrythmia) where a bradycardia was observed at the end of inspiratory phrenic neurogram. Thus, RSA for the WHBP was obtained by deducting the highest peak to the lowest through of the HR signal that was in synchrony to the inspiration. The typical RSA recording in rats would be 15 bpm (Potts *et al.*, 2000), although, the RSA activity may absent in some preparations (Paton, 1996b).

**Phrenic nerve discharge**

The phrenic nerve is the main motor supply of the diaphragm to produce diaphragmatic contractions. The phrenic nerve discharge indicates activity in the rhythmic respiratory cycle where its bursting activity reflect the corresponding respiratory brainstem network. The duration of the phrenic nerve discharges varied between 500-700 ms while the bursting rate was between 25-36 bursts/min (Potts *et al.*, 2000).

**Sympathetic Nerve Discharge**

Central sympathetic nerve discharge (SND) was recorded from the sympathetic chain at the lower thoracic level using a second glass suction electrode. The sympathetic chain discharge was synchronized with respiratory activity. The discharge of the sympathetic nerve was always in accordance to the burst of the phrenic nerve, but this is however not necessarily occurring in 1:1 phase relations (Barman & Gebber, 1976). There are three types of distinct relationship between the SND (recorded from external carotid postganglionic sympathetic nerve) and PND as observed in vagotomised cats **(Table 2.3)**.

**Table 2.3: The three types of relationship between Phrenic Nerve Discharge (PND) and Sympathetic Nerve Discharge (SND) in vagotomised cats identified by Barman and Gebber (1976)**

| Relationship | Nerve Discharge | Characteristic |
|---|---|---|
| Expiratory - Inspiratory | PND / SND | increase from a minimum in early expiration and reached a maximum during inspiration |
| Inspiratory | PND / SND | increase at the start of inspiration, maximal near peak inspiration, decayed with PND |
| Inspiratory- Expiratory | PND / SND | increase after the start of inspiration and reached maximum in early expiration |
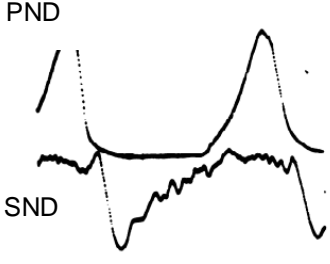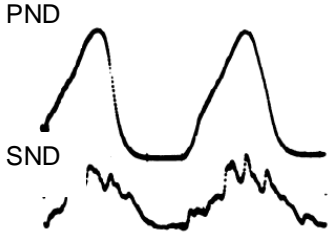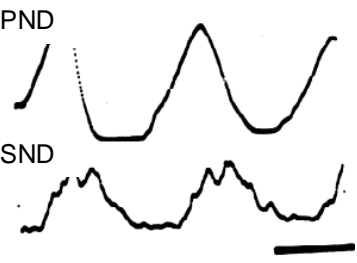
Paton et al has noted the possibility of artefacts due to the breathing movement in their SND. This was prevented by adding small amount of a muscle blocker (eg.vecuronium bromide) into the perfusate.

**Variable recordings**

Each respective nerve was attached to a glass suction electrode (borosilicate glass capillaries; World Precision Instruments, 1B150-4, outside diameter 1.50 mm, inside diameter 0.84 mm, length 10 cm) and connected to a head stage (Digitimer, NL 100) to be fed into a Neurolog amplifier (x 1000 amplification; Digitimer, NL 900D). Contaminated electrophysiological signals with 50/60 Hz noise and harmonics originating from power mains, power supplies and lighting were automatically eliminated by Humbug (Quest Scientific, Canada). The signals were also bandpass filtered between 50Hz and 4kHz and further digitised with a sampling frequency of 8 kHz and saved on computer using an interface (CED 1401, Cambridge Electronic Design, UK) for analysis on Spike 2 software offline.

# Chapter 3 Circadian variation of autonomic profiles in the working heart brainstem preparation

## 3.1 Introduction

### 3.1.1 Circadian Rhythm

Human physiological activity exhibits a dynamic oscillation pattern between the day and night and also the sleep-awake cycle. This 24 hours physiological variation is also known as the circadian cycle, originating from Latin *"circa"* around and *"diem"* one day. It is possible that this temporal pattern is part of the adaptation to sleep at night and wake in daytime. Our physiology during the day is governed for catabolic processes to facilitate with engaging the world. However, during the night our body is prepared for anabolic functions of growth, repair, consolidation and resetting for the next day (Panda, 2016). This cycle has important influences not only on cardiovascular activity but also hormonal release, metabolism, body temperature and other bodily functions. The work in this chapter will therefore examine if there are changes in cardiovascular, respiratory and autonomic variables in the WHBP with time of day which may influence future experiments.

### 3.1.2 SCN as the central clock of circadian rhythm is influenced with light

The diurnal rhythm of physiological functions are generated by an endogenous oscillator originating from the suprachiasmatic nucleus (SCN). The SCN acts as a central clock, consisting of multiple, autonomous, self-sustaining, oscillatory cells which are linked to produce co-ordinated, in-phase circadian signals (Zampieri *et al.*, 2014). These master oscillatory cells consist of interlocking gene activation-inactivation feedback loops; synthesising essential proteins overt physiological changes. Identified genes with circadian property in mammals are including circadian locomotor output cycles kaput

(*clock*), brain and muscle ARNT like protein 1 (*bmal*) and also period (*per*). The products generated from these genes oscillate over approximately 24 hours entrained over light/dark phase. Thus light is a primary environmental 'zeitgeber' or time giver on the circadian master clock in the SCN. The optic inputs detected from retinal photoreceptors are fed into the SCN through the retinohypothalamic tract. Initial tract tracing studies in rats with tritiated leucine or proline injection into the posterior chamber of the eye labelled the hypothalamic SCN bilaterally (Moore & Lenn, 1972). Earlier evidence on the SCN as central clocks include electrophysiological recording on the SCN of rat brain slices. These recordings revealed an endogenous circadian rhythmicity in the SCN, with unit discharge rates achieved the maximum activity during the day and reversed during the night (Shibata *et al.*, 1982).

### 3.1.3 PVN as a relay site for SCN mediated circadian influences on sympathetic nerve output

The SCN as a master circadian pacemaker plays a critical role in facilitating light entrained autonomic nervous system oscillation. Anatomical evidence from rats suggests the circadian rhythm information from the SCN is passed into hypothalamic paraventricular nucleus (PVN), (Buijs *et al.*, 1993; Teclemariam-Mesbah *et al.*, 1997) an important integrative site to influence the autonomic nervous system. Parallel to the SCN, the PVN also exhibited rhythmic expression of circadian genes (e.g. *per1*) where it reaches a peak in the late night in nocturnal laboratory rats. The *per* protein expression in the PVN is 180º out of phase in the reverse cycle rats, highlighting the light entrained rhythmicity of the nucleus similar to the SCN (Martin-Fairey *et al.*, 2015).

The PVN is located on both sides of the third ventricle of the hypothalamus where it contains larger magnocellular neurons and smaller parvocellular neurons (Badoer, 2000). The magnocellular neuron produced peptide hormones eg: vasopressin and oxytocin, transported to the posterior pituitary

73

where the hormones are released to the bloodstream to control diuresis and lead to blood pressure elevation. The parvocellular neurons on the other hand have additional functions by projecting into autonomic controlled regions such as the IML. Combination of retrograde tracer CTB into sympathetic cervical ganglion of rats with anterograde tracer Phaseolus vulgaris-luecoagglutinin (PHA-L) into the PVN revealed high PVN-fibre density on SPNs in the IML (Hosoya *et al.*, 1991). Similar tracing technique where CTB injected into the IML and PHA-L into the SCN shown the highest population of closely apposed labelled fibres and cell bodies is within the PVN (Vrang *et al.*, 1997). Taken together, these evidence suggesting circadian descending pathway originates from the SCN influences the sympathetic preganglionic neurons in the IML. This descending circadian pathway is mediated through inputs into the PVN. As such, short light exposure during dark phase rapidly elevates cFos expression in the arginine vasopressin neurons of SCN and the PVN (Santoso *et al.*, 2017). The vasopressinergic input from the PVN will then be directed onto the sympathetic preganglionic neurons where the sympathetic tone is discharged (Motawei *et al.*, 1999). The presence of these pathways therefore suggests that autonomic activity can be influenced by the circadian rhythm.

## 3.1.4 Diurnal activity of autonomic control in humans is manifested by sympathetic predominance in the morning and sympathetic withdrawal at night.

The sympathetic nervous system plays a critical role in generating the circadian rhythm in blood pressure (BP) control. The plasma adrenergic transmitter level is higher in humans during the day-time, with notable peaking observed in early morning (Grassi, 2009). In healthy individuals an enhanced morning surge in BP is commonly reported during the first 2-3 hours after waking from nocturnal sleep (Brotman *et al.*, 2008). Earlier evidence studying circadian vascular tone, using strain gauge plethysmography to measure

forearm vascular blood flow variation, revealed highest resistance and lowest flow during morning and *vice versa* during the night (Panza *et al.*, 1991). The circadian differences in blood flow and resistance were eliminated following phentolamine injection, suggesting α-receptor sympathetic-mediated vasoconstriction is a major determinant in the normally occurring circadian variation in arterial tone. Direct demonstration of sympathetic neural involvement in humans was obtained from microneurography, which revealed increases in muscle sympathetic nerve activity (MSNA) accompanying the morning BP surge (Narkiewicz *et al.*, 2002; Lambert *et al.*, 2014). The power of morning BP surges in healthy adults was found to be positively associated with MSNA during a cold pressor test, highlighting the sympathetic influence in determining the rate of BP rise during the morning period (Lambert *et al.*, 2014). Further trials on healthy participants also showed a strong correlation between the magnitude of morning BP surge with MSNA but not cardiac baroreflex sensitivity, reflecting changes in sympathetic tone rather than vagal reflexes in determining the morning BP surge (Johnson *et al.*, 2016).

In contrast, the autonomic control at night is associated with increased parasympathetic dominance over sympathetic. This was shown from early trials on healthy adults where the plasma epinephrine level dropped remarkably during the nocturnal sleep suggesting a sympathoadrenal latent phase at night (Dodt *et al.*, 1997). Malpas and Purdie analysed the circadian rhythmicity from HRV in healthy subjects by looking at the mean R-R interval and the standard deviation of the successive differences between R-R intervals (SDSD) for 30-minute periods using 24 hour Holter recordings (Malpas & Purdie, 1990). HRV was elevated during sleep, consistent with vagal predominance. In a different set of subjects that presented with vagal neuropathy (insulin dependent diabetics and alcoholics), the normal heart rate variation was reduced but the amplitude of the cycle and time of peak variability was not different to control. This postulates that the origin of circadian HRV variations was due to sympathetic withdrawal rather than parasympathetic elevation at night. Earlier trials on groups of hospitalized patients with a history of hypertension showed the LF power of the HRV

(associated with sympathetic activity) was significantly reduced meanwhile the HF power (reflecting predominantly parasympathetic activity) was significantly elevated at night, thus suggesting sympathetic withdrawal and elevation of the parasympathetic tone at this period of time (Furlan *et al.*, 1990). An HRV study on children also reported a similar circadian cardiac autonomic variation, characterized by a rise in HRV during sleep (Massin *et al.*, 2000). These studies indicate that sympathetic and parasympathetic influences on the cardiovascular system in humans vary with the time of day.

## 3.1.5 Diurnal activity of autonomic control in rats is manifested by sympathetic predominance in the dark phase.

Unlike humans, rats are known for their nocturnal nature where they are more active during the night. Locomotor activity recorded from revolutions of running wheels revealed rats had greater movements during the dark phase (Stephan & Zucker, 1972). A different study on the temporal pattern of rat locomotor activity recorded from telemetric recordings showed parallel ambulatory variation in mean heart rate and BP (Van Den Buuse, 1994). This suggests rat temporal locomotor variation is also associated with the cardiovascular temporal rhythm. Indeed, the telemetric recording revealed the LF/HF ratio on the light-phase (ie, akin to human night time) tended to be higher than those in the dark phase, suggesting predominant sympathetic nervous activity at night (Hashimoto *et al.*, 1999). The mean levels of plasma adrenaline and noradrenaline also were significantly higher during the nightime when rats are behaviourally active (De Boer & Van der Gugten, 1987). A dissection on rats' pineal gland, which receives rich innervation of sympathetic nerve endings, showed a peak noradrenaline content during the dark period (Wurtman & Axelrod, 1966). It is important to appreciate that these aforementioned studies have successfully showed the nocturnal sympathetic preferential pattern in rats through indirect measures. The direct measurement of the sympathetic activity from the sympathetic chain however requires

further investigation. Since the work in this thesis will examine sympathetic nerve activity, it is important to test for differences in such activity with time of day.

### 3.1.6 Research questions

There is a research gap in the literature examining a direct sympathetic nerve measurement in rats In particular, since this thesis uses the WHBP, it is important to determine if such differences exist in this preparation. The differences in the autonomic profile of the rats during the light and dark phases were therefore examined in the Working Heart Brainstem Preparation.

### 3.1.7 Research aims

- Understand the basic physiological functions in the WHBP
- Compare the autonomic and physiological profiles between different time points of the circadian cycle
- Finding the suitable WHBP model from different circadian cycle to be used in subsequent experiments.

### 3.1.8 Hypothesis

- The night-time rats will have a higher sympathetic nerve discharge in comparison to the day-time animals.
- The elevated sympathetic nerve discharge will be accompanied by differences in other physiological functions such as heart rate, perfusion pressure and also breathing rate.

## 3.2 Methods

The WHBP was prepared as detailed previously in Chapter 2 **(Section 2.2)**. Recordings were taken only after the animals displayed a stable eupnic respiratory activity, normally within 30 minutes after the initial reperfusion. Baseline recordings included HR, PND, SND, and also PP. The ramping pattern of the PND was stable for over than 2 hours, consistent with previous studies conducted in the WHBP of the rat (Potts *et al.*, 2000).

Primarily, animals from 2 different points in the circadian cycle were examined. The first group was the daytime animals (n=10, age 16-21 days) which have been caged in a normal lighting condition (lights on 7 am and off 7 pm). Another group of animals at similar age (n=20) were caged in the reversed lighting cabinet (switched on 7 pm and switched off 7 am). The reversed lighting group were acclimatised in this regime for 7 days before being used in the experiment. During transfer handling, light exposure on the nighttime animals were minimised by using a dark box.

The normality test for numerical datasets were appropriately explored with the Shapiro-Wilk test due to small sample size. The significant value of the normality test greater than 0.05 considered as normal, while below than 0.05 is considered to be deviated from a normal distribution.

To determine if the physiological functions differed between the daytime and nightime groups measured from the WHBP, an independent samples t-test was performed with $p < 0.05$ as the significance level for the normally distributed data. The non-normally distributed data was analysed with non-parametric analysis using 2 independent tests using IBM SPSS Statistics 21.

From all of the experiments performed, animals were later sub-grouped accordingly into their specific time of preparations. The preparations under light phase were done either at 1030 or 1430, while the recordings were conducted at the rat's dark phase equivalent at 2130 or 0230. One-way ANOVA test was used to determine any statistically significant differences

between the experimental stage (eg: 1030, 1430, 2130 and also 0230). Any statistical significant values from the ANOVA test were then confirmed with Fisher's Least Significant Difference (LSD) post hoc test.

## 3.3 Results

### 3.2.1 Baseline recording between day and night

Cardiorespiratory activity was recorded from the WHBP of rats at different times of day **(Figure 3.1)**. The recorded mean PP for the nightime animals (n=18, 61.6 ± 3.6 mmHg) was significantly higher than the daytime animals (n=10, 51.6 ± 2.2 mmHg, p= 0.024). The tonic discharge of the sympathetic chain in thoracic level was also significantly higher at night (n= 17, 4.7± 0.5 AUC) than during the day (n=8, 3.0 ± 0.6, p=0.011). The nightime animals displayed an increased PND frequency (Daytime: n=9, 12.8 ±1.1 RPM; Nightime: n=19 15.7 ± 0.6 RPM, p= 0.037). There was no statistical difference in heart rate between night (n=19, 306.4 ± 5.8 BPM) and day (n=10, 327.5 ± 13.5 BPM). There was also no statistically significant difference between cardiac vagal index measured from the RSA at day (n= 19, 9.5 ± 1.7 BPM) and nightime (n=9, 8.5 ± 1.6 BPM). The statistical summary can be found in **Figure 3.2** with further details on **Table 3.1**.

### 3.2.2 The physiological trend

Further analysis on the circadian profile of the WHBP preparation was later studied by sub-grouping accordingly to the time in which each experiment was performed **(Table 3.2 and Figure 3.3)**. The indicated times of experiments were equivalent to 10:30, 14:30 during the light phase, and 21:30 and 02:30 during the dark phase. The average HR of the rats started with highest point during the light phase at 10:30am (n=4, 333.4 ± 24.4 bpm), and slightly lower at 14:30pm (n= 6, 323.6 ± 17.5 bpm). The HR reached the lowest bpm at 21:30pm (n=11, 302.4 bpm ± 9.5 bpm) and slightly increased later at 02:30 am (n=8, 311.9 ± 4.1 bpm). However, a one-way ANOVA showed no

statistically significant differences in the HR of the preparations between each experimental time ($F_{(3, 25)}$ = 1.086, p = 0.373.

There was a statistically significant difference in PP between groups as determined by one-way ANOVA ($F_{(3, 24)}$ = 3.299, p = 0.038). A LSD post hoc test revealed the PP was significantly higher at 21:30 pm (n= 10, 67.5 ± 4.4 mmHg) compared to the PP at 10:30 am (n=4, 49.9± 3.9, p=0.021), 14:30 pm (n= 6, 52.7 ± 2.7, p=0.026) and 02:30 am (n=8, 54.3 ±4.8, p = 0.030).

The average RSA started low at 10:30 am (n=3, 7.1 ± 2.5 Δbpm), elevated at 14:30 pm (n=6,9.2 ± 1.5 Δbpm) and reached the peak at 21:30 pm (n=11, 10.4 ± 2.7 Δbpm). The RSA then dropped to 8.3 ± 1.8 Δbpm (n=8) at 02:30 pm. However, one-way ANOVA analysis on the RSA showed these are not statistically significant ($F_{(3,24)}$ = 0.265, p = 0.850).

The sympathetic activity recorded from low thoracic sympathetic chain showed a significant upward trend from evening until late nightime preparation. A statistically significant difference between groups are indicated with one-way ANOVA ($F_{(3, 21)}$ = 4.234, p = 0.017). A LSD post hoc test revealed the ∫SND was significantly higher at 02:30 am (n= 7, 5.9 ± 0.9 AUC) in comparison to 14:30 pm (n=4, 2.2 ± 0.5 AUC, p = 0.003) and 21:30 pm (n=10, 3.9 ± 0.3 AUC, p = 0.027). No significant differences were detected in the sympathetic nerve activity between the 10:30am and any other WHBP preparation.

The PND frequency doesn't show much variation between preparations at different times ($F_{(3, 24)}$ = 1.972, p = 0.145). This contrasts to when results from both groups of day time rats were compared with those from both groups of night time rats, where respiratory frequency was increased in rats from night time groups.
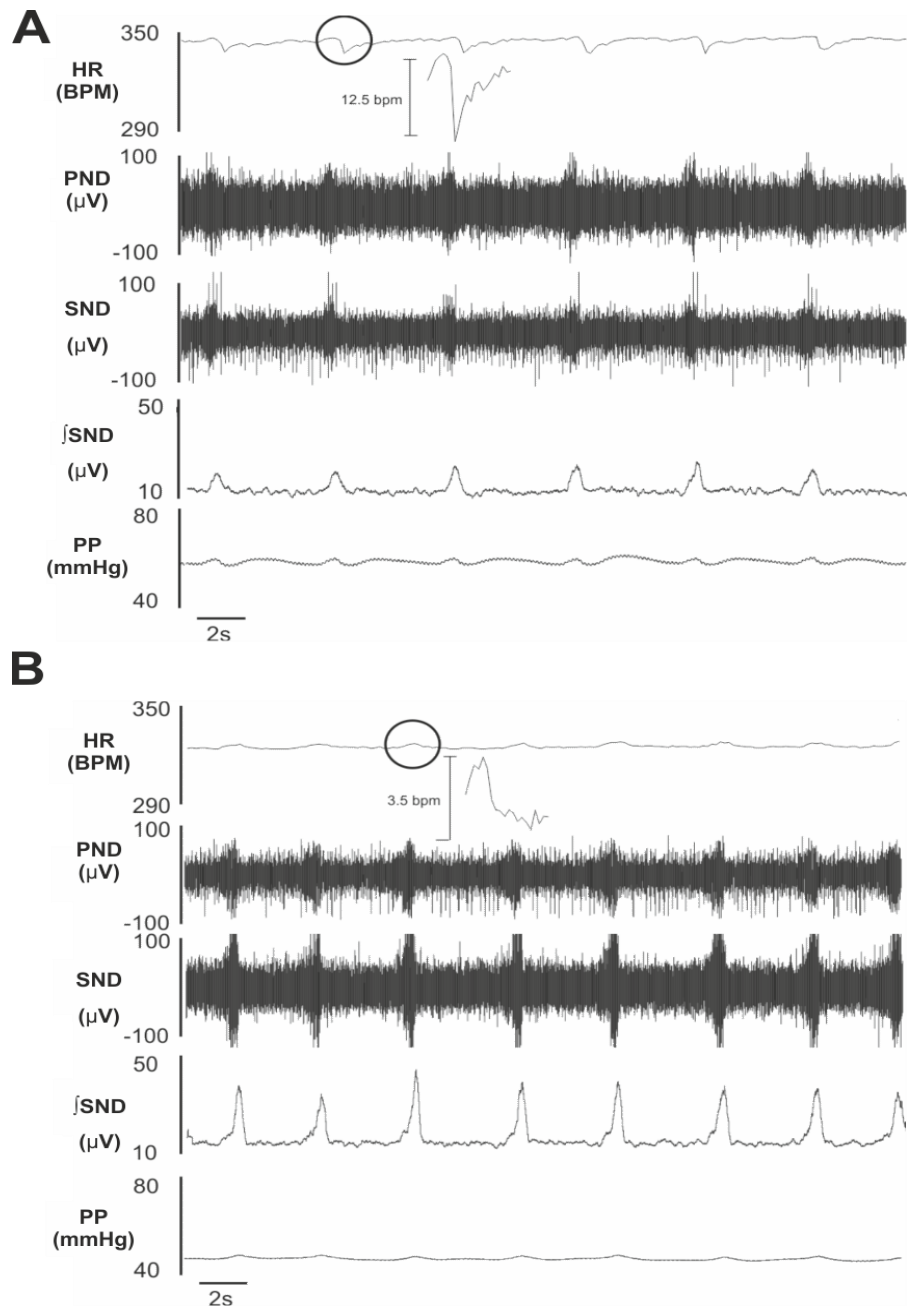
**Figure 3.1 The baseline of cardio respiratory activity recorded in the Working Heart Brainstem Preparation**

Examples of the baseline recording from the different timing of WHBP are shown in (A) daytime and (B) night-time. The RSA is measured from the dipping amplitude of HR (circled) that occurred concurrently with the PND. The sympathetic activities were measured from the area under the curve of the integrated SND. A striking sympathetic tone (SND) and respiratory frequency typically recorded from the nightime preparation. This was inconsistently accompanied by the perfusion pressure and also heart rate.
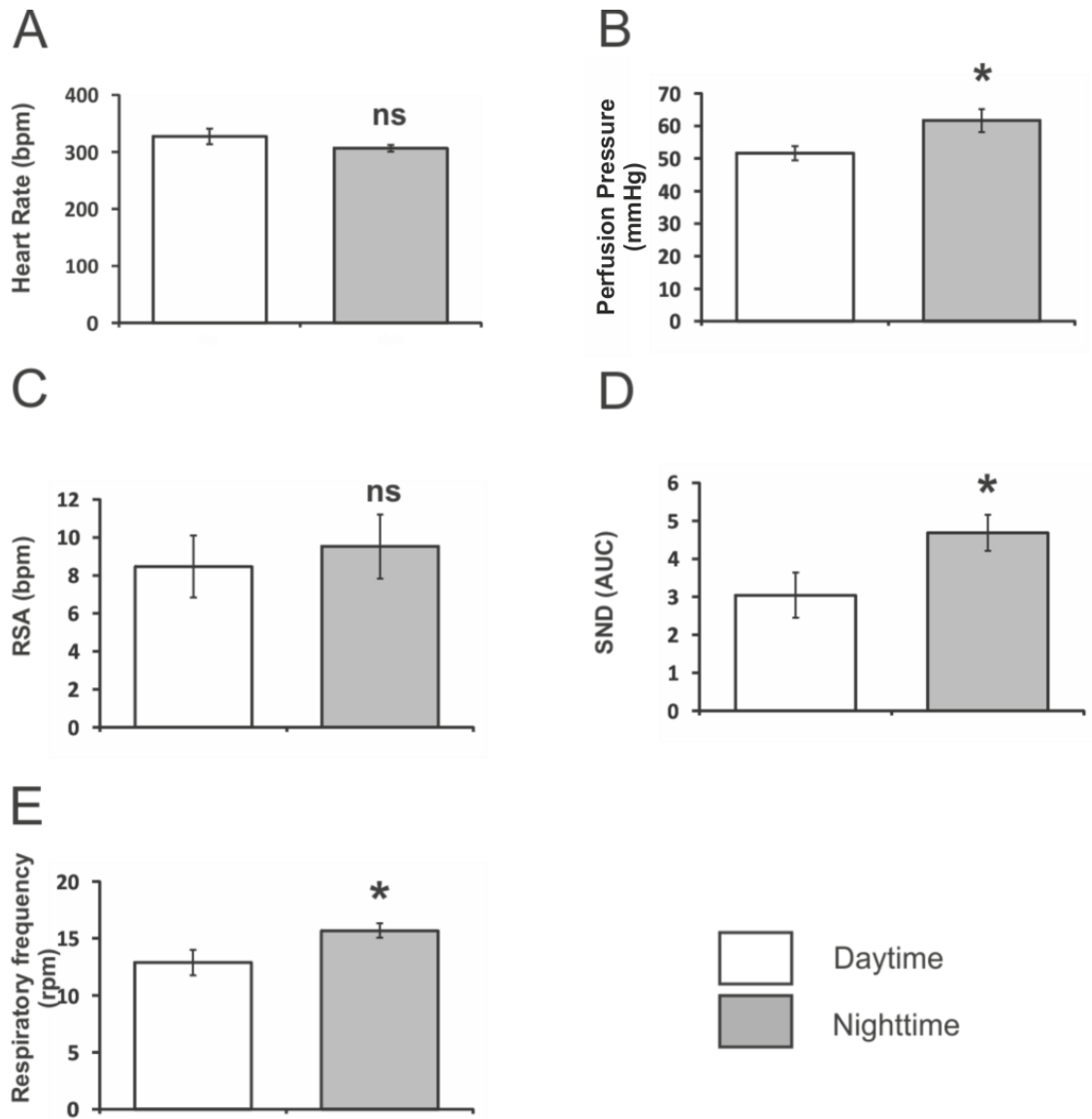
**Figure 3.2: The day-night animals displayed a circadian physiological profile in the WHBP preparation**

The B) perfusion pressure, D) sympathetic nerve activity and E) respiratory frequency in the night time animals were significantly higher than the daytime. Insignificant physiological profiles between groups were observed in the A) heart rate, and C) respiratory sinus arrhythmia. *, $p < 0.05$; **, $p < 0.01$; *** $p, < 0.005$. Statistical details included on Table 4.1 below.

**Table 3.1 The statistical details of physiological profile in different circadian cycle from WHBP preparation**

| | | N | Mean | Std err | Min | Max | *P* value |
|---|---|---|---|---|---|---|---|
| HR (bpm) | Day | 10 | 327.5 | 13.5 | 250.4 | 403.2 | 0.115 |
| | **Night** | 19 | 306.4 | 5.8 | 220.4 | 327.4 | |
| PP (mmHg) | Day | 10 | 51.6 | 2.2 | 38.1 | 59.9 | 0.024 |
| | **Night** | 18 | 61.6 | 3.6 | 37.6 | 91.1 | |
| RSA (Δbpm) | Day | 9 | 8.5 | 1.6 | 1.9 | 16.3 | 0.923 |
| | **Night** | 19 | 9.5 | 1.7 | 2.8 | 29.5 | |
| ∫SND (AUC) | Day | 8 | 3.0 | 0.6 | 1.5 | 7.0 | 0.011 |
| | **Night** | 17 | 4.7 | 0.5 | 2.5 | 9.7 | |
| ƒ PND (rpm) | Day | 9 | 12.8 | 1.1 | 8.0 | 17.0 | 0.037 |
| | **Night** | 19 | 15.7 | 0.6 | 8.0 | 19.0 | |
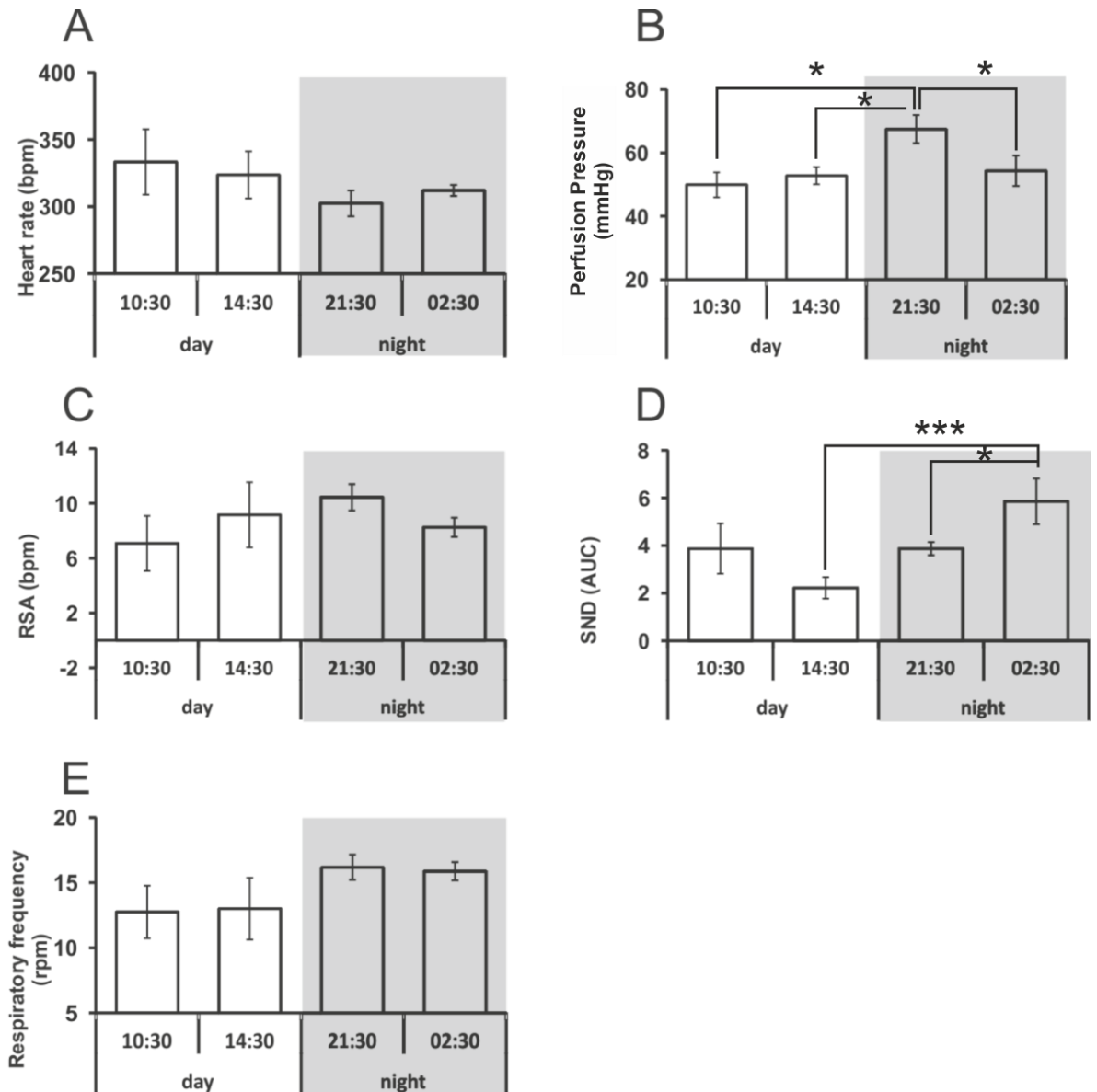
**Figure 3.3: The physiological profiles from the Working Heart Brainstem preparation at the four different recording times**

There are no significant differences at different time points between heart rate (A), RSA (C), respiratory frequency (E). In contrast, perfusion pressure (B) and SND (D) were higher at night. *, $p<0.05$; **, $p<0.01$; *** p, $< 0.005$. Statistical details included on Table 4.2 below.

**Table 3.2: The statistical details of physiological profiles from different timings of the WHBP preparation**

| | | Time | N | Mean | Std err | Min | Max | *P* value |
|---|---|---|---|---|---|---|---|---|
| **HR (bpm)** | **Day** | 10:30 | 4 | 333.4 | 24.4 | 298.75 | 403.29 | |
| | | 14:30 | 6 | 323.6 | 17.5 | 250.1 | 364.12 | ns |
| | **Night** | 21:30 | 11 | 302.4 | 9.5 | 220.45 | 328.03 | |
| | | 02:30 | 8 | 311.9 | 4.1 | 287.31 | 326.73 | |
| **PP (mmHg)** | **Day** | 10:30 | 4 | 49.9 | 3.9 | 38.18 | 54.55 | 0.021 |
| | | 14:30 | 6 | 52.8 | 2.8 | 45.02 | 59.93 | 0.026 |
| | **Night** | 21:30 | 10 | 67.5 | 4.4 | 49.12 | 91.1 | Max |
| | | 02:30 | 8 | 54.3 | 4.8 | 37.63 | 76.28 | 0.030 |
| **RSA (Δ bpm)** | **Day** | 10:30 | 3 | 7.1 | 2.5 | 3.9 | 12.05 | |
| | | 14:30 | 6 | 9.2 | 1.5 | 1.92 | 16.33 | ns |
| | **Night** | 21:30 | 11 | 10.4 | 2.7 | 3.15 | 29.51 | |
| | | 02:30 | 8 | 8.3 | 1.8 | 2.83 | 15.39 | |
| **∫SND (AUC)** | **Day** | 10:30 | 4 | 3.9 | 1.1 | 8 | 17 | ns |
| | | 14:30 | 4 | 2.2 | 0.5 | 9 | 16 | 0.003 |
| | **Night** | 21:30 | 10 | 3.9 | 0.3 | 8 | 19 | 0.027 |
| | | 02:30 | 7 | 5.9 | 0.9 | 12 | 19 | Max |
| **Resp *f* (rpm)** | **Day** | 10:30 | 4 | 12.8 | 2.1 | 2.64 | 7.03 | |
| | | 14:30 | 5 | 13.0 | 2.4 | 1.55 | 2.89 | ns |
| | **Night** | 21:30 | 11 | 16.2 | 0.9 | 2.46 | 5.32 | |
| | | 02:30 | 8 | 15.9 | 0.7 | 2.83 | 9.66 | |

## 3.4 Discussion

### 3.4.1 Main findings

In this study, the circadian cardio-respiratory profiles of rats that have been acclimatized either into a light phase or dark phase using the WHBP were assessed. PP, SND and PND were significantly higher during the night phase than the light phase. In contrast, HR and RSA were not significantly different between day and night. The animals were then sub grouped according to the time of day of recording and significant differences between PP and SND were detected. The presence of these differences and their relevance to the WHBP and subsequent studies in this thesis will be discussed below.

### 3.4.2 Perfusion pressure and sympathetic nerve activity exhibit circadian variance in the WHBP.

The circadian variation in maintenance and control of blood pressure has long been recognized in humans (Millar-Craig *et al.,* 1978; Krauchi & Wirz-Justice, 1994) and laboratory animals (Janssen *et al.,* 1994; Van Den Buuse, 1994). Consistent with these findings, circadian influences on PP were detected in the WHBP in this study, albeit opposite to human timings - the PP was significantly higher during the nighttime, with a peak at 2130 at night and lowest at 1030 in the morning.

The significant physiological variation in PP may be underpinned by the differences in the sympathetic nerve activity observed in the diurnal and nocturnal WHBP preparations. Such circadian patterns of SND as well as BP are found with humans. MSNA recording from healthy subjects in dark phase while sleeping (overnight) showed decreases in sympathetic outflow specifically during non-rapid eye movement (non-REM) sleep and

progressively into deeper sleeping stages (Okada *et al.*, 1991). The decrease in the sympathetic efferent outflow during the non-REM sleep stages were associated with decrease in arterial pressure and heart rate (Somers *et al.*, 1993). The rapid eye movement (REM) sleeping stage which is most manifest toward the end of sleep, before arousal, showed profound sympathetic activation with the HR and BP returning to levels similar to those during wakefulness (Somers *et al.*, 1993). A major influence on rhythms in SND (and by association, blood pressure) appears to be the SCN. A bright light exposure (15 minutes at 5000 lx) in healthy subjects increased the sympathetic nerve activity as measured directly from their muscle sympathetic nerves. The elevated MSNA further increased and became significant during post - bright light exposure (Saito *et al.*, 1996).

Unlike humans, direct measurement of the sympathetic nerve activity in an effort to study the circadian variation in rodents is scarce. The nearest study was performed in rats where the sympathetic nerve activity measured indirectly through plasma noradrenaline and adrenaline level in free moving rats, collected hourly during 12 hour light and dark period. It was found that the circulating adrenaline and noradrenaline were significantly higher during the nightime, along with the more active behaviour pattern (e.g.: grooming, feeding, drinking, resting) (De Boer & Van der Gugten, 1987). Similarly, a 24 hour telemetric recording of heart rate variability showed higher LF/HF ratio in the dark-phase, suggesting predominant sympathetic nervous activity at night (Hashimoto *et al.*, 1999). Hence, the experiments in this chapter are consistent with different circadian autonomic profiles between humans and rats, but both exhibiting a circadian rhythm. This is evident as the current WHBP preparation showed the sympathetic activity was significantly higher at night, with the highest levels noted in the 2130 preparation.

### 3.4.3 Persistence of Circadian Rhythms in PP and SND in WHBP

An important point to note is that the circadian rhythms in PP, SND and PND persisted in the WHBP, in which the hypothalamus has been removed. As discussed earlier in the Introduction (Section 3.3.2) circadian rhythms are set by the neuronal network from the SCN, how do these rhythms persist in its absence? Notably, circadian rhythms are driven by gene expression changes in the master clock in the SCN, but these serve to entrain similar rhythms in gene expression in cells of other organs and tissues. For example, oscillations of clock genes (*per2, bmal1* and *clock*) have been reported in CNS regions controlling the baroreflex functions, such as the NTS and RVLM (Herichová *et al.*, 2007). How fluctuations in expression of these genes influence the behaviour of neurons in these areas, for e.g. by controlling expression of other genes such as ion channels, is unknown. Indeed, it is not known if specific cells are under circadian influence, or indeed how other regions controlling autonomic outflow, such as the IML, may also display circadian rhythms. Crucially, since the WHBP is a short term preparation, it is clear that circadian changes in the brainstem circuits controlling PP and SND are sufficient to influence these activities. Future studies may address the changes in specific cell types and how they contribute to the circadian differences observed in this study.

### 3.4.4 Respiratory rate and circadian influences in WHBP

In these studies, respiratory rate (as measured by PND) was significantly higher in nighttime rats. This is consistent with observations in adult rats, which when placed into a plethysmography chamber for 3 consecutive days (12 hour L: D) showed substantial breathing oscillation, particularly during the dark phase (Seifert & Mortola, 2002). Using a similar chamber method, freely moving rats were found to have an increased ventilation in the dark phase, driven by an increased respiratory frequency (Stephenson *et al.*, 2001).

However, these previous studies have examined awake animals, which were free to move and such movements may contribute to the increased ventilation. Since the WHBP is static, the increased PND is not driven by movement: this suggests that there are changes in the respiratory pattern generator network itself that leads to the increased PND. PND was therefore decreased in the light phase, when rats are more likely to be asleep. Such a decrease in respiratory drive could play a role in the expression of Ondine's Curse (aka congenital chronic hypoventilation syndrome), when the central drive for respiration is already diminished and reflex control of $CO_2$ levels via the retrotrapezoid nucleus circuitry may come to the fore (Guyenet, 2008).

### 3.4.5  Is vagal tone affected by the circadian rhythm?

Unlike the sympathetic nerve activity, variation in the parasympathetic tone in relation to the circadian rhythm is debatable. From our WHBP record, indirect measurement of the cardiac vagal tone by examining respiratory sinus arrhythmia did not significantly vary between the day and night time. It was previously postulated that the autonomic control of the parasympathetic is not entrained by the light/dark phase since the circadian HRV variation persisted in vagal neuropathy subjects (Malpas & Purdie, 1990). Recent evidence from SCN damaged patients that underwent overnight ambulatory polysomnography did not have a significant HRV across the sleep stages in comparison to healthy controls (Joustra *et al.*, 2016). This suggests the SCN has no primary role in the parasympathetic autonomic control since sleeping phase is frequently associated with cardiac vagal pre-dominance. Joustra's observation is essentially contradicted by another study where the parasympathetic- associated HRV profiles of healthy volunteers showed a day-night pattern, marked by peak at nighttime and plateau at daytime (Bonnemeier *et al.*, 2003).

Furthermore, a neuroanatomical study using a series of retrograde viral tracers suggests the alternating sympathetic-parasympathetic nerve activity is

controlled by segregated pre-autonomic neurons in the hypothalamus. Injection of Pseudorabies virus (BGAL)-PRV into the sympathetically denervated liver (so the virus infects vagus nerve only), and GFP-PRV injected simultaneously into the adrenal (to infect the sympathetic nerve only) has stained separate pre-autonomic neurons in the PVN as well as the SCN (Buijs *et al.*, 2003). The presence of pre-sympathetic and pre-parasympathetic neurons projection also can be seen in the NTS, the main cardiovascular autonomic integration centre. This proposes the SCN balances sympathetic and parasympathetic outputs to peripheral organs through separate pre-autonomic neurons where the PVN and NTS are involved in the interactions (Buijs *et al.*, 2003). However, careful interpretation on the neuroanatomical result is required as there is a possibility that different organs were just projecting to different targets in the central nervous system. Also, functional significance of this differential autonomic neuronal projection into the hypothalamic circadian centre (eg: SCN) needs further investigation.

### 3.4.6 Future application

The study on diurnal rhythms is relevant to cardiovascular disease since the normal diurnal variation is altered in manifesting cardiovascular disease (Shaw *et al.*, 2001) associated with increased end organ damage (Foley & DuBois, 1937) and associated with acute cardiovascular events (Boscan *et al.*, 2002). Cardiovascular events also exhibit 24-h variability in occurrence with a prominent peak between 06:00 h and noon (Youcef *et al.*, 2014), parallel with the diurnal rhythmicity of sympathetic vasoconstriction activity suggesting autonomic blood pressure control may participate in triggering acute cardiovascular events (Panza *et al.*, 1991). The diurnal sympathetic rhythm obtained in humans is, however, contrary to the current WHBP findings, where heightened sympathetic activity was observed during the dark phase. Unfortunately, the vast majority of studies has been carried out on rats and mice during the daytime when the nocturnal animals are at rest.

Therefore, while studying the physiological functions in nocturnal animals during the daytime does not make invalid results, it needs to be considered during interpretation process.

### 3.4.7 Conclusion

This chapter is the first to examine the autonomic and physiological functions of rats in different parts of the circadian cycle using the WHBP. A key finding was that circadian differences in SND, PP and PND were consistent with those previously observed in intact animals and displayed a reverse cycle to that in humans. This is the first observation that SND was significantly higher in nighttime WHBPs. It is not yet clear if the differences in the physiological responses between day and nightime animals are also modulated by the parasympathetic nervous system. However, it is important to note these differences when designing experiments in rats that examine autonomic and respiratory activity.

# Chapter 4 An anatomical and functional study of the central afferent nerve projections from the tragus of the external ear

## 4.1 Introduction

Different sites of stimulation of the auricle that is termed transcutaneous vagal nerve stimulation (tVNS) include the tragus, concha and cymba concha since there is ABVN innervation into these regions (**see General Introduction section 1.3.7**). Since Clancy et al 2014 showed a decrease in sympathetic nerve activity via tragus stimulation in humans, this chapter examined the central projections of sensory afferents innervating the tragus, using the rat model. In addition, the effects of tragus stimulation on cardiorespiratory function in the WHBP were investigated.

### 4.1.1 Functional effects of tragus stimulation

Current evidence suggests tragus stimulation modulates autonomic control of the heart. In heathy human subjects (20- 60 years old),15 minutes of tragus stimulation (200μs, 30 Hz, 1-50 mA) shifted the cardiac autonomic function toward parasympathetic predominance as indicated from HRV analysis (Clancy *et al.*, 2014). This was accompanied by a significant decrease in the muscle sympathetic nerve activity (MSNA) during tVNS recorded from muscle microneurography. The observed reduction in MSNA with tVNS could help explain the therapeutic potential of tragus stimulation in cardiovascular diseases characterised by sympathoexcitation (He *et al.*, 2012; Murray *et al.*, 2016).

Experimental models have assisted investigations into tVNS via the tragus and point to potential therapeutic uses. In dogs in which atrial fibrillation (AF) had been induced using rapid atrial pacing, low level stimulation of the right tragus (LLTS) dampened the fibrillation (Yu *et al.*, 2013). Longer LLTS (9 hours at 80% below threshold) stimulation delivered along with atrial pacing on anaesthetized dogs prevented the loss of connexin proteins (e.g.: Cx 40 and Cx 43) in atrial tissues that were measured through Western Blot. This

suggests the anti-fibrillatory effect posed by the LLTS is through the defence against cardiac remodelling and preservation of its electrical conduction via gap junction (eg: Cx40 and Cx43) (Chen *et al.*, 2015). Indeed, the LLTS effects on remodelling of the left ventricle have been studied specifically after myocardial infarction. Applying the LLTS twice per day for 90 days significantly improved cardiovascular system performance measured via ventricular contractility and diastolic function, reduced infarct size, decreased nonspecific inflammatory and fibrosis markers thus suggesting attenuation of cardiac remodelling  (Wang *et al.*, 2014). These cardio protective effects were accompanied with plasma noradrenaline reduction, suggesting inhibition in central sympathetic nerve activity. Reduction of sympathetic output by LLTS was supported in a recent study in anaesthetised dogs (Zhou *et al.*, 2016). Cardiac sympathetic hyperactivity was induced by a high-voltage electrical stimulation (20Hz, 0.1 ms, 10-70 V) on the right stellate ganglion (RSG), which significantly increased sinus rate in a voltage-dependent fashion (Zhou *et al.*, 2016). The sinus node acceleration and neural activity recorded from the right stellate ganglion (RSG) were, however, attenuated after 3 hours of the LLTS (20 Hz, 2 ms, voltage 80% below threshold). Furthermore, the neural related protein expression (cFos and NGF) in the RSG measured using qPCR and Western blot were significantly lower in the LLTS group. Electrophysiological recording from the RSG showed attenuation of its neural activity after 3 hours of LLTS, suggesting inhibition of sympathetically induced sinus node acceleration (Zhou *et al.*, 2016).

Patients attending for AF ablation procedure were treated with an hour of LLTS (20Hz, 50% below threshold) under the influence of general anaesthesia (Stavrakis *et al.*, 2015). Similar anti-fibrillatory effects were reported in these people as were observed in the animal models, in addition to suppressed proinflammatory factors like TNFα and CRP. Considering that tVNS via the tragus is easy to apply, reduces sympathetic nerve activity in humans and has positive effects on cardiovascular disease models, further investigation into pathways and mechanisms appears warranted.

## 4.1.2 Central afferent projections from the tragus

As noted in the Introduction, the external ear of mammals receives a relatively large sensory afferent innervation, with the three innervating nerves exhibiting overlapping, but distinct, distributions. The central portion of the auricle appears to be innervated differently to the peripheral portion: in cats, injection of horseradish peroxidase (HRP) into the central auricular region resulted in retrogradely labelled afferent cell bodies predominantly in the ganglia of cranial nerves, whilst peripheral auricular (tragus included) injections revealed labelled neurons predominantly in C1-C4 spinal ganglia (Satomi & Takahashi, 1990). In a different approach, human cadaveric dissection of the nerves innervating the human auricle identified three innervating nerves namely the Auricular branch of the vagus nerve (ABVN), the greater auricular nerve (GAN) and also a branch of the trigeminal nerve, the Auriculotemporal nerve (ATN). These sensory nerves cover the auricular area at a variable degree in the respective dermatomes - the tragus has an almost even distribution of the GAN and also ABVN at 45% and 46% respectively (General Introduction Section 1.3.1).

Previous anatomical studies observed an overlap of the central projection from the GAN and ABVN into the dorsal horn of the upper cervical and a main autonomic relay centre, the NTS. The application of HRP on the GAN in rabbits revealed afferent cell bodies in the ipsilateral dorsal root ganglion ($C_2$-$C_3$) and the superior cervical ganglion, thus suggesting its origins from the cervical plexus (Liu & Hu, 1988). Nerve fibres were detected in the dorsal column of the upper cervical spinal cord and strongly stained in laminae I-V at the $C_2$. Extending rostrally, the afferent GAN also has intense labelling in the cranial nerve nuclei in the medulla, accounting for caudal subnucleus of the spinal trigeminal nerve, the solitary nucleus, and also medial and lateral cuneate nuclei. ABVN central projection has been studied earlier in cats and rats where the sensory endings terminated ipsilaterally on the solitary

nucleus, spinal trigeminal nucleus, rostral cuneate nucleus, in addition to the spinal dorsal horn of the upper cervical (Nomura & Mizuno, 1984; He *et al.*, 2013). The frequent termination of afferent staining from the auricle on the NTS has been believed to be the explanatory mechanism for autonomic modulation from ear stimulation, hence was termed the Auriculovagal Afferent Pathway (He *et al.*, 2013).

## 4.2 Research gap

To date, there have been no reports on the central projections of the tragus in an effort to understand its beneficial potential in modulating cardiac autonomic control. The nearest study was injection of HRP into peripheral region in cats auricle (tragus included) where primary afferents were labelled in the cervical and spinal ganglion (Satomi & Takahashi, 1990). In rats, CTB was injected into the auricular concha of rats where labelled afferent terminals were observed on the lateral NTS along with the spinal trigeminal nucleus, cuneate nucleus and also spinal dorsal horn of 2-3 cervical segments (He *et al.*, 2013). This however might not reflect the sensory nerve innervation into the tragus as human cadaver examination showed that the cymba concha is 100% innervated by the ABVN, while the tragus has a great mixture of ABVN and also GAN (Peuker & Filler, 2002). The tracing study on cats by Satomi and Takahashi, 1990 also showed that the HRP injection from the concha is mainly detected within cranial ganglia (superior vagus, trigeminal) while peripheral injections (tragus included) concentrated within the spinal ganglia (C1-C4). Thus mapping out the primary afferent projections from the tragus would facilitate better understanding and interpretation on the effects elicited from the tragus stimulation. The cardiorespiratory effects of tragus stimulation in the absence of anaesthetic were examined in the Working Heart Brainstem Preparation. Selective de-afferentation was performed to examine which afferents potentially influenced the cardiorespiratory effects of tragus stimulation.

## 4.3 Hypothesis

- The tragus afferents project into the NTS
- Tragus stimulation will cause a sympatho-inhibition in the WHBP.
- This sympatho-inhibition from tragus stimulation is mediated by the auricular branch of the vagus nerve.

## 4.4 Aim

The aims of this study were:

1. To map the afferent central projections of the tragus in rats using the neuronal tracer Cholera Toxin B (CTB).

2. To examine potential cell contacts of the tragus afferents using immunohistochemistry.

3. To determine the effects of tragus stimulation on cardiorespiratory activity in in the WHBP.

4. To examine potential pathways mediating tragus stimulation by cutting specific nerves and examining if tragus stimulation elicited similar effects as in fully intact animals.

## 4.5 Methods

### 4.5.1 General Methods

The general methods that been used in this chapter has been discussed in details in the general methods chapter. This includes the injection of CTB into the tragus **(Section 2.1)** and the WHBP **(Section 2.2)**. All the animals (n=30) used in the WHBP experiments were night phase animals that been acclimatized inside a reverse cycle cabinet for at least 7 days. 3 groups of animals been studied:

1) Fully intact (n=10)

2) Right cervical vagotomised (n=10)

3) C1-C3 transected animals (n=10).

### 4.5.2 The Working Heart Brainstem Preparation (WHBP) Stimulation timeline

After the preparation has settled in by displaying eupnoeic breathing pattern for at least 30 minutes, baseline parameters were recorded. These include the heart rate (HR), perfusion pressure (PP), sympathetic nerve discharge (SND) and also phrenic nerve discharge (PND). Indirect measurement of respiratory sinus arrhythmia (RSA) was measured by mean changes in the HR in response to breathing cycle. The right tragus stimulation was performed using a *DS3* Constant Current Isolated Stimulator (Digitimer Ltd, UK) connected to a modified metal ear clip **(Figure 4.1)**. The stimulation was applied for 5 minutes at 100 Hz, 2.5 mA with any current leakage grounded. The effects of post stimulation was compared immediately (post-stim) and much later (recovery). The effects of tragus stimulation was further examined in intervention WHBP group.
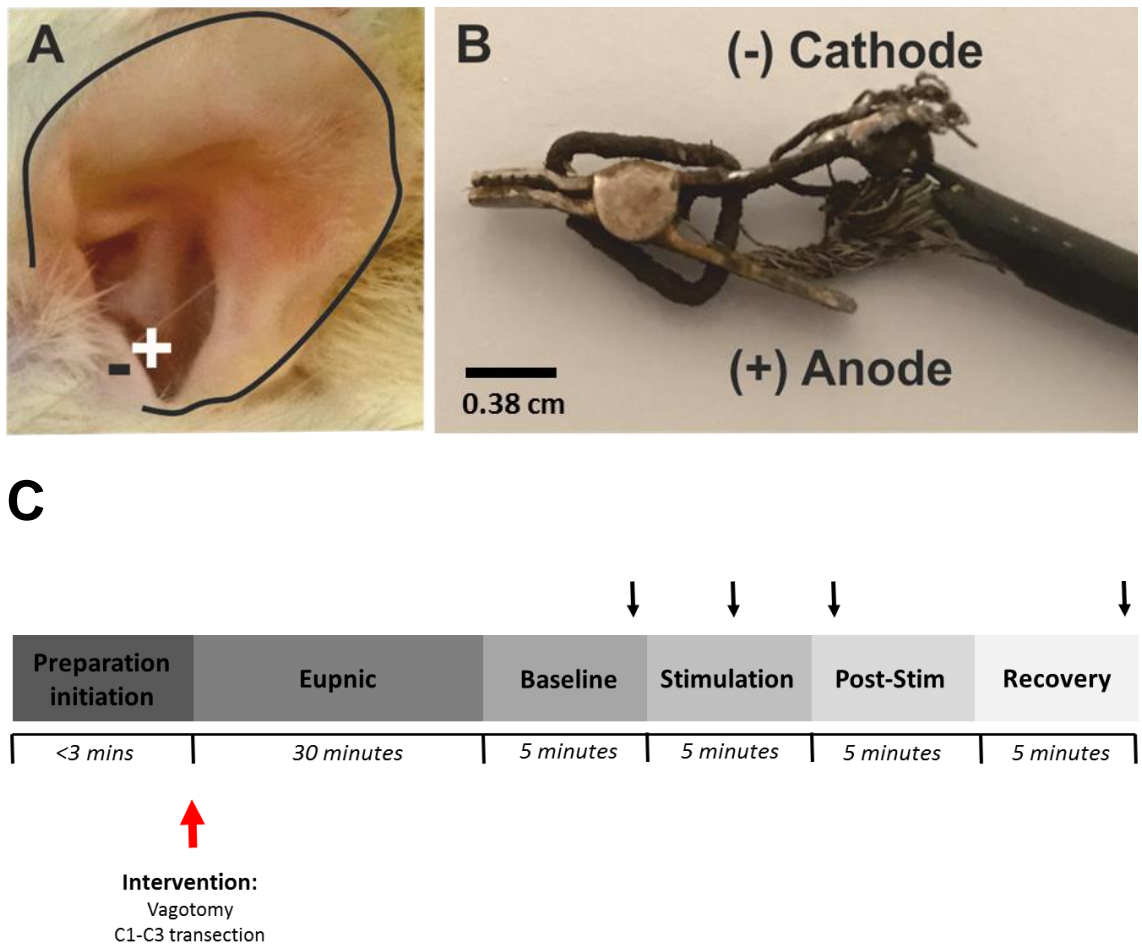
**Figure 4.1: The tragus stimulation during WHBP experiment**

The electrical stimuli was applied on the A) the tragus using alligator clip. B) the cathode was applied on the outer tragus and anode on the inner tragus. C) Experimental parameters were recorded after the preparation has reached the eupnic breathing pattern for at least 30 minutes. The top black arrows indicate specific timings when the parameters were recorded. The effects of tragus stimulation were analysed and compared during baseline, stimulation, post-stimulation and recovery. The effects of tragus stimulation also compared in groups that received intervention procedure immediately after initiation of the WHBP (red arrow).

### 4.5.3 Sectioning of the cervical vagus nerve

In some preparations the effects of sectioning the cervical vagus nerve on tragus evoked responses was investigated. Dissection of the vagus nerve began after animals were decerebrated and before the preparations were taken into the recording chamber. Dissection was initiated by removal of the superficial muscle layers on the right side (ipsilateral to the ear stimulation site). The sternohyoid muscle, a narrow band of muscle lying nearest to the trachea, was removed, exposing the carotid bifurcation beneath. At this point, vagus nerve is visible lying next to the common carotid artery surrounded by a layer of sheath. Careful identification was required as the superior cervical sympathetic ganglion also lies nearby. The vagus nerve was carefully isolated from the sheath that attached to the common carotid artery and a thread was tied around the vagus nerve trunk. This thread was used to pull the nerve gently away during the WHBP preparation while iris scissors were utilised to cut the nerve without touching the surrounding tissues. With practice, this whole dissection process took between 2-3 minutes. It was important to make sure the whole dissection finished as quickly as possible for better viability of the nerve recording in the WHBP preparation (Docherty *et al.*, 2005).

### 4.5.4 Dissections of the dorsal roots of C2-C3

Following the decerebration procedure, posterior neck muscles that covered the upper cervical cord axis were dissected and vertebrae were exposed. The spinous processes were carefully laminectomized **(Figure 4.2)**. Ipsilateral to the site of the stimulation, the dorsal roots from the first till third cervical spinal were cut using springbow dissecting scissors. This dissection took 2-3 minutes.
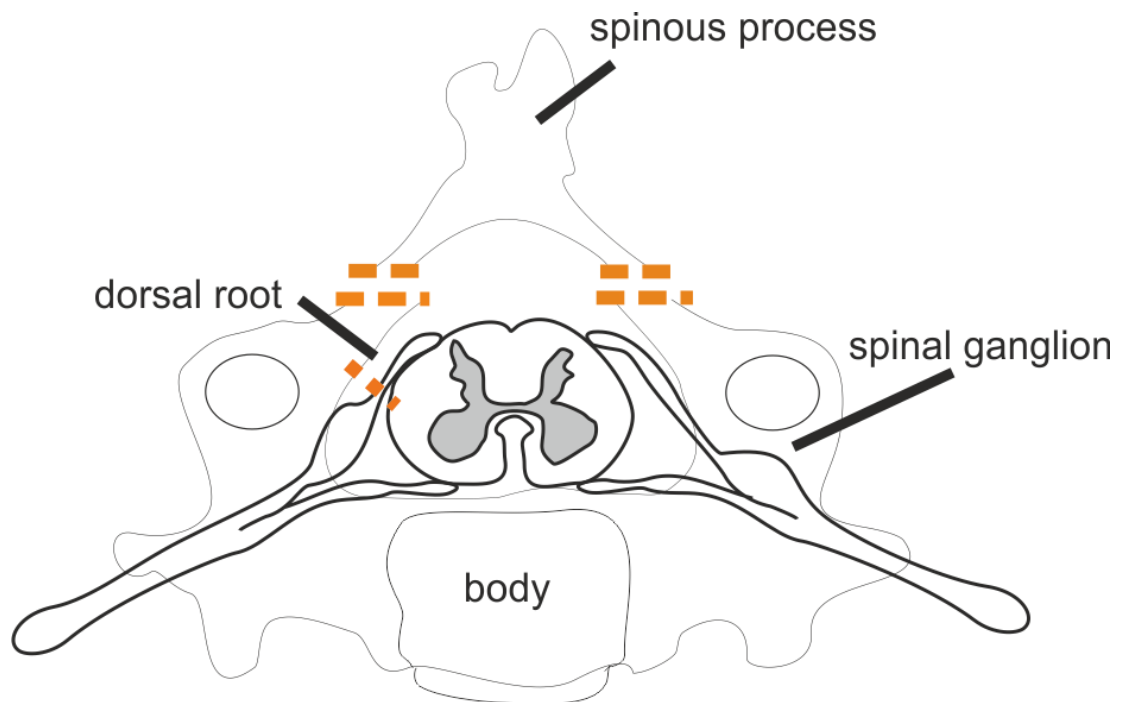
**Figure 4.2: The schematic diagram for upper cervical (C1-C3) dissection in WHBP**

The upper cervical spinal cords were exposed by removal of the spinous process. The ipsilateral dorsal root from the stimulation site was carefully cut. The coloured dotted lines represent the cutting areas that need to be made.

### 4.5.5 Statistical Analysis

The normality test for numerical datasets were appropriately explored with the Shapiro-Wilk test due to small sample size. The significant value of the normality test greater than 0.05 considered as normal, while below than 0.05 is considered to be deviated from a normal distribution.

For normal distributed data, the effects of electrical stimulation on the tragus were compared between baseline and other time points with repeated

measure ANOVA. Any statistical significant values from the ANOVA test were then confirmed with Fisher's Least Significant Difference (LSD) post hoc test.

To determine if the physiological functions differed between 2 groups only (in comparing the effects of vagotomy on physiological parameters of the WHBP), an independent samples t-test was performed with $p<0.05$ as the significance level for the normally distributed data.

The non-normally distributed data was analysed with non-parametric analysis (Friedman test) using IBM SPSS Statistics 21. Identification of the significant points were made with the Wilcoxon signed-ranked test.

## 4.6 Results

### 4.6.1 Localisation of the central afferent labelling from the tragus

Rat brains were examined starting from the level of the $4^{th}$ ventricle (Bregma -10.04 mm) to upper cervical cord in C4. The areas labelled with CTB within the CNS were ipsilateral to the injected tragus and were identical for each of the animals **(Figure 4.3)**. In the rostral brainstem (Bregma -12.72mm) there was labelling of the Paratrigeminal nucleus (Pa5) **(Figure 4.3A)**. In the lower brainstem level (Bregma -14.08 mm) a larger area of afferent termination was observed in the Spinal trigeminal tract (Sp5) extending towards cuneate nucleus (Cu) **(Figure 4.3B)**. In the most caudal brainstem (Bregma -14.60 mm) the afferents labelled from Cu and extended ventromedially to the NTS covering the lateral, dorsomedial, and also medial of the NTS **(Figure 4.3C)**. Double labelling with ChAT showed rare CTB labelled structures in close proximity to the ChAT labelled cells in the medial NTS **(Figure 4.3Ci)**.

In the upper cervical cord (C1-C3) there was substantial CTB labelling within the dorsal horn, in varying laminae **(Figure 4.4)**. In C2, a large staining area covered laminae I, III, and IV but not laminae II **(Figure 4.4B)**. The main termination of CTB labelled from the tragus was detected in the section of C3 covering laminae III and IV **( Figure 4.4C)**. No CTB staining was observed distal to the rostral part of C3. Double labelling with ChAT suggested potential cell contacts in laminae IV only in all aforementioned cervical levels.

Other potential cell contacts are also identified using monoclonal antibodies listed from general methodology. It must be noted that no cell type examined appeared significantly innervated by the afferents and therefore quantification was not undertaken. Calb-28k which is highly expressed in laminae II of the dorsal horn was detected to have infrequent appositions from the CTB terminations **(Figure 4.5A and Figure 4.5Ai)**. Parv, another calcium binding protein, was potentially contacted by the afferent terminals in the Pa5 of the

brainstem **(Figure 4.5B and Figure 4.5Bi)**. Potential afferent contacts onto GABA-ergic cells were observed rarely **(Figure 4.5B and Figure 4.5Bi)**. NK1R, which has high distribution in superficial laminae (e.g.: laminae I) was also infrequently contacted with the CTB terminations.
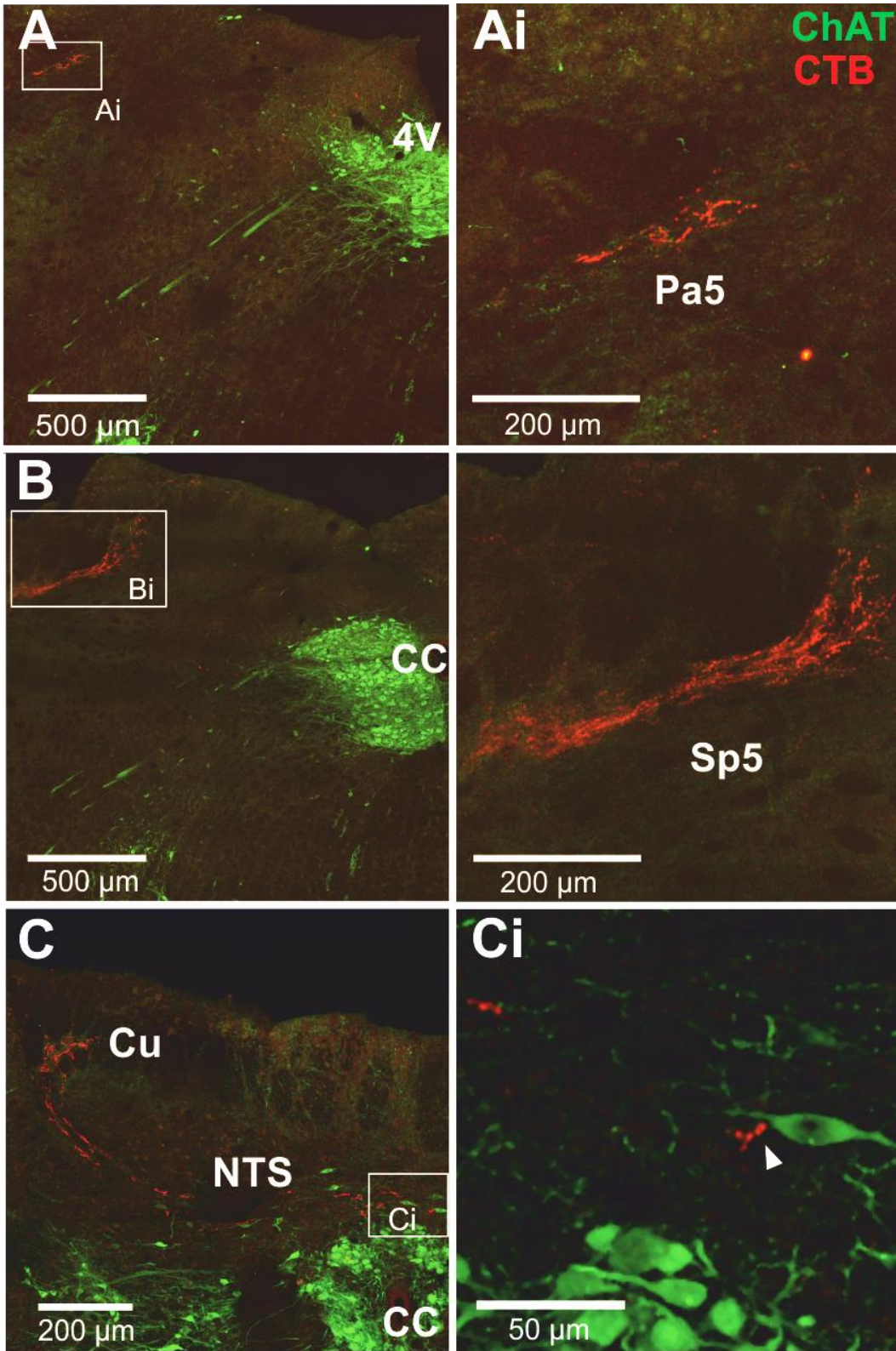
**Figure 4.3: Labelled afferents in the brainstem following injection of CTB into the tragus, with co-staining for ChAT immunofluorescence**

A) Rostral brainstem with afferents labelled in the Pa5 (magnified: Ai). B) Afferents more caudally seen in SP5 (magnified:Bi). C) Labelled afferents course from Cu to dorso-medio lateral NTS. Example of a rare apposition between a labelled afferent and a ChAT immunoreactive cell (Ci). Pa5- paratrigeminal nucleus, Sp5- spinal trigeminal tract, Cu-cuneate nucleus, NTS- nucleus tractus solitarius, ChAT – Choline acetyl transferase, CTB – Cholera Toxin B .
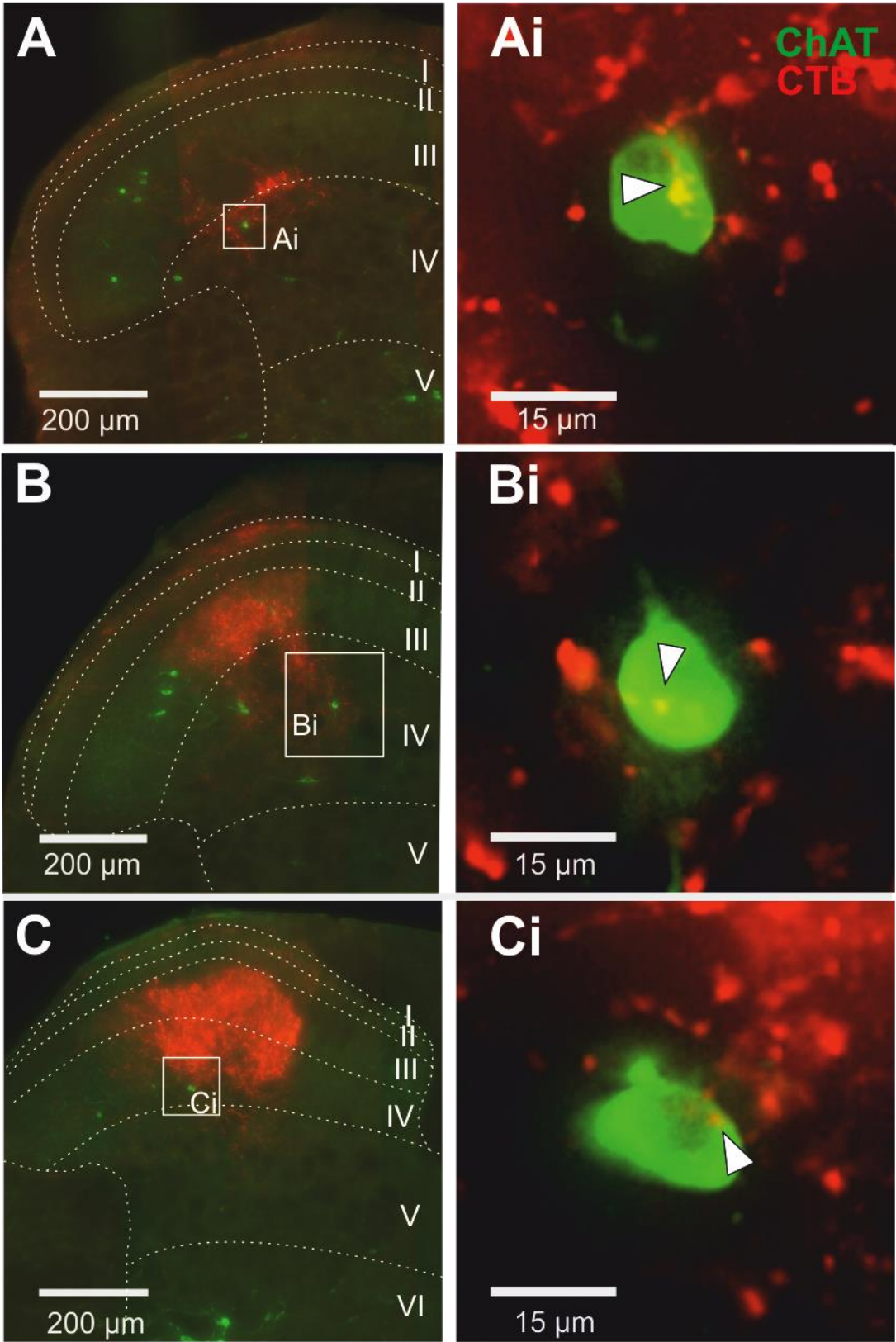
**Figure 4.4: CTB-positive afferents labelled in the upper cervical cord following injection of CTB into the tragus, detected with double staining of CTB and ChAT immunofluorescence**

A) Cervical slice at C1 with CTB-positive afferents terminating in laminae III and IV. B) Cervical slice at C2 with CTB-positive afferents terminating in laminae I, III and IV. C) Cervical slice at C2 with CTB-positive afferents terminating in laminae I, III and IV. Ai-Ci) Potential cell contact of the labelled afferents with ChAT positive cells mostly detected in laminae IV. ChAT – Choline acetyl transferase, CTB – Cholera Toxin B.
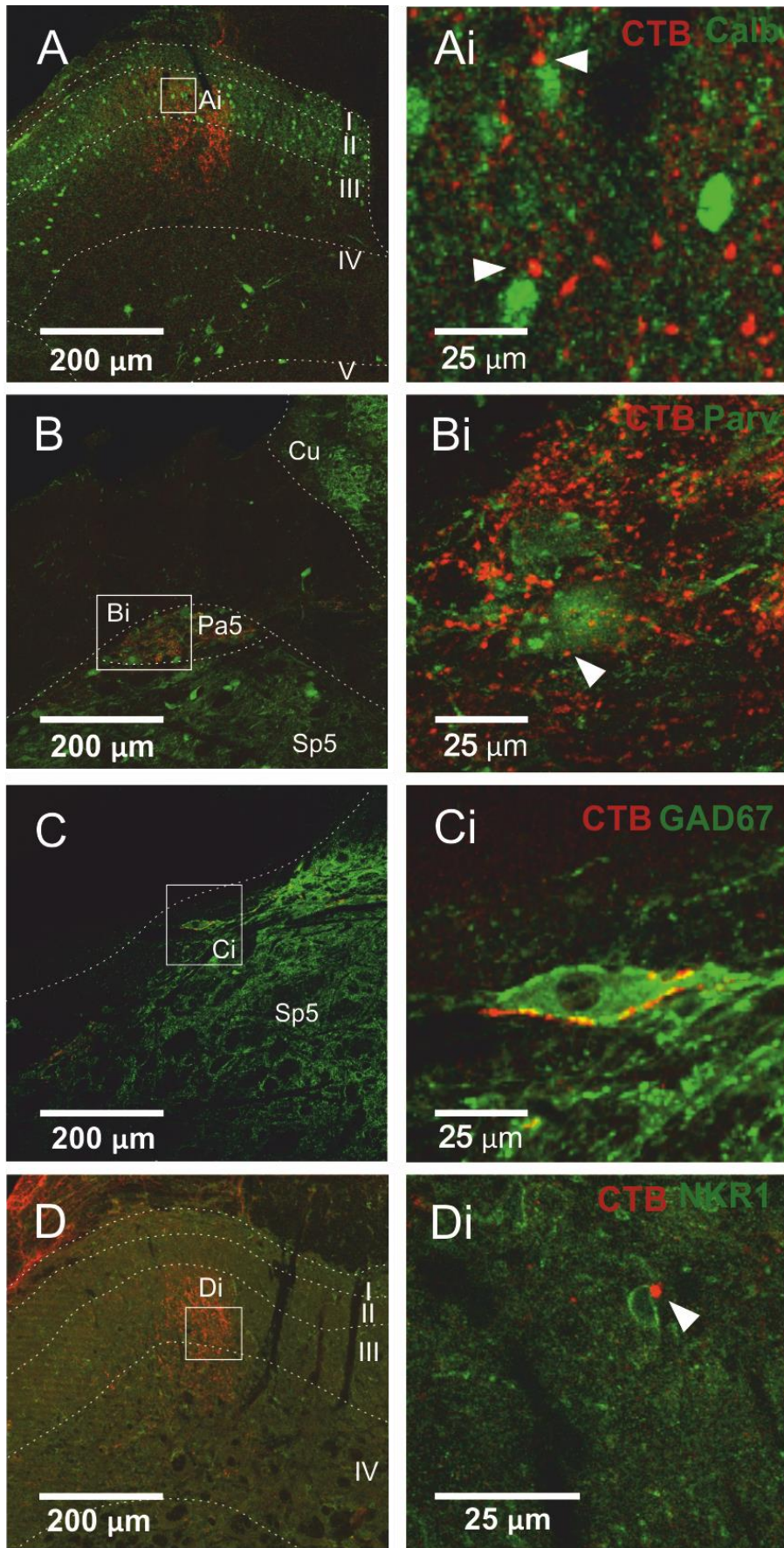
**Figure 4.5: CTB labelled afferents (red) in various locations of spinal cord and brainstem with examples of infrequent appositions to potential post synaptic cell types (green)**

A) Infrequent apposition of the CTB afferent terminals with Calb cells were observed in laminae II of the dorsal horn. B) Brainstem section where afferents apposed Parv positive neuron. C) Dorsolateral Sp5 with a rare example of potential apposition between CTB labelled afferents and GAD 67 immunoreactivity D) Abundant NKR1 positive cells in laminae I of the dorsal horn have infrequent contact with the CTB terminations. All potential contacts are depicted on (Ai-Di) and shown by arrows where appropriate. CTB – Cholera Toxin B, Calb – Calcium binding protein, Sp5 – spinal trigeminal tract, GAD 67 – glutamic acid decarboxylase 67, NKR1 – neurokinin receptor 1, Parv – parvalbumin ,Pa5 – paratrigeminal nucleus, Cu – cuneate nucleus.

## 4.6.2 Effects of tragus stimulation on heart rate, sympathetic nerve discharge, perfusion pressure and phrenic nerve discharge.

HR was recorded from the ECG signal of the phrenic nerve with the average taken for 1 minute before the stimulation began (301.2 ± 11.4 bpm, n=10) **(Figure 4.6).** Tragus stimulation significantly reduced the HR $(F(1.74,13.95)=1.58$, p = 0.02). During stimulation, the HR was reduced to 297.9 ± 11.5 bpm (p=0.034) and persisted at post-stimulation (297.6 ± 11.6 bpm p=0.045). During the recovery period (10 minutes after stimulation stopped), HR was not significantly different from the baseline (299.8 ± 11.6 bpm) (p=0.17). These results indicate tragus stimulation causes a short term heart depressor response in the WHBP.

PP recorded from the distal end of the aorta had a baseline average of 55.4 ± 5.0 mm Hg. Tragus stimulation significantly lowered PP from the baseline, $\chi^2(3)=6.120, p=0.033$ to 53.9 ± 5.1 mm Hg (p=0.008). It further reduced during the post-stimulation period (52.8 ± 5.1) (p=0.003). This depressor effect persisted during the recovery period, at least 5 minutes after the stimulation stopped (52.7 ± 5.0) (p=0.038). Thus the vasodepressor response outlasted the HR bradycardiac response.

The baseline RSA was 7.23 ± 1.17 bpm. Electrical stimulation of the tragus did not significantly affect the RSA at any of the time points $(F(1.14,10.263) = 0.985$, p = 0.356). (Stimulation; 7.15 ± 1.10 bpm; p=0.831;Post stimulation; 7.33 ± 0.96 bpm; p=0.93; Recovery; 9.05 ± 1.40; p=0.367).

There was a significant reduction in the ∫SND from the baseline 4.87 ± 0.52 AUC $(F(1.44, 12.93) = 12.66$, p = 0.002). Electrical tragal stimulation significantly lowered the ∫SND during post-stimulation (3.70 AUC ± 0.36; p=0.003) and also during the recovery period (3.17 ± 1.18 AUC; p=0.004).

Baseline respiratory rate (16.3 ± 1.04 rpm) determined from PND did not significantly alter during the stimulation (16.0 ± 1.14 rpm; p=0.26), post

stimulation (15.7 ± 1.20) (0=0.20) and during the recovery period (16.4 ± 1.35 rpm) (p=0.83).

The duration of inspiratory, expiratory and total respiratory phases did not differ significantly during the experiments **(Table 4.1)**.
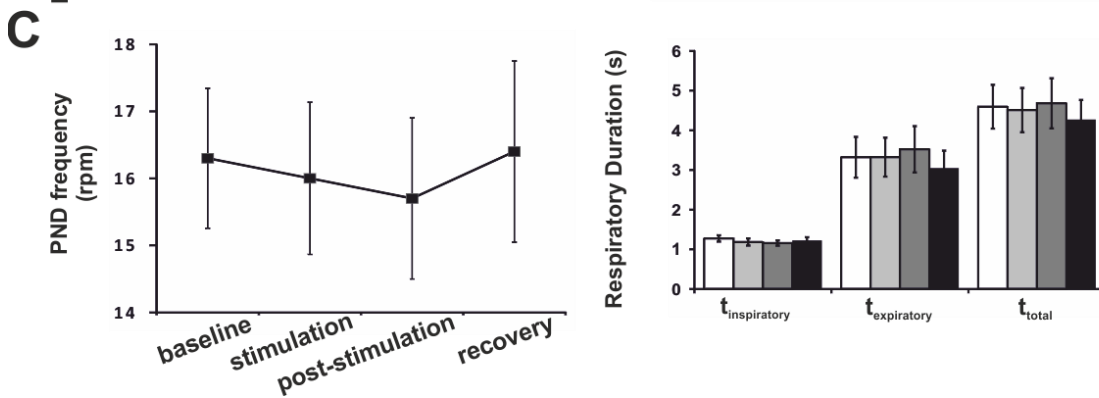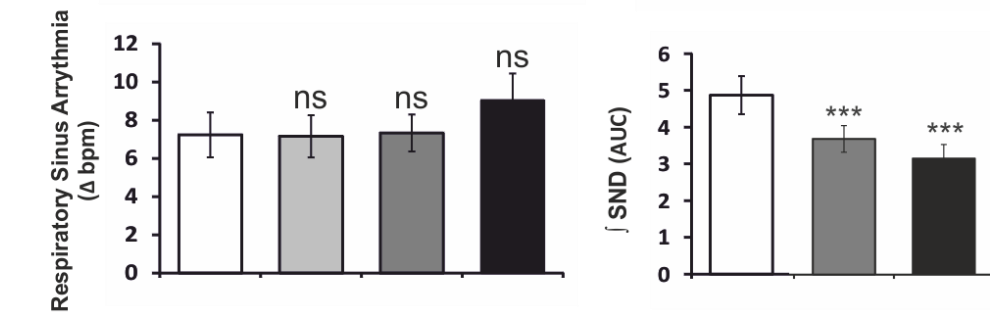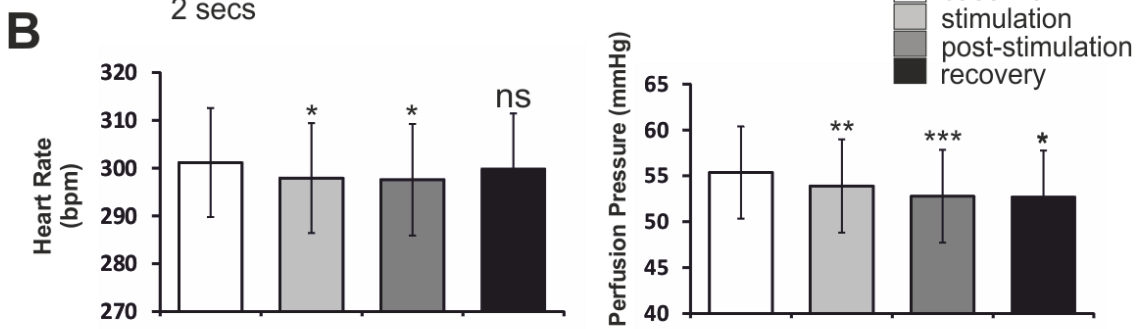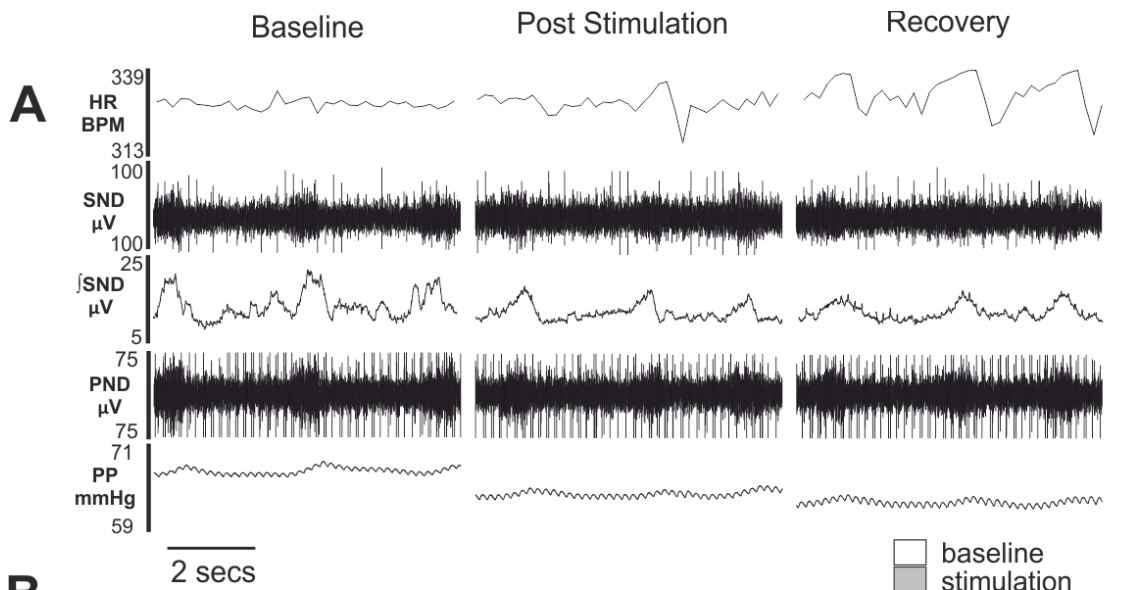
**Figure 4.6: The effects of tragus stimulation on autonomic and respiratory variables in the Working Heart Brainstem Preparation**

Original traces of the WHBP at A) 3 different time points: baseline, post stimulation (immediately after stimulation), and also recovery (10 minutes after stimulation stopped). No measurements of the SND nerve recording were taken during stimulation due to the presence of stimulus related noise that could not be eliminated. B) Group data (n=10) indicating HR, PP, RSA, and SND during baseline, stimulation (SND excluded), post-stimulation and recovery. No significant reduction was observed in the respiration of the animals due to tragus stimulation. *, $p<0.05$; **, $p < 0.01$; ***, $p<0.005$. WHBP - working heart brainstem preparation, HR – heart rate, PP - perfusion pressure, RSA – respiratory sinus arrhythmia, SND – sympathetic nerve discharge.

**Table 4.1: Duration of respiratory phases (seconds) did not change upon tragus stimulation**

| | | Ti (s) | Te (s) | Ttot (s) |
|---|---|---|---|---|
| Baseline | Average | 1.27 | 3.32 | 4.59 |
| | Std error | 0.08 | 0.51 | 0.55 |
| Stimulation | Average | 1.19 | 3.32 | 4.51 |
| | Std error | 0.09 | 0.49 | 0.56 |
| | P value | 0.169 | 0.878 | 0.333 |
| Post stimulation | Average | 1.16 | 3.52 | 4.68 |
| | Std error | 0.07 | 0.58 | 0.63 |
| | P value | 0.059 | 0.093 | 0.445 |
| Recovery | Average | 1.23 | 3.05 | 4.27 |
| | Std error | 0.08 | 0.44 | 0.49 |
| | P value | 0.959 | 0.285 | 0.139 |

### 4.6.3 The effects of vagotomy on tragus stimulation induced changes.

To determine if vagal efferent nerves were involved in responses to tragus stimulation, physiological parameters were recorded pre- and post-cervical vagal vagotomy **(Table 4.2 and Figure 4.7)**. RSA was significantly reduced by unilateral right sided vagotomy (9.7 ± 4.0 bpm VS 4.2 ± 1.1 bpm; p=0.009), reflecting vagal involvement. A typical example of the vagal tone reduction measured from the heart beat variation can be seen on **(Figure 4.7A)**. Basal HR (309.5 ± 5.6 bpm) significantly increased following cervical vagotomy (319.9 ± 4.8 bpm, p=0.009). Similarly, respiratory frequency also increased after the vagotomy (16.7 ± 1.5 rpm VS 19.0 ± 1.4 rpm, p=0.005). There was only a small, but statistically significant (p=0.012), drop in the PP after vagotomy (57.9 ± 3.3 mmHg VS 57.2 ± 3.3 mmHg). The baseline integrated sympathetic activity (3.7 ± 0.2 AUC) was not significantly altered after the vagotomy (4.0 ± 0.2 AUC; p=0.406).

Tragus stimulation in the vagotomised groups elicited no significant effects on the HR, PP and also the RSA **(Table 4.3 and Figure 4.8)**. Repeated measures ANOVA revealed significant reduction in SND $F_{(2,14)}=4.064$,p=0.041 during recovery period (4.0 ± 0.2 AUC VS 3.2 ± 0.3; p=0.048). In contrast, PND rate significantly increased $F_{(3,27)}=3.676$, p = 0.024 during the recovery period (19.0 ± 1.4 rpm VS 20.2 ± 1.6; p=0.044). Further analysis on respiration revealed the significant value increase in breathing frequency lies in the reduction of the expiratory phase during the recovery period **(Table 4.4)**.
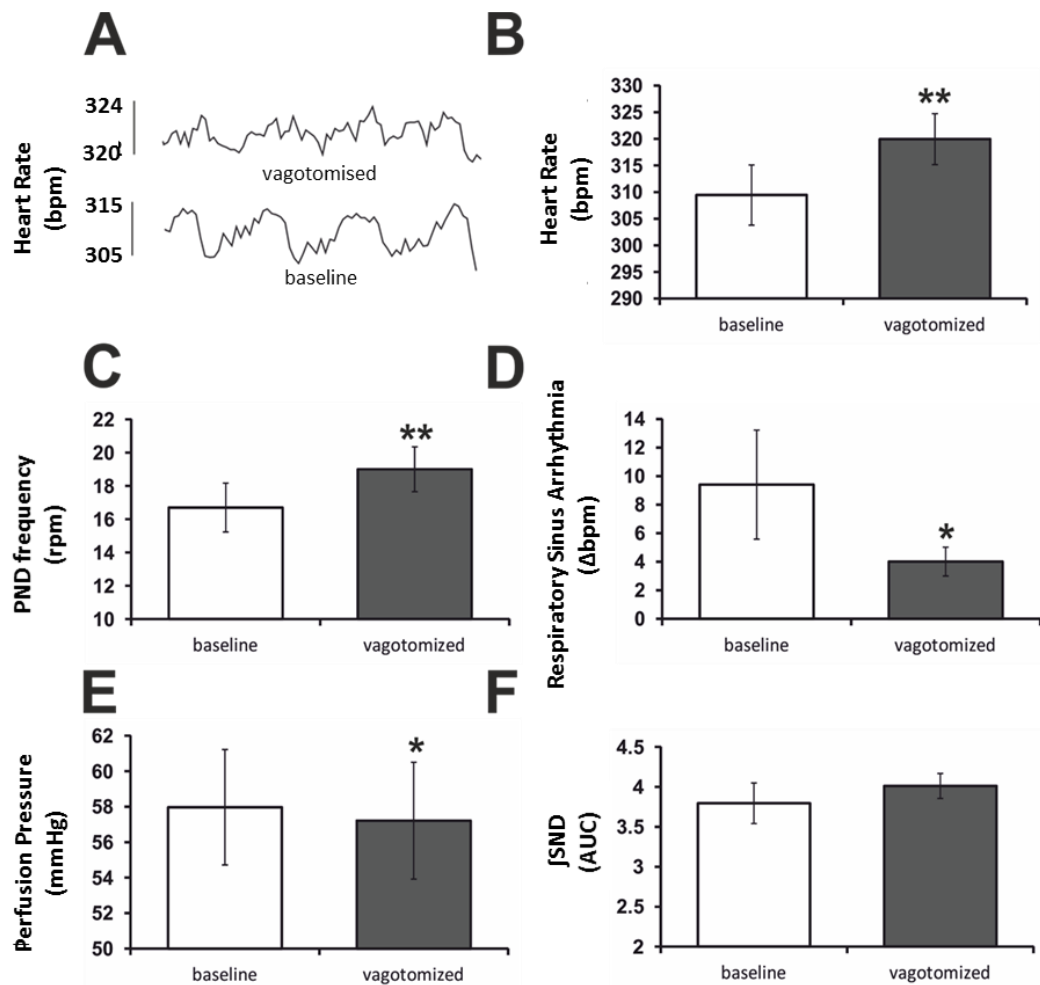
**Figure 4.7: The effect of right cervical vagotomy on the physiological properties in WHBP**

A) Raw traces of the apparent RSA recorded in non-vagotomised (bottom) in comparison to the vagotomised prep (top). B, C) Ipsilateral vagotomy on the WHBP animals significantly increased the HR and breathing frequencies D, E) PP significantly reduced after vagotomy. F) SND was not affected by vagotomy. *, p<0.05; **, p < 0.01; ***, p<0.005. WHBP - working heart brainstem preparation, HR – heart rate, PP - perfusion pressure, RSA – respiratory sinus arrhythmia, SND – sympathetic nerve discharge.

**Table 4.2: Effects of vagotomy on measured variables**

|  |  | N | Mean | Std err | Min | Max | P value |
|---|---|---|---|---|---|---|---|
| HR (bpm) | Baseline | 10 | 309.45 | 5.64 | 275.10 | 329.33 | 0.009** |
|  | Vagotomized | 10 | 319.95 | 4.78 | 294.83 | 346.27 | |
| PP (mmHg) | Baseline | 10 | 57.97 | 3.26 | 44.17 | 73.37 | 0.012* |
|  | Vagotomized | 10 | 57.21 | 3.29 | 43.68 | 74.05 | |
| RSA (Δ bpm) | Baseline | 10 | 9.77 | 4.04 | 2.46 | 40.28 | 0.015* |
|  | Vagotomized | 10 | 4.22 | 1.05 | 1.80 | 11.46 | |
| ∫SND (AUC) | Baseline | 8 | 3.79 | 0.25 | 2.74 | 4.85 | 0.406 |
|  | Vagotomized | 8 | 4.01 | 0.16 | 3.31 | 4.48 | |
| PND (rpm) | Baseline | 10 | 16.70 | 1.47 | 10 | 24 | 0.005** |
|  | Vagotomized | 10 | 19.00 | 1.35 | 13 | 24 | |

**Figure 4.8: The effect of tragus stimulation on physiological parameters recorded from the Working Heart Brainstem Preparation of the vagotomised animals**

Tragus stimulation on the ipsilateral vagotomised animals did not significantly affect HR (A), PP (B) or RSA (C). (D) The integrated SND was significantly inhibited during the recovery period. (E) The breathing activity significantly increased during the recovery period. *, $p<0.05$; **, $p < 0.01$; ***, $p<0.005$. WHBP - working heart brainstem preparation, HR – heart rate, PP - perfusion pressure, RSA – respiratory sinus arrhythmia, SND – sympathetic nerve discharge.

**Table 4.3: Tragus stimulation in the vagotomised WHBP significantly altered the ∫SND and PND rate during the recovery period**

| | | N | Mean | Std err | Min | Max | P value |
|---|---|---|---|---|---|---|---|
| **HR (bpm)** | **Vagotomised** | 10 | 319.95 | 4.78 | 294.83 | 346.27 | |
| | **Stimulation** | 10 | 318.89 | 5.03 | 288.60 | 341.96 | 0.529 |
| | **Post Stimulation** | 10 | 317.65 | 5.03 | 287.04 | 339.23 | 0.248 |
| | **Recovery** | 10 | 316.86 | 4.95 | 282.27 | 334.06 | 0.221 |
| **PP (mmHg)** | **Vagotomised** | 10 | 57.21 | 3.29 | 43.68 | 74.05 | |
| | **Stimulation** | 10 | 57.40 | 3.21 | 43.44 | 74.38 | 0.564 |
| | **Post Stimulation** | 10 | 57.91 | 3.65 | 43.52 | 80.65 | 0.352 |
| | **Recovery** | 10 | 58.32 | 4.07 | 43.88 | 86.66 | 0.434 |
| **RSA (Δbpm)** | **Vagotomised** | 10 | 4.22 | 1.05 | 1.80 | 11.46 | |
| | **Stimulation** | 10 | 4.63 | 1.58 | 1.83 | 16.69 | 0.678 |
| | **Post Stimulation** | 10 | 3.72 | 1.11 | 1.23 | 11.92 | 0.086 |
| | **Recovery** | 10 | 3.70 | 1.07 | 1.09 | 11.40 | 0.068 |
| **∫SND (AUC)** | **Vagotomised** | 8 | 4.01 | 0.16 | 3.31 | 4.48 | |
| | **Post Stimulation** | 8 | 3.45 | 0.21 | 3.31 | 4.48 | 0.069 |
| | **Recovery** | 8 | 3.24 | 0.30 | 1.75 | 4.58 | 0.041* |
| **PND rate (rpm)** | **Vagotomised** | 10 | 19.00 | 1.35 | 13 | 24 | |
| | **Stimulation** | 10 | 19.10 | 1.69 | 12 | 26 | 0.832 |
| | **Post Stimulation** | 10 | 20.30 | 1.78 | 13 | 30 | 0.064 |
| | **Recovery** | 10 | 20.20 | 1.63 | 13 | 28 | 0.044* |

**Table 4.4: Significant changes of the expiratory and total phase duration (seconds) in response to tragus stimulation in vagotomised WHBP**

| | | Ti (s) | Te (s) | Ttot (s) |
|---|---|---|---|---|
| **Baseline** | **Average** | 0.91 | 2.85 | 3.76 |
| | **Std error** | 0.03 | 0.23 | 0.23 |
| **Stimulation** | **Average** | 0.88 | 2.67 | 3.55 |
| | **Stderror** | 0.06 | 0.29 | 0.27 |
| | **P value** | 0.603 | 0.275 | 0.103 |
| **Post stimulation** | **Average** | 0.91 | 2.67 | 3.57 |
| | **Stderror** | 0.05 | 0.26 | 0.25 |
| | **P value** | 0.832 | 0.205 | 0.166 |
| **Recovery** | **Average** | 0.90 | 2.35 | 3.25 |
| | **Stderror** | 0.05 | 0.21 | 0.21 |
| | **P value** | 0.848 | 0.003** | 0.006** |

## 4.6.4 Functional study to determine the effect of tragus stimulation following upper cervical (C1-C3) afferent nerve section

In the anatomical study, significant afferent labelling from the tragus was visualised in the dorsal horn of the C1-C3 segments of the spinal cord. We were intrigued if afferent projections from the tragus into these classical sensory pathways had a role in autonomic respiratory modification due to electrical stimulation. Here the functionality of this sensory innervation was tested by cutting the afferent nerves in the WHBP and examining the physiological effects **(Table 4.5 and Figure 4.9)** due to tragus stimulation.

The recorded HR before the stimulation was 277.4 ± 17.4 bpm (n=10). Repeated measures ANOVA revealed a significant elevation of HR after tragus stimulation $F_{(1.4, 12.2)}$=4.4,p=0.048 (287.4 ± 17.2 bpm, p=0.047), post stimulation (294.6 ± 16.2p= 0.038). Further increases in HR were observed during the recovery (307.6 ± 18.4 bpm, p=0.038).

The basal average of the PP recorded from the distal end of the aorta was 65.4 ± 5.1 mm Hg. Tragus stimulation did not significantly affect the PP (64.2 ± 5.2 mm Hg). The PP significantly reduced ($\chi^2(3)$=12.720,p=0.022) to 63.0 ± 5.4 mmHg when the stimulation stopped p=0.037 (. The arterial depressor effect persisted until the recovery period (61.9 ± 5.9 mmHg) (p=0.028).

The recorded RSA baseline was 15.36 ± 3.76 Δbpm. Electrical stimulation on the tragus did not significantly affect the RSA during the stimulation (13.4 ± 3.0 Δbpm; p=0.093). During post stimulation, however, the RSA significantly dropped $F_{(1.2,10.9)}$=5.5, p=0.034 with the reduction maintained during the recovery (Post stimulation; 8.66 ± 1.4 Δbpm; p=0.043; Recovery; 9.08 ± 1.9; p=0.036).

The integrated SND from the lower thoracic level was initially recorded at 3.82 ± 0.72 AUC. Electrical stimulation of the tragus had no effect on the sympathetic nerve activity at any of the time points (Post stimulation= 3.81± 0.75 AUC; p = 0.693) (Recovery= 2.97± 0.53 AUC; p = 0.141).

The effects of tragus stimulation also were measured on the respiratory frequency of the preparations $F_{(1.1, 7.9)} = 8.1$, $p = 0.020$ as well as the duration of the inspiratory/expiratory phase. The baseline respiratory rate (17.8 ± 1.47 rpm) was significantly increased during the stimulation (18.6 ± 1.6 rpm)($p = 0.006$). Further elevation on respiratory activity was seen during the post stimulation (20.3 ± 1.63) ($p < 0.001$) and also recovery (21.0 ± 2.3 rpm) ($p = 0.019$). Statistical analysis on the inspiratory, expiratory and total respiratory duration however showed non-significant changes due to the stimulation. The details of this analysis are included in **Table 4.6.**

A

| | Baseline | Post-Stimulation | Recovery |

HR BPM
310
280
10 bpm
4 bpm
3.5 bpm

SND µV
75
-75

∫SND µV
20
10

PND µV
75
-75

AP mmHg
70
55

1 sec

B

Heart Rate (bpm)

C

Pressure (mmHg)

D

RSA (bpm)

E

∫SND (AUC)

F

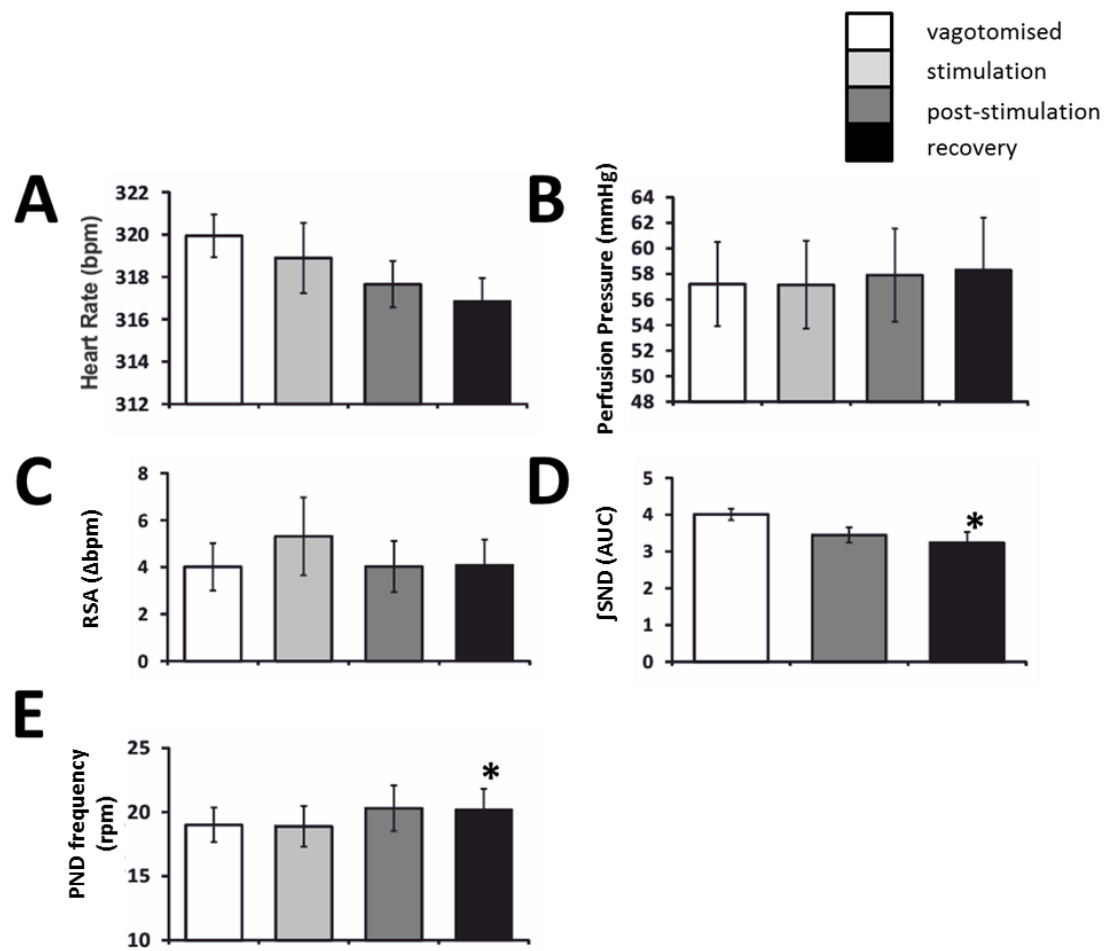Respiratory frequency (rpm)

Baseline
stimulation
post-stimulation
recovery
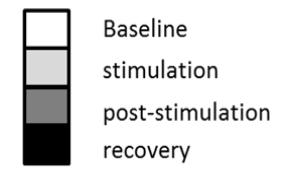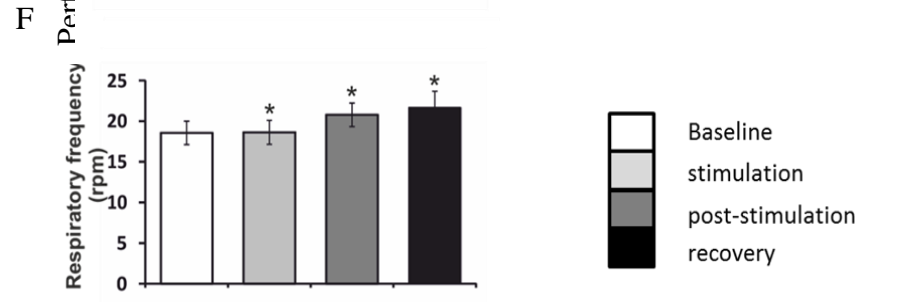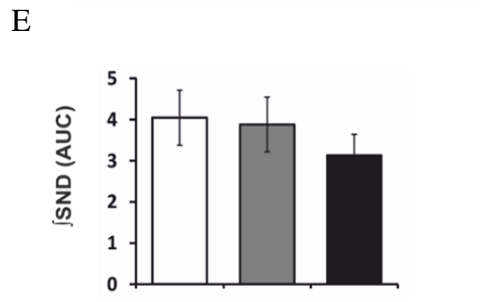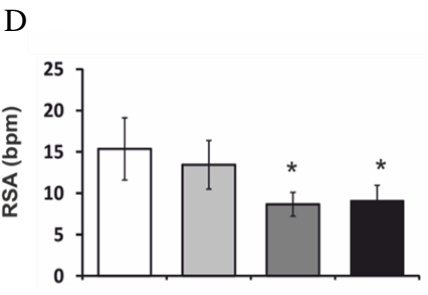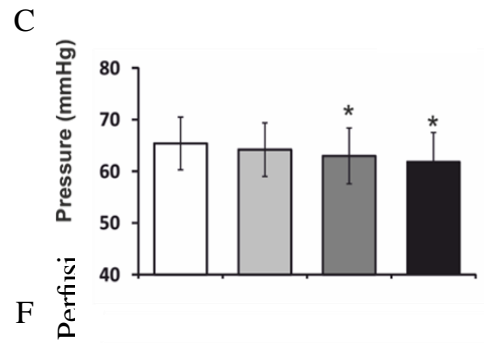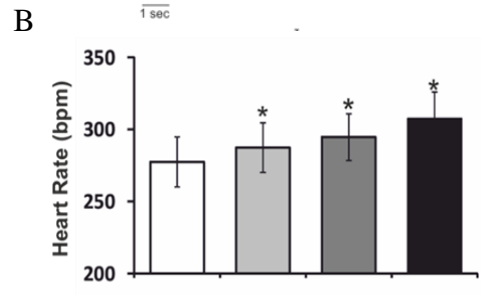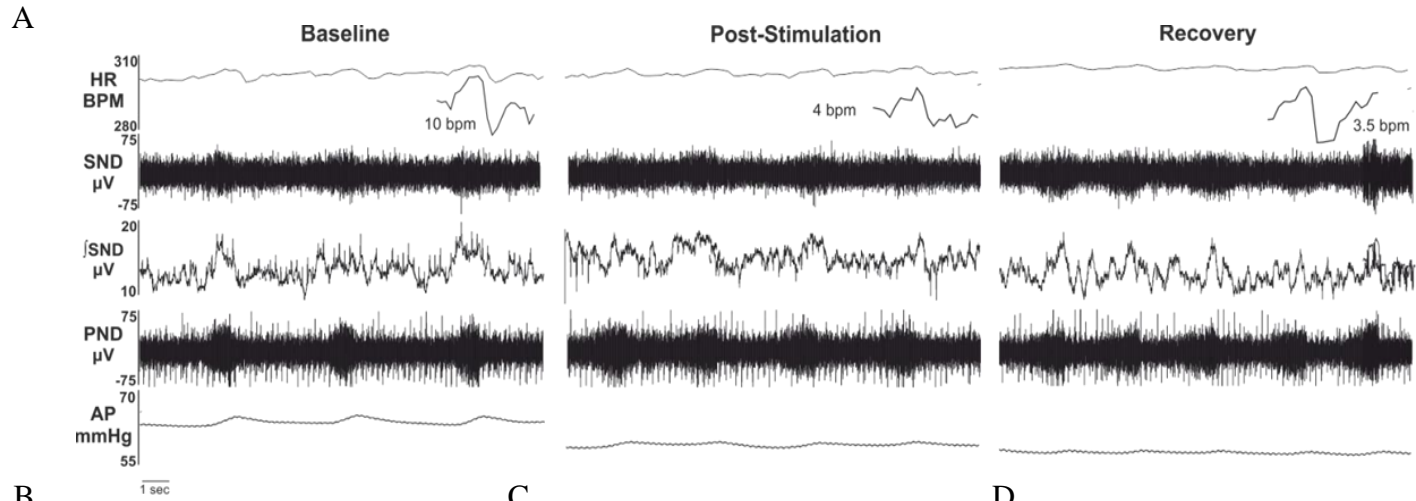
**Figure 4.9: The effect of tragus stimulation on physiological variables recorded from the Working Heart Brainstem Preparation of the upper cervical afferent nerve severed animals (C1-C3)**

Tragus stimulation in the upper cervical nerve severed animals significantly reduced the arterial pressure and also the RSA after the stimulation stopped. The HR and respiratory frequency immediately increased due to the stimulation where the elevation is maintained until the recovery period. The SND and respiratory duration showed no effects in response to the ear stimulation. *, $p < 0.05$; **, $p < 0.01$; ***, $p < 0.005$. HR – heart rate, RSA – respiratory sinus arrhythmia, SND – sympathetic nerve discharge.

**Table 4.5: Tragus stimulation in the upper cervical nerve transected WHBP significantly caused physiological alteration without affecting the sympathetic activity**

| | | N | Mean | Std err | Min | Max | P value |
|---|---|---|---|---|---|---|---|
| **HR (bpm)** | **Baseline** | 10 | 277.41 | 17.35 | 193.87 | 373.11 | |
| | **Stimulation** | 10 | 287.39 | 17.15 | 196.22 | 368.64 | 0.047* |
| | **Post stimulation** | 10 | 294.63 | 16.20 | 238.56 | 369.03 | 0.038* |
| | **Recovery** | 10 | 307.58 | 18.38 | 238.07 | 411.91 | 0.038* |
| **PP (mmHg)** | **Baseline** | 10 | 65.39 | 5.11 | 48.59 | 107.79 | |
| | **Stimulation** | 10 | 64.18 | 5.18 | 47.72 | 107.38 | 0.093 |
| | **Post stimulation** | 10 | 62.96 | 5.40 | 46.52 | 107.43 | 0.037* |
| | **Recovery** | 10 | 61.89 | 5.62 | 45.21 | 107.18 | 0.028* |
| **RSA (Δ bpm)** | **Baseline** | 10 | 15.36 | 3.76 | 1.10 | 33.46 | |
| | **Stimulation** | 10 | 13.44 | 2.95 | 1.29 | 28.08 | 0.169 |
| | **Post stimulation** | 10 | 8.66 | 1.44 | 1.49 | 14.20 | 0.043* |
| | **Recovery** | 10 | 9.077 | 1.88 | 0.88 | 17.65 | 0.036* |
| **∫SND (AUC)** | **Baseline** | 8 | 3.82 | 0.72 | 0.83 | 6.65 | |
| | **Stimulation** | 8 | 3.34 | 0.59 | 1.16 | 5.90 | 0.197 |
| | **Post stimulation** | 8 | 3.81 | 0.75 | 1.03 | 6.89 | 0.693 |
| | **Recovery** | 8 | 2.97 | 0.53 | 1.16 | 4.75 | 0.141 |
| **PND frequency (rpm)** | **Baseline** | 8 | 17.75 | 1.47 | 10 | 22 | |
| | **Stimulation** | 8 | 18.63 | 1.58 | 10 | 23 | 0.006** |
| | **Post stimulation** | 8 | 20.25 | 1.63 | 12 | 25 | 0.001*** |
| | **Recovery** | 8 | 21.00 | 2.30 | 10 | 30 | 0.019** |

**Table 4.6: No changes of respiratory phase duration in response to tragus stimulation**

|  |  | Ti (s) | Te (s) | Ttot (s) |
|---|---|---|---|---|
| **Baseline** | **Average** | **1.40** | **3.10** | **4.49** |
|  | **Std error** | **0.14** | **0.65** | **0.71** |
| **Stimulation** | **Average** | **1.43** | **2.90** | **4.33** |
|  | **Stderror** | **0.10** | **0.55** | **0.56** |
|  | **P value** | **0.78** | **0.221** | **0.46** |
| **Post stimulation** | **Average** | **1.37** | **2.49** | **3.86** |
|  | **Stderror** | **0.11** | **0.39** | **0.38** |
|  | **P value** | **0.58** | **0.166** | **0.21** |
| **Recovery** | **Average** | **1.28** | **2.23** | **3.51** |
|  | **Stderror** | **0.09** | **0.36** | **0.36** |
|  | **P value** | **0.58** | **0.120** | **0.13** |

## 4.7 Discussion

The major findings from these anatomical and functional studies include:

- The main termination sites for afferents labelled from the tragus were in the upper cervical spinal cord, especially C2 and C3.
- In the brainstem, the NTS and Pa5 received afferent inputs, with the Pa5 more densely innervated than the NTS.
- The anterogradely labelled afferents make rare close appositions with ChAT, Calb-28k, Parv, NKR1, and GAD67 immunoreactive cells.
- Tragus stimulation elicited a decrease in HR and PP, accompanied by a sympathoinhibition. The RSA and breathing activity were not changed.
- The decrease in cardiovascular parameters were absent when tragus stimulation was applied in the vagotomized preparation. Sympathoinhibition was observed during the post-stimulation period, alongside an increase in respiratory frequency.
- Sympathoinhibition was absent when tragus stimulation was applied in upper cervical afferent nerve transected preparations. This was accompanied by a significant increase in HR and respiratory activity. The PP and RSA were decreased after stimulation.

The summary for these changes can be found in **Table 4.7** below.

**Table 4.7: Summary of major effects of tragus stimulation in different WHBP preparations (ns = no significant change)**

| Preparation | HR | PP | RSA | SND | PND |
|---|---|---|---|---|---|
| Fully intact | ↓ | ↓ | ns | ↓ | ns |
| Vagotomized | ns | ns | ns | ↓ | ↑ |
| C1 – C3 transected | ↑ | ↓ | ↓ | ns | ↑ |

## 4.7.1 The cervical spinal cord dorsal horn is a major termination site for sensory afferents from the tragus.

A significant finding was that the major sensory projections from the tragus were to the dorsal horn of the C1-C3 cervical spinal cord. The labelled afferents on the upper cervical cord covered laminae I, III & IV. Similar labelling in the dorsal horn has been mentioned previously when CTB was injected into the inner concha of rats, but no images or other analyses were shown (He *et al.*, 2013). This is therefore the first study to reveal the large extent of afferent signalling from the tragus to the cervical spinal cord.

**Afferent projections from the tragus to the upper cervical dorsal horn participate in responses to tragus stimulation.**

Since neuronal tracing from the tragus revealed primary afferents terminating in the superficial and deep laminae of the upper cervical spinal cord (C1-C3), the potential contribution of these afferents to tragus evoked responses was tested by transecting the upper cervical dorsal roots. Interestingly, the sympathoinhibition normally elicited by tragus stimulation was absent following sectioning of these cervical nerves. Therefore, this suggests the

afferents projecting into the dorsal horn play an important role in mediating the sympathoinhibition from tragus stimulation.

Upper cervical spinal cord influences on autonomic cardiovascular control has been observed in various spinal cord stimulation (SCS) studies. An early spinal cord stimulation study (including lower cervical levels) in non-acute coronary syndrome patients showed a decrease in resting HR during stimulation that was pharmacologically shown to be mediated by a sympathoinhibition (Meglio *et al.*, 1987). In another study in anaesthetised rats, SCS resulted in an increase in peripheral circulation in the muscle and skin measured using laser Doppler flowmetry which was mediated by sympathoinhibition as it was inhibited by postganglionic $\alpha-$adrenoceptor blockade (Linderoth *et al.*, 1994). Since such spinal cord stimulation is mediated by electrodes placed adjacent to the dorsal surface of the spinal cord, it is easy to envisage how this could activate the primary afferent fibres and terminals within the dorsal horn, leading to sympathoinhibition similar to that observed to tragus stimulation.

Curiously, the decrease in HR usually observed to tragus stimulation was reversed to an increase on stimulation after C1-C3 nerve section. It seems possible that the increase in HR is mediated by a decrease in parasympathetic outflow in these preparations, since the vagally mediated respiratory sinus arrhythmia decreased and SND did not change. Direct recordings of cardiac vagal nerve in future studies would clarify this issue. Nevertheless, the changes suggest that another afferent pathway from the tragus can also influence autonomic outflow, likely mediated via brainstem afferents.

**Possible neuronal pathways via the cervical cord dorsal horn mediating the effects of tragus stimulation**

Dorsal horn neurons are typically associated with conveying sensory information from the skin and internal organs into the spinothalamic tract for pain perception processing (Todd, 2010). However, although less well appreciated, neurons in the superficial laminae of the cervical dorsal horn also provide synaptic input into cardiovascular and respiratory centres in the medullary reticular formation. Injections of anterograde tracer into the superficial (I-II) of the cervical dorsal horn in rats revealed projections predominantly concentrated in the medial part of the commissural subnuclei of the NTS at caudal levels, whilst the deeper laminae showed predominant labelled fibres and terminals only in the ventrolateral and dorsolateral portions of the caudal NTS (Gamboa-Esteves *et al.*, 2001). In a similar experiment, anterograde neuronal tracer microinjection covering laminae I-V of the cervical spinal dorsal horn of rats, which revealed labelled axons in the medial, dorsomedial and commissural subdivisions of the caudal NTS, with most of the staining ipsilaterally (Potts *et al.*, 2002). In addition, projections to other brainstem regions involved in autonomic control were also observed – including the caudal and rostral ventrolateral medulla, which play a significant role in the control of autonomic function. Hence, this suggests afferent projections from the tragus can indirectly influence brainstem regions involved in autonomic and respiratory function via the cervical spinal cord. Future studies could investigate this proposition by injecting the tragus with viruses that travel only in the anterograde direction, such as select rabies viruses (Zampieri *et al.*, 2014).

There is also a possibility that some of the effects of activating cervical sensory afferents are mediated through connections within the spinal cord. For example, application of glutamate pledgets to the dorsal surface of rat C1-C2 spinal cord increased intercostal nerve and phrenic nerve activity and this persisted after spinal transection at rostral C1, indicating it was a spinally mediated response (Lu *et al.*, 2004). However, the pledget application of

glutamate is likely to activate many neurons, making it difficult to identify the activated pathways. There are neurons in the cervical spinal cord that are pre-sympathetic as they are labelled following transneuronal virus application to the stellate ganglion (Jansen & Loewy, 1997), but they are located laterally in the white matter and so appear unlikely to be innervated by the tragus afferents, although their dendritic architecture is unknown and it is possible that these dendrites lie within the afferent termination fields. The circuitry underlying the cervical cord mediation of tragus evoked responses therefore requires further examination.

## 4.7.2 Pa5 is likely to be involved in the tragus evoked responses

Following injection of CTB into the tragus, a prominent projection was to the Pa5 in the brainstem. The Pa5 is a small collection of neurons within the dorsal lateral medullary spinal trigeminal tract that receives input from the jugular ganglion since injection of $CTB_{488}$ into the Pa5 of guinea pigs labelled jugular ganglion neurons, whilst injection of $CTB_{555}$ into the NTS labelled predominantly the nodose ganglion (McGovern et al., 2015). The input from the jugular ganglion to the Pa5 is consistent with observations in the cat that the ABVN sensory somata are within the jugular ganglion (Nomura & Mizuno, 1984) and the Pa5 tragus projections observed in this study.

Previous studies have revealed roles for the Pa5 consistent with a role in mediating the tragus influences on cardiovascular and respiratory function. The Pa5 also receives sensory input from airways - anterograde trans-neuronal viral tracing from the trachea of rats identified tracheal sensory inputs towards the Pa5 that were relayed in the brainstem to the spinal trigeminal complex (McGovern et al., 2015). This input is involved in respiratory reflexes, revealed by a study performed on guinea pigs with a selective recurrent laryngeal nerve section to remove nodose ganglion inputs (eliminating the cough reflex), but leaving afferents via the jugular ganglion intact. Electrical laryngeal stimulation evoked a frequency dependent respiratory slowing and

a mild decrease in blood pressure. Both of these responses were abolished when the Pa5 was inhibited by muscimol injections (Driessen *et al.*, 2015). The respiratory slowing is similar to the trend observed when the tragus was stimulated in the intact WHBP (but significance was not achieved), but opposite to that when the C1-C3 nerves were sectioned where PND increased to tragus stimulation. Indeed, the increase in PND in response to tragus stimulation in the C1-C3 nerve sectioned WHBP is similar to phrenic nerve responses in fictive cough evoked by mechanical or electrical stimulation of the trachea (Baekey *et al.*, 2001). Since approximately 4% of the population coughs when cleaning their ears, the so-called Arnold's reflex (Murray *et al.*, 2016), this may reflect a role for the tragus afferents to the Pa5 in some cases.

In addition to a role in respiratory control, neurons in Pa5 have been suggested to have a role in baroreceptor reflex modulation. Electrophysiological recording from Pa5 neurons in anaesthetic free rats showed that a large percentage (~35%) increased firing rate in response to intravenous phenylepinephrine injection (Yu & Lindsey, 2003). The functional role of the Pa5 in baroreflex control was later tested in anaesthetic free rats that underwent Pa5 ablation. Not only was a reduction in the baroreceptor reflex sensitivity ($\Delta HR/\Delta AP$) observed, resting AP and HR decreased, whilst respiratory rate increased; comparable to basal changes on lesioned NTS rats (Yu & Lindsey, 2003). It therefore seems possible that the tragus projections to the Pa5 could be involved in the stimulation evoked autonomic and respiratory changes.

### 4.7.3 The afferent projection from the tragus to the NTS is limited

Although the NTS is the main target for vagal and glossopharyngeal sensory afferents (Grélot *et al.*, 1989), very few labelled afferents were found in the NTS following tragus injections of CTB in this study. This is similar to labelling from the concha, which was minimal and restricted to the medial NTS (He *et al.*, 2013). Although according to human cadaveric dissections both of these

auricular regions are vagally innervated, they are also innervated by other nerves (Peuker & Filler, 2002). Therefore, the projection to the NTS may reflect that each of these areas only receives a small innervation from the ABVN. There have been no studies where the ABVN in rats has been specifically labelled, probably due to relative inaccessibility for recovery surgery. However, in cats application of HRP to the ABVN also resulted in labelling that was not predominantly in the NTS, but rather the spinal trigeminal nucleus and cervical cord dorsal horn (Nomura & Mizuno, 1984). It is therefore possible that the NTS is not in fact a major target of the ABVN sensory afferents.

The lack of projection from the external ear direct to the NTS appears at first glance contradictory to a functional study - when the auricular dermatomes in anaesthetised rats were stimulated by electrical stimulation (100 Hz, 1mA) or manual acupuncture and the pattern of cardiovascular and gastric responses were documented. A mild depressor response (6%-12%) was noted in the BP, HR, and intragastric pressure from manual and electrical stimulation of the ear regardless of the stimulation area (Gao *et al.*, 2008). Further, manual stimulation on the auricular area with the ABVN innervation (e.g. concha) revealed significant activation of the neurons in the NTS with cardiac related activity (presumed baroreceptive cells) which was associated with inhibition of the AP and HR (Gao *et al.*, 2011). However, it is possible that the pathway underlying activation of these NTS 'baroreceptive' neurons is not through the NTS, but through the spinal cord cervical dorsal horn as discussed above.

## 4.7.4 Comparison with effects of tragal stimulation in humans

Tragus stimulation in rats WHBP showed reduction in the central sympathetic chain where the inhibition remained during the 10 minutes of post-stimulation. This was a main highlight of this study since there no other literature has ever performed similar stimulation in anaesthetic free animal models and demonstrated sympathoinhibition directly from the sympathetic nerve. The nearest direct sympathetic demonstration due to tragus stimulation was done

in healthy human subjects (200µs, 30 Hz, 1-50 mA, 15 minutes stimulation) in which a significant muscle sympathetic nerve reduction was measured during the stimulation (Clancy *et al.*, 2014). The cardiovascular autonomic control measured from the HRV analysis indicated a shift towards parasympathetic predominance. The autonomic parameters in Clancy's study did not return fully to baseline in 15 minutes post-stimulation, similar to the maintained sympathoinhibition seen here. This sympathoinhibition may have some therapeutic usefulness since 1 hour of low-level tragus electrical stimulation suppressed atrial fibrillation in patients with induced AF (Stavrakis *et al.*, 2015). However, the interpretation of the pathways underlying the tragus evoked effects may need to be reconsidered. Clancy *et al.* (2014) and Murray *et al.* (2016) suggested that tVNS works via a sensory projection to the NTS which interacts with the circuitry established to be involved in sympathetic control, but since there were few afferents in the NTS in this study this seems unlikely (assuming rat and humans share similar anatomy). Rather, it seems more likely that the afferents to the spinal cord are involved in the sympatho - inhibition as this was absent in the C1-C3 sectioned animals. This may influence future stimulation sites in humans since different areas in the external ear receive different degrees of innervation from the ABVN, the auriculo-temporal nerve and the great auricular nerve (GAN). Indeed, since the GAN provides significant input to the cervical spinal cord dorsal horn, the autonomic and respiratory effects of direct stimulation of the relevant auricular areas could be interesting.

### 4.7.5 Does tragus stimulation involve vagal efferent activation to cause heart rate decreases?

When tragus stimulation experiments were performed in the vagotomised preparations, there was no significant decrease in heart rate, which could suggest that vagal efferent activation was involved. However, there was a downward trend in the HR responses in these vagotomised preparations and in the intact WHBP, there was no change in RSA, seeming to exclude a

change in vagal activity but rather point to the reduced sympathetic nerve activity as the reason for the decreases in heart rate. On the other hand, tragus stimulation elicited inhibition of atrial remodelling and atrial fibrillation induced by atrial pacing, was eliminated in bi-vagal transected anaesthetized dogs, suggesting that vagal efferent fibres to play a role in the cardiovascular response to tVNS (Yu *et al.*, 2013). Direct recordings of cardiac vagal nerve activity during tragus stimulation could resolve these differences.

## 4.7.6 Does the autonomic changes from tragus stimulation is affecting the respiratory frequency?

Breathing is an activity that requires contraction of respiratory muscles which are coordinated by the respiratory motor control system. This requires integration of inputs from the brainstem, spinal cord, and also peripheral nerves. The autonomic control of the breathing arises through the chemoreflex, as discussed earlier in the Introduction. In controlled WHBP conditions (e.g.: stable oxygen and carbon dioxide levels, and pH) respiratory activity was expected to remain constant. Any changes in respiratory activity from ear stimulation is non-autonomic related (e.g.: Pa5 activation). Indeed, as seen in all stimulation experiments in this chapter the sympathoinhibition was not accompanied by changes in respiratory activity.

### 4.7.7 Potential postsynaptic targets of anterogradely labelled afferents from the tragus

To determine if a particular neurochemical cell type was innervated by the tragal afferents, potential postsynaptic targets were identified using immunofluorescence. Despite staining for a number of markers known to be present in second order neurons (ChAT, calbindin, NK1R, GAD67), no one cell type received significant innervation. Considering the diverse projections from the tragus to different brain regions, further studies will need to conduct a systematic review of postsynaptic targets in each region, perhaps using a different strategy for cell type markers in each region.

## 4.8 Conclusions

Sensory afferents from the rat tragus projected heavily to the dorsal horn of the upper cervical spinal cord, and in the brainstem significantly to the Pa5 but to a lesser extent in the NTS. Potential neurochemical characteristics of the postsynaptic targets were ChAT, Calb, Parv, NKR1 and GAD67 cells, although no one group was densely innervated. Stimulating the tragus resulted in sympathoinhibition recorded from the lower thoracic sympathetic chain, accompanied by a decrease in HR and PP. Since the neuronal tracing showed the upper cervical cord was significantly innervated by afferents originating from the tragus, the importance of this sensory afferent innervation to tragus evoked responses was then tested in C1-C3 ipsilateral nerve transected WHBP. The absence of sympathoinhibition in this preparation suggest reductions in sympathetic nerve activity were mediated through these projections.

# Chapter 5 An anatomical and functional study of the central afferent nerve projections innervating from the rat earlobe

## 5.1 Introduction

In the previous chapter, electrical stimulation of the tragus reduced the sympathetic nerve discharge from the lower thoracic sympathetic chain. This was consistent with a previous human study where tVNS reduced muscle sympathetic nerve activity measured using microneurography (Clancy *et al.*, 2014). It was postulated that the effects of tragus stimulation were due to activation of the ABVN. However, injection of the neuronal tracer CTB into the tragus resulted in dense afferent labelling in the dorsal horn of the upper cervical spinal cord, in addition to the NTS and Pa5 in the medulla oblongata. This suggests a major non-vagal sensory innervation of the tragus. Indeed, human cadaver examination suggested that the tragus also receives innervation from the GAN, almost to the same degree as the ABVN. The GAN is composed from the cervical plexus of the C2 and C3 spinal nerve and provides sensory innervation for the skin surrounding the auricular area. The potential relevance of GAN innervation in tragus stimulation was then examined through upper cervical transection WHBP. The sympathetic inhibition which was present in the fully intact and vagotomised preparations was absent in this preparation. This suggests involvement of the GAN innervation in the autonomic responses to tragus stimulation.

A previous study by Peuker and Filler 2002 suggested that the GAN is the only nerve innervating the human ear lobule (Peuker & Filler, 2002). Assuming that GAN innervation within the lobule is similar in rats, this auricular region was stimulated in the WHBP preparation. Further, afferent projections from the lobule were studied with CTB to try to understand the central activation pathways for any physiological effects.

### 5.1.1 Anatomy of the Great Auricular Nerve

An early anatomical study to determine the origin and course of the GAN was performed in rabbits. The GAN receives a major contribution from the anterior primary division of the third cervical nerve, with a smaller extent from the posterior primary division of the second cervical nerve (Weddell *et al.*, 1955a) **(Figure 5.1A)**. In humans, the GAN leaves the cervical plexus winding around the posterior margin of the sternocleidomastoid muscle. It penetrates the parotid capsule antero-superiorly before separated into the anterior and posterior terminal branches **(Figure 5.1B)** (Ginsberg & Eicher, 2000). While the anterior branch supplies the skin covering the parotid gland and lower pre-auricular region, this bifurcation also introduce the posterior branch that is destined to reach the posterior aspect of the auricle (Weddell *et al.*, 1955a; Weddell *et al.*, 1955b). As its name suggest, there is a large GAN innervation into the postero-inferior region of the auricle principally covering the area of the tail of helix, scapha and also the lobule of the auricle as seen in rabbits and humans (Figure 5.1C) (Peuker & Filler, 2002). In different parts of the auricle, the posterior branch of GAN communicates with the auricular branch of the vagus nerve and also with the posterior auricular branch of the facial nerve (the Auriculotemporal Nerve).

The application of HRP on the central cut end of GAN nerve (region of sternocleidomastoids) in rabbits revealed afferent cell bodies in the ipsilateral dorsal root ganglion (C2-C3) and the superior cervical ganglion (Liu & Hu, 1988). Nerve fibres were detected in the dorsal column of the upper cervical spinal cord and strongly stained in laminae I-V at the C2 level. The afferent GAN projection also has intense labelling in the cranial nerve nuclei in the medulla, including caudal subnucleus of the spinal trigeminal nerve, the solitary nucleus predominantly within the dorsal and interstitial subnuclei, and also medial and lateral cuneate nuclei (Liu & Hu, 1988). The convergence of the GAN primary afferents on the upper cervical cord, trigeminal tract and the NTS was then suggested to play a role on the transmission of somatovisceral sensations. The projection of afferents from the lobule of the rat has, however, never been tested.

141
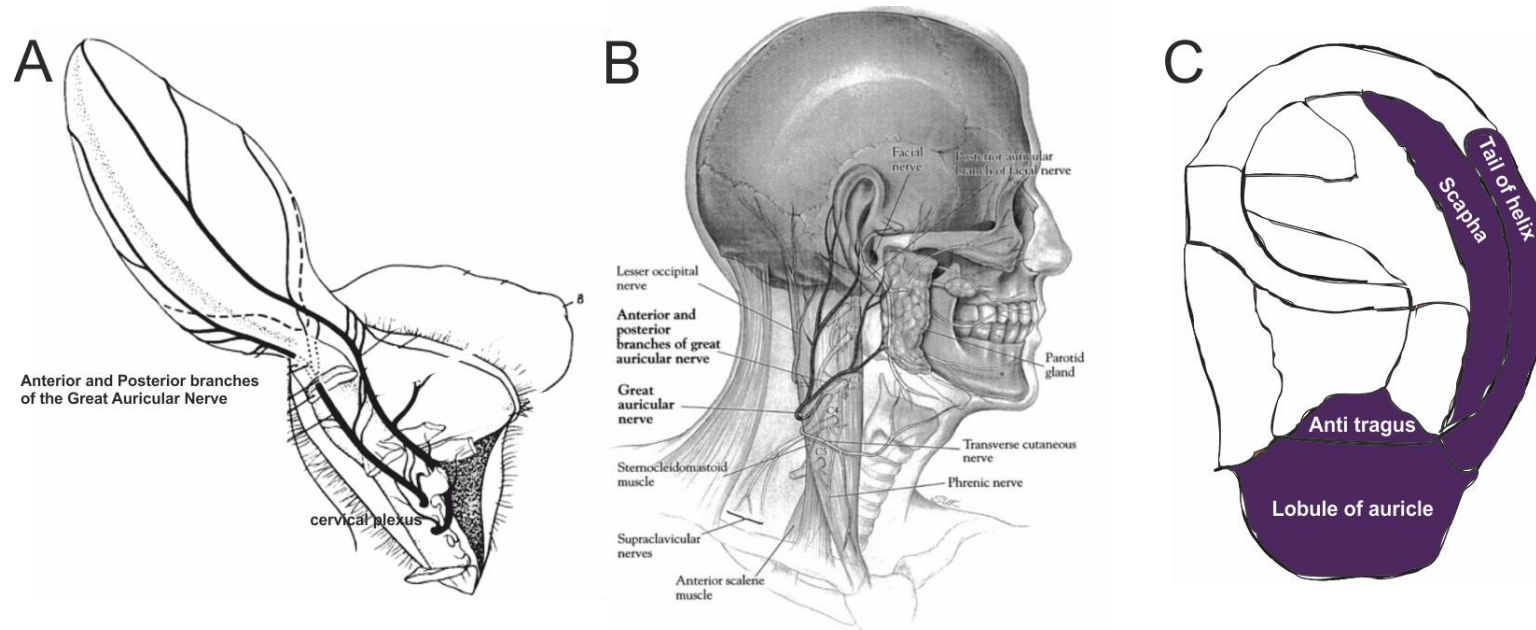
**Figure 5.1: Diagrammatic representation of the Great Auricular Nerve (GAN) origin from the cervical plexus and its major dermatome distribution area**

A) In rabbits, the GAN emerged from the cervical plexus originating from C2-C3 coursing superiorly and anteriorly, dividing into anterior and posterior branches. B) In humans, the GAN lies beneath the sternocleidomastoid muscle before changing course to the auricle area. C) Peripheral innervation of the GAN into humans auricle dermatome solely concentrated within the area tail of helix, scapha, anti-tragus and lobule of auricle. Source of image A) Weddell *et al.* (1955a), B) Ginsberg and Eicher (2000), C) Peuker and Filler (2002).

### 5.1.2 Physiological function of Greater Auricular Nerve

The GAN relays sensory information - such as tactile, thermal, and also pain sensations detected from the skin overlying the parotid gland, external ear and posterior auricular region. Functional sensations in the regions with GAN distributions were disturbed in some patients who underwent conventional parotidectomy procedures, where the GAN is occasionally sacrificed (Patel *et al.*, 2001; Ryan & Fee, 2006, 2009). Numerous difficulties have been listed from different studies where the GAN sensory loss lead to medical conditions (e.g.:- anaesthesia, paraesthesia), functional deficits (e.g.: difficulties when shaving, wearing earphones) thus increase risk of traumatic injuries, and also increase risk of neuromas. These medical side effects are however tolerable and improved in a long post-operative period, with the recovery potentially due to the regeneration of the GAN nerve fibres (Patel *et al.*, 2001). Pharmacological blockade of GAN assisted with ultrasound imaging among healthy volunteers reported total sensory loss by pin prick tests in several auricular areas. These include the tail of helix, antitragus and also ear lobe (Thallaj *et al.*, 2010). The benefits of this medical intervention would be specifically for patients with "Red ear syndrome", a rare condition with burning pain or discomfort from tactile stimulation. Patients who received this treatment reported to be symptom free for 8-week during control examination (Selekler *et al.*, 2009).

## 5.2   Research gap

Chapter 4 revealed that tragus stimulation instigated neuromodulation of the cardio-respiratory system in rats. Due to afferent heterogeneity in the tragus, it is unclear if the neuronal changes were elicited by the ABVN and/or GAN. Since the earlobe has exclusive innervation of the GAN at least in humans (Peuker & Filler, 2002) and rabbits (Weddell *et al.*, 1955a),the effects of lobe

stimulation in the rat WHBP were tested. In addition, the central sensory projections from the earlobe of the rat were examined.

## 5.3  Aims

- To determine the central projection of afferents from the ear lobule
- To determine the effects of lobule stimulation in the WHBP

## 5.4  Hypothesis:

- The major central sensory projection from the rat earlobe is to the cervical cord dorsal horn

- Ear lobe stimulation will cause a sympatho-inhibition similar to tragus stimulation.

## 5.5  Methodology

### 5.5.1 General Methodology

The neuronal tracing procedures that been used in this chapter has been discussed in detail in the General methodology **(Section 2.1)**. CTB was injected into the lobule of the ear to label afferents from there to the CNS. Since tragus injections did not detect any particular post synaptic cell phenotype, double labelling for different neurochemical cell types was not typically performed. CTB was localised with ChAT, since ChAT facilitates identification of preganglionic and motor nuclei.

The earlobe stimulation procedure are similar to that in tragus stimulation (Chapter 4 for ear stimulation). Briefly a DS3 Constant Current Isolated Stimulator (Digitimer Ltd, UK) connected to a modified metal ear clip attached to the right earlobe. Ear lobe stimulation was applied for 5 minutes (100 Hz, 2.5 mA) and the effects were compared during baseline, stimulation, post-stim

and also recovery period. The animals used in the WHBP are nighttime animals (n=10).

### 5.5.2 Statistical Analysis

The normality test for numerical datasets were appropriately explored with the Shapiro-Wilk test due to small sample size. The significant value of the normality test greater than 0.05 considered as normal, while below than 0.05 is considered to be deviated from a normal distribution.

For normal distributed data, the effects of electrical stimulation on the tragus were compared between baseline and other time points with repeated measure ANOVA. Any statistical significant values from the ANOVA test were then confirmed with Fisher's Least Significant Difference (LSD) post hoc test.

The non-normally distributed data was analysed with non-parametric analysis (Friedman test) using IBM SPSS Statistics 21. Identification of the significant points were made with the Wilcoxon signed-ranked test.

## 5.6   Results

### 5.6.1 Afferent labelling from the lobule

The perfused rat brains were sectioned and examined between Bregma -10.04 mm to upper C4 spinal segment. Areas with CTB labelling were ipsilateral and almost identical for each animal (n=4). Labelled afferents were detected in the Pa5 of the rostral brainstem sections (Bregma -13.30mm and Bregma -13.68) **(Figure 5.2A and Figure 5.2B)**. The mid brainstem section (Bregma -13.80 mm) has CTB labelled afferents observed within the Cu, extending medially towards the NTS **(Figure 5.2C)**. In the lower mid brainstem

region (Bregma -14.30), CTB labelled afferents were most prominent in the cuneate fasciculus (cf), along with a small termination in the NTS **(Figure 5.2D)**. In the most caudal brainstem section (Bregma -14.60 mm), only cf has CTB labelled afferents originating from the earlobe **(Figure 5.2E)**. CTB labelled afferents in mid brainstem were consistently observed within the region of ventrolateral NTS, although this labelling was sparse **(Figure 5.3)**.

CTB labelled afferents were detected in the dorsal horn of the upper cervical cord (C1-C4 levels) where close appositions with ChAT cells were occasionally observed **(Figure 5.4)**. A small area with labelled afferents was observed in the medio-dorsal aspect of laminae IV of C1 (**Figure 5.4A)**. In C2, labelling covered a larger area, including some of the central regions of laminae III, and IV **(Figure 5.4B)**. The largest degree of labelling was consistently observed in C3, covering a greater portion of the mediodorsal aspect of laminae III and IV, bordering but not intruding into lamina II **(Figure 5.4C)**.
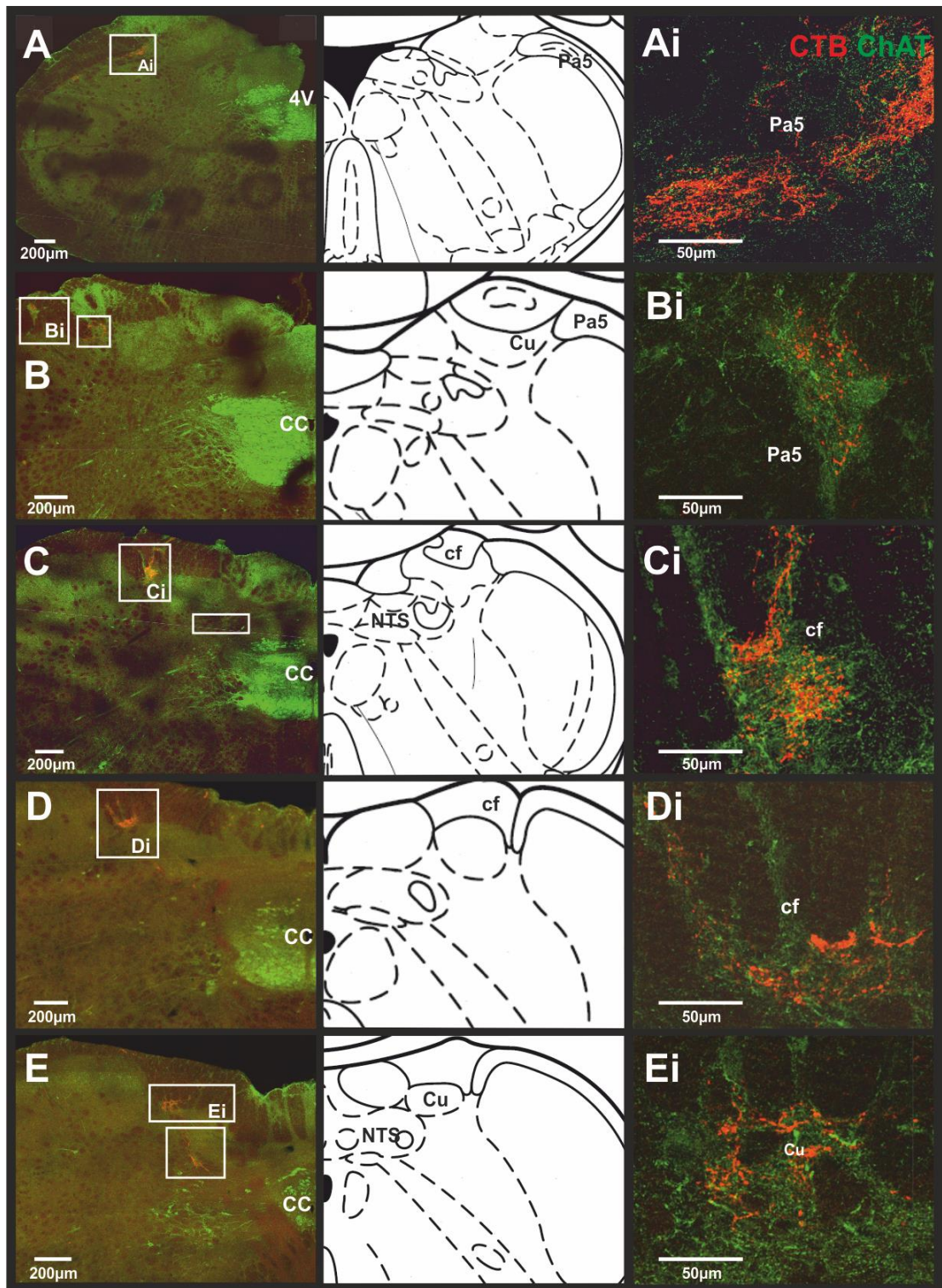
**Figure 5.2: Photomontages of the brainstem at different rostrocaudal levels with CTB-positive afferents labelled following cutaneous injection of CTB into the lobule (red) detected with ChAT immunofluorescence (green)**

A, B) Rostral brainstem sections with CTB labelled afferents evident in Pa5. C,D,E) Afferents labelled in the Cu, cf and also the NTS. (Ai-Ei) Magnified images illustrating labelled afferents. All terminating afferents are ipsilateral to the injection side. CC – central canal, NTS- nucleus tractus solitarius, cf- cuneate fasciculus, Cu- cuneate nucleus.
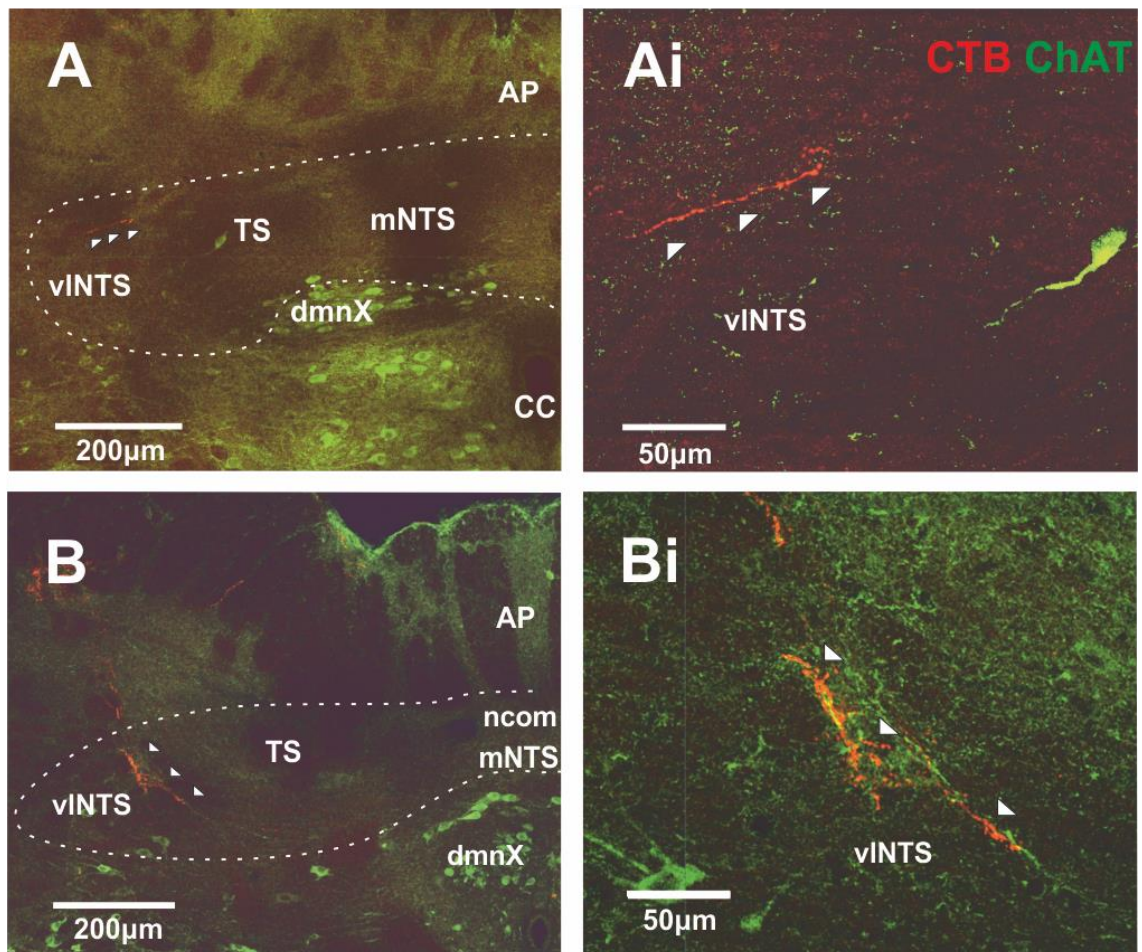
**Figure 5.3: CTB-positive afferents in the NTS region following injection into the lobule**

A) Example of a single, small labelled afferent in the ventrolateral NTS in rostral brainstem (magnified: Ai). B) Moving caudally, moderate labelled afferents also detected in the vlNTS Ai-Bi) Magnified figures for each of the labelled afferents in the NTS. NTS- nucleus tractus solitaries, CC – central canal, AP – area postrema, mNTS- medial NTS, ncom- commissural nuclei, TS- tractus solitaries, dmnX- dorsal nucleus of the vagus nerve.
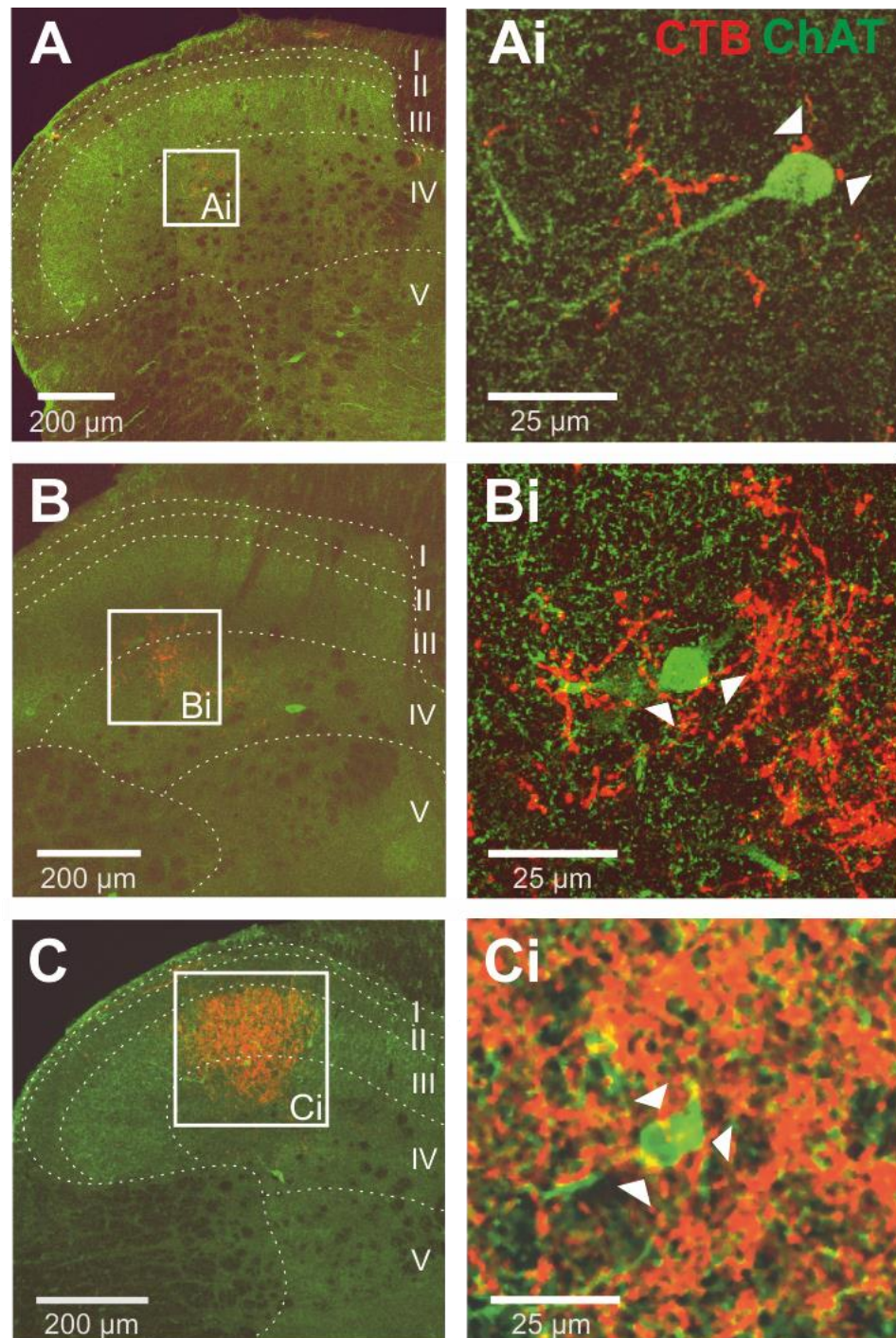
**Figure 5.4: CTB-positive afferents in the upper cervical cord following cutaneous injection of CTB into the lobule, detected with double staining of CTB and ChAT immunofluorescence.**

A) Cervical section at C1 with CTB-positive afferents terminating in laminae IV. B) Cervical section at C2 with CTB-positive afferents terminating in laminae III and IV. C) Cervical section at C3 with CTB-positive afferents largely terminating in laminae III and IV.

### 5.6.2 Functional study on lobule stimulation

The raw tracers on the effects of earlobe stimulation can be found on **Figure 5.5**. In general, lobule stimulation reduced RSA, SND and increase the PND frequency. The HR and PP was not affected by the stimulation.

Average HR (n=10) at baseline was 308.3 ± 5.1 bpm and this was not significantly affected by stimulation or during recovery (Stimulation = 310.4 ± 6.3 bpm; p=0.29; Post-stimulation=312.3 ± 6.17 bpm; p=0.16; Recovery = 314.2 ± 5.09 bpm; p=0.07) **(Figure 5.6A)**. Average PP from the distal aorta had a basal average of 68.3 ± 3.7 mm Hg, which was not significantly changed by stimulation (Stimulation = 67.7 ± 3.6 mm Hg; p=0.18; Post-stimulation=66.9 ± 3.47 mm Hg; p=0.08; Recovery = 66.1 ± 3.29 mm Hg; p=0.06) **(Figure 5.6B)**.

RSA during the baseline was 12.08 ± 3.18 Δbpm. Electrical stimulation of the lobule significantly reduced the RSA $\chi^2(3)=16.6, p=0.001$ during the stimulation (9.97 ± 2.3 Δbpm; p=0.015). During post stimulation, the RSA further dropped (7.17 ± 1.5 Δbpm; p=0.041) and such reduction continued into the recovery period (5.80 ± 1.3 Δbpm; p=0.033) **(Figure 5.6C)**.

The sympathetic nerve discharge measured directly from the sympathetic chain of the lower thoracic level was 4.27 ± 0.66 AUC at baseline. This SND was significantly reduced $\chi^2(2)=15.2, p=0.001$ after stimulation (2.88 ± 0.64 AUC; p=0.049). The sympatho-depressor effects were maintained during the recovery period (2.59 ± 0.55 AUC; p =0.036) **(Figure 5.6D)**.

The baseline respiratory rate (14.1 ± 1.54 rpm) was significantly increased $\chi^2(3)=16.2, p=0.001$ during the stimulation (16.2 ± 1.7 rpm;p=0.041). Further elevation of respiratory activity was also seen during the post stimulation (17.9 ± 3.2;p=0.009) and during the recovery (18.0 ± 3.1 rpm;p<0.008) **(Figure 5.6E)**. Statistical analysis on the duration of the different respiratory phases however revealed no significant alterations due to the stimulation. The only significant changes were in the total duration of the respiration during the recovery period, which was significantly reduced from the baseline (Baseline

151

4.37 ± 0.6 rpm vs Recovery 4.10 ± 0.7 rpm; P=0.004) **(Figure 5.6F)**. Further details of this analysis are included in **Table 5.1 and Table 5.2.**
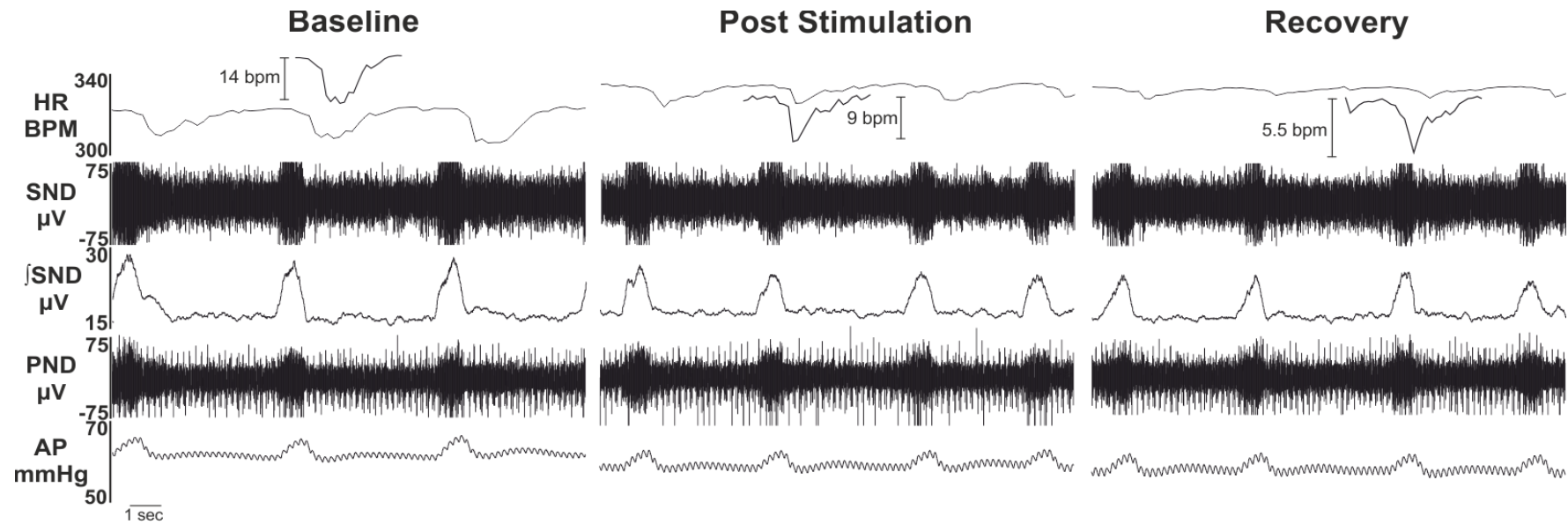
**Figure 5.5: Typical example of original traces recorded from lobule stimulation.**

Following lobule stimulation HR and PP were not significantly altered, RSA and the SND were reduced and, respiratory frequency increased. Original traces during the stimulation period were omitted due to stimulation artefact in nerve recordings. HR – heart rate, PP – perfusion pressure, RSA – respiratory sinus arrhythmia, SND – sympathetic nerve discharge.
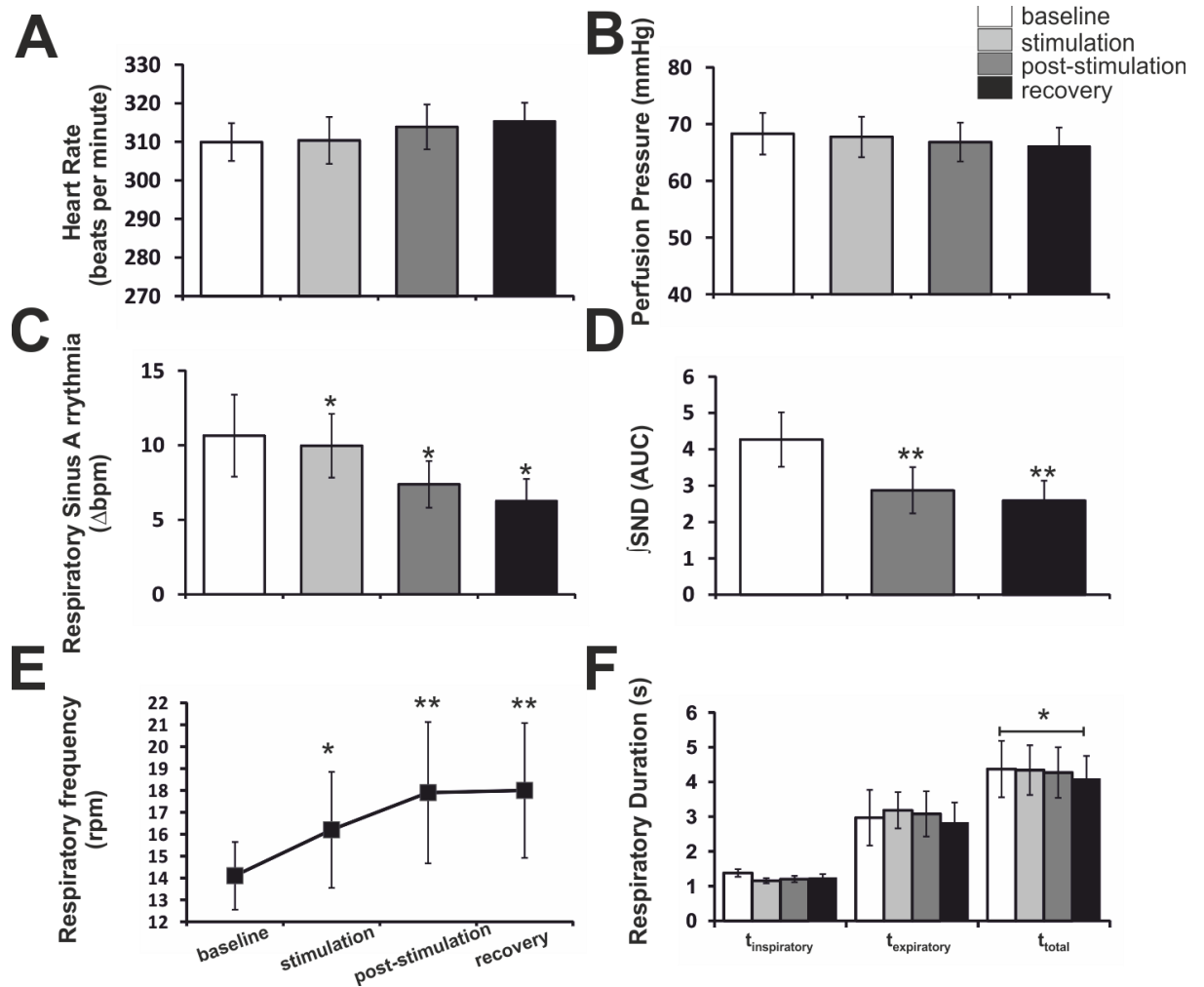
**Figure 5.6: The effect of lobule stimulation on autonomic and respiratory control in the Working Heart Brainstem Preparation**

Lobule stimulation did not significantly affect HR or PP, but did significantly reduce the RSA and SND. The respiratory frequency significantly increased during stimulation and persisted during the recovery period. The duration of the total respiratory cycle only showed significant reduction during the recovery. HR – heart rate, PP – perfusion pressure, RSA – respiratory sinus arrhythmia, SND – sympathetic nerve discharge.*, $p<0.05$; **, $p < 0.01$; ***, $p<0.005$.

154

**Table 5.1: Group data indicating that earlobe stimulation significantly caused sympathetic (SND) and parasympathetic (RSA) inhibition along with respiratory activation (PND rate)**

| | | N | Mean | Std err | Min | Max | P value |
|---|---|---|---|---|---|---|---|
| HR (bpm) | Baseline | 10 | 308.29 | 5.06 | 267.64 | 327.75 | |
| | Stimulation | 10 | 310.39 | 6.34 | 261.63 | 341.39 | 0.288 |
| | Post stimulation | 10 | 312.34 | 6.17 | 265.04 | 342.79 | 0.157 |
| | Recovery | 10 | 314.21 | 5.09 | 282.26 | 344.70 | 0.070 |
| PP (mmHg) | Baseline | 10 | 68.29 | 3.67 | 48.17 | 86.85 | |
| | Stimulation | 10 | 67.74 | 3.57 | 47.75 | 84.81 | 0.177 |
| | Post stimulation | 10 | 66.93 | 3.47 | 47.96 | 81.42 | 0.078 |
| | Recovery | 10 | 66.10 | 3.29 | 48.52 | 79.66 | 0.063 |
| RSA ($\Delta$bpm) | Baseline | 9 | 12.08 | 3.18 | 4.18 | 29.51 | |
| | Stimulation | 9 | 9.97 | 2.37 | 3.50 | 20.26 | 0.015* |
| | Post stimulation | 9 | 7.17 | 1.53 | 2.82 | 15.82 | 0.041* |
| | Recovery | 9 | 5.80 | 1.29 | 2.61 | 13.56 | 0.033* |
| ∫SND (AUC) | Baseline | 10 | 4.27 | 0.66 | 2.70 | 9.66 | |
| | Post stimulation | 10 | 2.88 | 0.64 | 0.90 | 7.51 | 0.005** |
| | Recovery | 10 | 2.59 | 0.55 | 0.49 | 6.37 | 0.005** |
| PND rate (rpm) | Baseline | 10 | 14.1 | 1.54 | 8 | 24 | |
| | Stimulation | 10 | 16.2 | 1.65 | 7 | 37 | 0.041* |
| | Post stimulation | 10 | 17.9 | 3.23 | 7 | 44 | 0.009** |
| | Recovery | 10 | 18.0 | 3.08 | 7 | 43 | 0.008** |

**Table 5.2: Statistical evaluation of the respiratory phase duration in response to earlobe stimulation**

|  |  | Ti | Te | Ttot |
|---|---|---|---|---|
| **Baseline** | **Average** | 1.40 | 2.97 | 4.37 |
|  | **Std error** | 0.13 | 0.57 | 0.60 |
| **Stimulation** | **Average** | 1.15 | 3.18 | 4.34 |
|  | **Std error** | 0.10 | 0.64 | 0.71 |
|  | **P value** | 0.087 | 0.273 | 0.797 |
| **Post stimulation** | **Average** | 1.20 | 3.08 | 4.27 |
|  | **Std error** | 0.10 | 0.65 | 0.75 |
|  | **P value** | 0.303 | 0.273 | 0.100 |
| **Recovery** | **Average** | 1.25 | 2.84 | 4.10 |
|  | **Std error** | 0.11 | 0.64 | 0.74 |
|  | **P value** | 0.386 | 0.103 | 0.040* |

## 5.7    Discussion

This is the first study to examine the central sensory afferent projection of the earlobe of the rat and the effect of its stimulation on autonomic and respiratory control. The main findings from this anatomical and functional study include:

- The main termination sites were observed in the upper cervical spinal cord, especially C2 and C3. In the brainstem the paratrigeminal nucleus was densely innervated and a minor projection was also observed to the NTS. .
- Electrical stimulation of the earlobe did not evoke any changes in heart rate or arterial pressure.
- Respiratory rate increased during and after the stimulation.
- Cardiac parasympathetic function measured from the RSA was significantly reduced by stimulation.
- Thoracic sympathetic nerve discharge was significantly reduced by the stimulation.

Since some elements may overlap with outcomes discussed in chapter 4, they will be noted briefly here and comparisons made in more detail in chapter 6.

### 5.7.1  Projections of afferents from the earlobe

The ear lobe has been shown to be solely innervated by the GAN at least in humans and majorly in rabbits (Weddell *et al*., 1955b; Peuker & Filler, 2002). Neuronal tracer application of HRP on isolated GAN in rabbits primarily labelled ipsilateral dorsal root ganglion cells in C2 – C3, with the labelled fibres distributed in the dorsal horn of the upper 4 cervical segments (Liu & Hu, 1988). Similar observations on the upper cervical innervation were made when HRP was applied on the cutaneous nerve of the caudal surface of the pinna of young dog pups , an area that is equivalent to human earlobe (Chien *et al*., 1996). The current neuronal tracing study confirms in rats that the

afferent innervation and central projection pattern appears similar to the species in these aforementioned studies (Liu & Hu, 1988; Chien *et al.*, 1996; Peuker & Filler, 2002), with the labelled afferents predominantly within deeper laminae of the upper cervical cord (laminae III-IV).

In addition to dorsal horn in the upper cervical region there were also labelled afferents in the brainstem Pa5 and, to a minor degree, the NTS. These areas were detected as afferent targets in the previous isolated GAN tracing study in rabbits (Liu & Hu, 1988) as well as GAN innervated region in the caudal surface (earlobe included) of dog ear (Chien *et al.*, 1996). This is of potential functional relevance as the Pa5 can modulate autonomic function (See Chapter 4 and 6) (Ciriello & Calaresu, 1981; Sousa & Lindsey, 2009). Interestingly, a study in humans to examine the activated pathway from earlobe stimulation (potentially through GAN activation) using fMRI did not show activation in any autonomic related regions, but did notice activation of the spinal trigeminal nucleus, which may include the Pa5 as it could be difficult to differentiate using fMRI (Frangos *et al.*, 2015). Thus the central sensory projections of the earlobe in the rat may be similar to those observed or the GAN and/or similar auricular areas in other species.

## 5.7.2  Functional consequences of ear lobe stimulation in the WHBP

Stimulation of the earlobe did not evoke any changes in heart rate or arterial pressure, but increased respiratory rate. In contrast, RSA and SND both decreased. The increase in respiratory rate and decrease in RSA was different to tragus stimulation, where no differences were observed (see Chapter 6 for more detailed comparison).

How can earlobe stimulation cause a decrease in RSA (and presumably parasympathetic activity) and sympathetic nerve discharge? The main afferent termination sites were in the cervical cord dorsal horn lamina 4 and the Pa5 in the brainstem, so comparison to previous studies stimulating these

areas could shed some light (see also Chapters 4 and 6). As discussed in the previous chapter (Chapter 4), spinal cord stimulation has been linked with the autonomic control of the heart as measured in non-cardiac related patients (Meglio *et al.*, 1987) and also anaesthetised rats (Linderoth *et al.*, 1994). In our stimulation study, significant reduction in sympathetic nerve activity during the post stimulation and recovery period, however were not accompanied by any cardiovascular changes. This probably could be explained by locality of the cardiovascular effects induced by the cervical spinal cord stimulation (cSCS). As such, stimulating the upper cervical (C3) in anaesthetized adult rats induced a significant vasodilation in the peripheral vasculature in the cerebral circulation that measured from the cerebral blood flow (Sagher & Huang, 2000). The increase in cerebral blood flow was not accompanied by significant changes in systemic blood pressure. The cerebral flow measurements had a peak 30 to 45 seconds after the stimulation and gradually returned to baseline after 5 minutes. The systemic BP however remained unchanged. This suggests high specificity of the stimulation effects in vasculature control. Indeed, cSCS on the higher upper cervical (C1) induced greater cerebral blood flow changes to that the C3, and the C6 stimulated level did not significantly cause changes (Sagher & Huang, 2000). Since cerebral circulation has been removed in the WHBP it will clearly not be possible to detect any changes in this and it is perhaps not surprising that no changes were observed in perfusion pressure.

The autonomic properties of local spinal region on cats was determined by intraspinal stimulation was applied through electrode place on various C2 regions (Illert & Gabriel, 1972). An excitatory region to cause elevation in BP, renal and splanchnic sympathetic activity were found converged within the dorsal part of the lateral funiculus and laminae II-VII of the grey matter. In contrast, an inhibitory regions were revealed resided within the ventral funiculus, and also head of the dorsal horn (superficial laminae). Stimulation on both regions resulted changed BP and sympathetic nerve activity independent to each other. Considering species variation between the current investigation and Illert's findings, it is unclear if the immunoreactive labelled

afferents from the tragus lies within excitatory, inhibitory, or transitory region (Illert & Gabriel, 1972). However, the significant reduction in SND without being companied by the HR or PP suggests that these are in transitory.

### 5.7.3 Does ear lobe stimulation affect vagal modulation?

Here, stimulating the GAN innervated area in the rat ear lobe caused vagal inhibition as measured from the RSA. Other regions with sole GAN into human ear would include the tail of helix, scapha, and also anti-tragus. Consistent with the results in this chapter, electrical and manual acupuncture in the tail of helix of the ear in the rat (likely to exert GAN activation), caused a mild depressor response on the blood pressure in anaesthetized rats (6% - 12% decrease from baseline) (Gao *et al.*, 2008). In addition, a small bradycardia response was reported from electroacupuncture applied on the GAN innervated region, suggesting autonomic cardiovascular changes evoked from the stimulation. In future studies it would be preferable to identify effects on the vagus by recording directly from the cardiac vagus nerve (O'Leary & Jones, 2003).

Outcomes of human studies are consistent with these current findings. Five minutes of SCS (between upper cervical to mid thoracic) at an amplitude to generate paraesthesia in patients who were in a treatment for chronic pain, caused significant increases in HR (Kalmár *et al.*, 2013) The increase in HR may have been due to vagal withdrawal since the HF component of the was significantly reduced during the SCS stimulation (Kalmár *et al.*, 2013). However, these results were contradictory to another SCS study performed in obese patients (Sobocki *et al.*, 2013). The cSCS (C1-C2) in obese patients who underwent the treatment for 12 hour per day for 8 weeks significantly reduced body weight as well as increase in all HRV parameters, with the most pronounced effect in HF power that reflects parasympathetic activity (Sobocki *et al.*, 2013). Referring to the differences on length of stimulation (5 minutes VS 12 hour) applied in current study and both of the previous SCS studies

might explain variation observed within vagal component of the cardiac. Furthermore, since Clancy et al reported that the starting HRV influenced the response to tragal stimulation, perhaps a similar relationship exists for SCS, where SCS increases the lower HRV of obese patients.

.

## 5.8 Conclusion

The central afferent projection from the earlobe is similar to that from the tragus. The labelled afferent terminations can be seen in medullary regions (NTS, Pa5, and Cu) but the main termination was in the dorsal horn of the upper cervical spinal cord. Electrical stimulation of the earlobe caused sympathoinhibition in the lower thoracic chain. Interestingly, the vagal tone was also significantly reduced and this was accompanied by increased respiratory activity.

# Chapter 6 General Discussion

## 6.1    Summary of findings

### 6.1.1 The physiological profile of the WHBP animals exhibits a circadian variation.

The functional evidence presented in the first results chapter indicates the presence of physiological functions that vary with the dark/light phase recorded in the WHBP. The physiological functions were marked with higher perfusion pressure in the night time preparations, as well as increased respiratory activity. Direct demonstration of sympathetic neural involvement was evident from increased activity recorded from the lower thoracic sympathetic chain.  Sub-grouping the preparations according to specific time of the experimentation (e.g.: 10:30, 14:30, 21:30, and 2:30) revealed preferential peaking in perfusion pressure during the early dark phase. Sympathetic nerve activity on the other hand peaked during the late dark phase. These differences were consistent with those previously observed in intact rodents where the plasma epinephrine and norepinephrine were notably higher during the night time (De Boer & Van der Gugten, 1987).  The circadian variation in autonomic plasma markers  were  in  reverse to that in humans (Dodt *et al.*, 1997). Hence, the differences in these autonomic profiles needed to be acknowledged when designing experiments in rats. The WHBP findings in this chapter provided a basis to utilize the night-time animals in the ear stimulation experiments in Chapter 4 and 5.  Further, these findings suggest that experiments conducted on rats during the day time need to acknowledge that this is their sleeping phase, with potentially different outcomes than observed in the night time, awake phase. This could have implications for studies in which translation to human trials is a primary objective.

163

## 6.1.2 Auricular stimulation at the tragus and lobe both evoke a sympathoinhibition.

A common outcome for both studies was that stimulation at both the tragus (Chapter 4) and the lobe (Chapter 5) resulted in an inhibition of sympathetic nerve discharge. The cardiovascular depressor responses following electroacupuncture as reported by Gao *et al.* (2008) were well in agreement with sympathoinhibition observed from current WHBP stimulations. Electrical acupuncture (100 Hz, 1.0 mA) in the tail of helix of the ear in the rat (potentially GAN activation), caused a mild depressor response on the blood pressure (-10 mmHg) in anaesthetized rats (Gao *et al.*, 2008). In addition, a small bradycardia response (-8 bpm) was reported from tail of helix electroacupuncture. Similarly, electrical stimulation on the conchae (presumably innervated by the ABVN) gave a mild arterial depressor (-7mmHg) and bradycardia (-6 bpm) responses. The sympathoinhibition observed from tragus stimulated WHBP was accompanied by a reduction in cardiovascular parameters, but not necessarily in earlobe stimulation **(Figure 6.1).** This is interesting since both studies utilized a similar auricular stimulation frequency (100 Hz, 2.5 mA) and targeted similar auricular nerves (eg: GAN/ABVN).
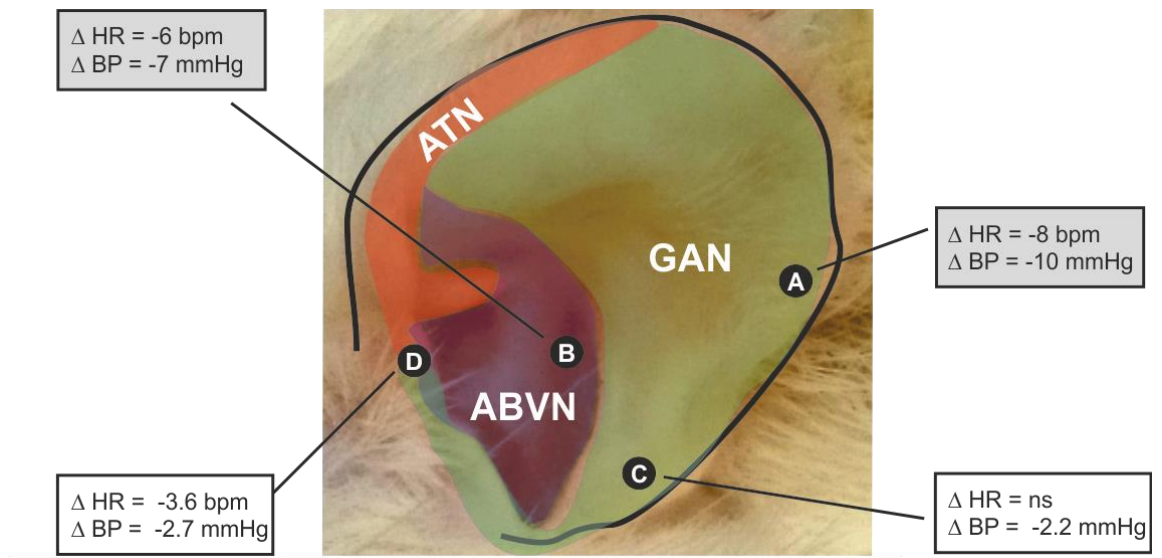
**Figure 6.1: Presumptive auricular sensory nerve innervation of rat ear and summary of cardiovascular effects of stimulation at different sites**

The outcome of electrical stimulation (100 Hz, 1 mA) on tail of A) helix and B) conchae of anaesthetized rats resulted in cardiovascular inhibition (Gao *et al.*, 2008). Similar stimulation frequency (100 Hz, 2.5 mA) on C) earlobe and D) tragus in WHBP also caused cardiovascular inhibition (except for HR in earlobe). ATN- Auriculotemporal Nerve, ABVN – Auricular Branch of the Vagus Nerve, GAN- Great Auricular Nerve.

As covered earlier in General Introduction (**Section 1.3.7**), the effects of ABVN stimulation (tragus/conchae) on ANS activity in healthy volunteers are rather conflicting. In brief, manual acupuncture on the concha increased HRV component of the cardiac vagal tone but not sympathetic (Haker *et al.*, 2000). Electrical stimulation on the tragus (30 Hz, 10-50 mA) shifted the HRV of healthy volunteers towards parasympathetic predominance while microneurography from the peroneal nerve recorded reduction in sympathetic nerve activity (Clancy *et al.*, 2014). In another study, no changes were detected in HRV after one hour of right sided concha stimulation (De Couck *et al.*, 2017). The use of HRV to describe sympatho-vagal balance in these studies may lead to the disagreements since the reliability of the aforementioned method to measure autonomic function has been questioned (Billman, 2007; Shaffer *et al.*, 2014). Thus, the current WHBP study in providing a direct sympathetic nerve measurement demonstrates additional evidence on autonomic modulation from tragus stimulation.

Easy accessibility of the auricular stimulation has been suggested as an inexpensive alternative treatment of "vagal nerve stimulation" for autonomic imbalance (Murray *et al.*, 2016), a clinical feature for failing heart. In particular, accelerated heart beat is one of the common outcomes of sympathoexcitation in heart failure associated with an adverse prognosis. As such, electrical stimulation on the right stellate ganglion (RSG) to induce sympathetic hyperactivity resulted in sinus tachycardia in anaesthetized dogs (Zhou *et al.*, 2016). Duel stimulation onto the RSG and tragus (20 Hz, 2 millisecond pulse width) suppressed the RSG neural hyperactivation as seen from neural gene expression of cFos and neuronal growth factor. Furthermore, the cardiac sympathetic dominance was reduced as seen in the reduction of the LF/HF ratio of the HRV (Zhou *et al.*, 2016). The effects of longer period tragus stimulation demonstrated sympathoinhibition in myocardial infarcted dogs as revealed by lower plasma norepinephrine. (Wang *et al.*, 2014). These autonomic changes were coupled by improved ventricular functions (contractility and diastolic), smaller infarction size, and lower plasma cytokine.

Unlike tragus, there are limited studies that focused on autonomic changes following earlobe stimulation (presumably through the GAN). This possibly due to prominent application of earlobe stimulation; also commonly known as Cranial Electrotherapy stimulation in the treatment of non-autonomic conditions such as depression, anxiety, insomnia and pain (Horowitz, 2013). The sympathoinhibition observed after earlobe stimulation in the WHBP thus provides a novel evidence of the GAN autonomic functions, similar to the ABVN.

## 6.1.3 What pathways underlie the sympathoinhibition from the lobe and tragus?

The current neuronal tracing studies from the GAN and the ABVN innervation areas, showed a similar central termination pattern. The only study on central projections from the isolated ABVN was done in cats using HRP. Principally, labelled neurons were found in the jugular ganglion but none in the nodose ganglion of the vagus. Labelled afferent projections were evident in brainstem in the cuneate nucleus and trigeminal nucleus as well as in dorsal horn at C1-C3 levels (Nomura & Mizuno, 1984). Similarly, application of HRP into the GAN in rabbits showed prime convergence of sensory afferent terminals in the dorsal horn of the upper cervical regions (C1-C3) particularly the C2 in laminae I-V. Additional labelled terminal fibres were detected in the cuneate nuclei and nucleus of the spinal tract (Liu & Hu, 1988). The similarity in isolated ABVN to the GAN raised a question if the previous neurotracing studies had properly differentiated these 2 nerves. Furthermore, their results were almost equivalent to what was seen from the current non-isolated auricular nerves innervating into the tragus or earlobe **(Table 6.1)**.

Due to primary afferent innervation into the dorsal horn of the upper cervical cord, the significance of this innervation was later tested with C1-C3 ipsilateral nerve transections. In turn, the sympathoinhibition was absent in this preparation, suggesting that upper cervical afferents can modulate autonomic

167

activity. Stimulating neck muscle afferents that project into the rats upper cervical (C2) in WHBP study increased vascular resistance and with a little reduction of HR (Edwards *et al.*, 2015). This physiological outcome was opposite to the current study when electrical stimuli was applied on the tragus of cervical transected preparations, highlighting the loss of autonomic modulating pathway. As discussed earlier in Chapter 4 **(see 4.7.1)** and 5 **(see 5.7.3)**, spinal cord stimulation on the upper cervical segments has been linked to autonomic modulation of cardiovascular control in animal (Linderoth *et al.*, 1994; Sagher & Huang, 2000) and human (Meglio *et al.*, 1987) studies. Taken together, these studies suggest a pivotal role of afferents terminating into upper cervical region for modulating central autonomic control.

The current proposed activation pathway **(Figure 6.2)** is contrary to our initial expectation where vagal afferents were thought to be activated upon auricular stimulation (He *et al.*, 2013). fMRI evidence on the ABVN stimulation in cymba conchae (and GAN in earlobe as control) in healthy humans showed widespread activation in the ipsilateral NTS (Frangos *et al.*, 2015). Similar fMRI experiment to stimulate the ABVN in posterior side of the outer auditory canal showed robust decreases in blood oxygenation level dependent (BOLD) signal in the area of the nucleus of the vagus nerve as well as the NTS (Kraus *et al.*, 2013). In most recent fMRI evidence on healthy volunteers, ABVN stimulation in the tragus, wall of ear canal, cymba conchae caused significant activation of the NTS (Yakunina *et al.*, 2016).

Direct activation of the NTS from auricular stimulation is, however, inconsistent with our own and other findings. Auricular afferent labelling in the NTS is sparse in cats (Nomura & Mizuno, 1984) and in rats (this thesis). An alternative pathway may be that the NTS is activated via the spinal cord (see Figure 6.2). The aforementioned fMRI studies (Kraus *et al.*, 2013; Frangos *et al.*, 2015; Yakunina *et al.*, 2016) only reported on brain activity changes occurred within the brainstem, but not in the upper cervical region. We showed a primary convergence of somatosensory afferent from the stimulation sites terminated into dorsal horn of the upper cervical. Cutting this projection eliminates the sympathoinhibitory effects that presence in normal WHBP ear

stimulation.  Neuronal projection from the upper cervical dorsal horn into the NTS has also been documented in rats (Gamboa-Esteves *et al.*, 2001) thus suggesting that the somatosensory afferent neurons in the dorsal horn are the first order of activation while NTS are the second order.  Future imaging studies on humans may reveal if the cervical dorsal horn is indeed activated by auricular stimulation.
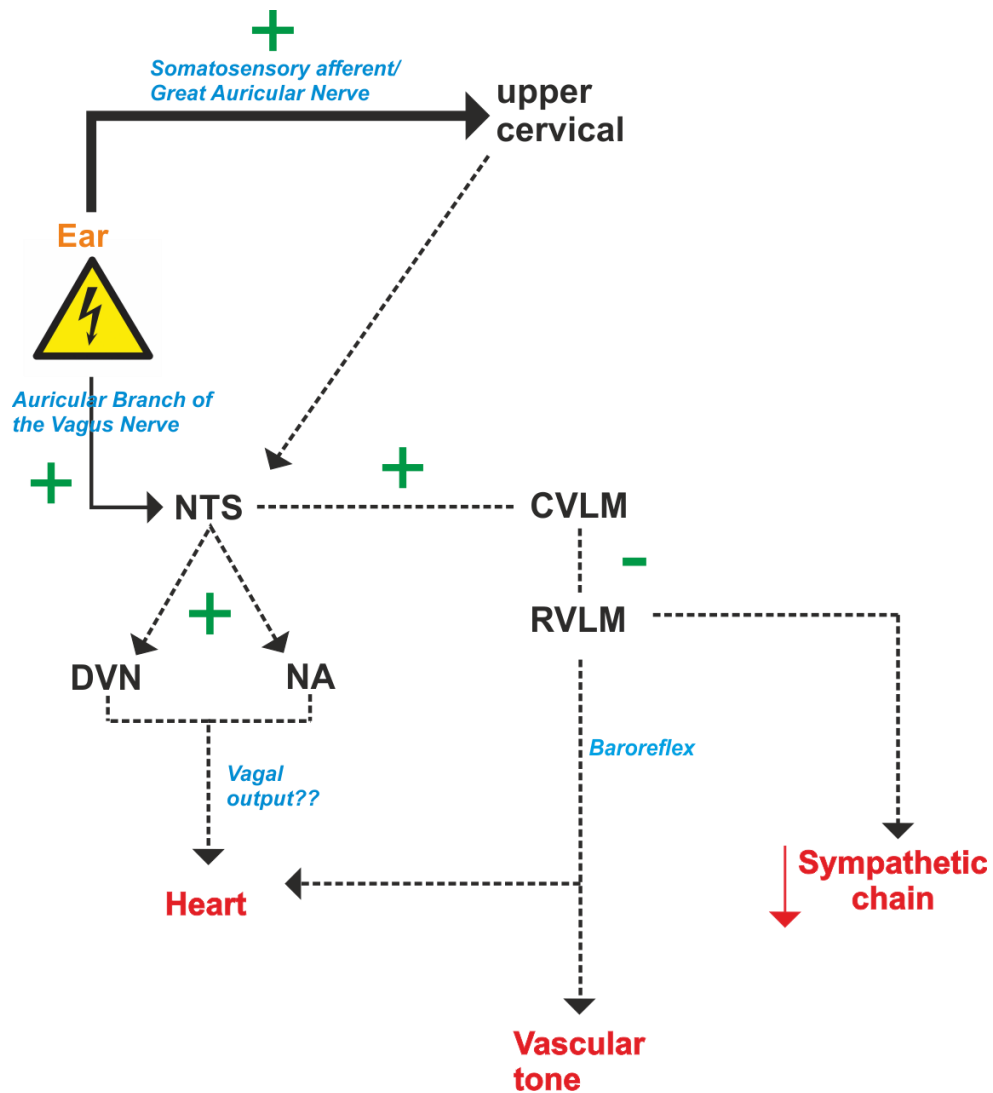
**Figure 6.2: Potential pathways mediating effects of tragus stimulation on cardiovascular autonomic functions**

Stimulation of the ear (e.g.: tragus, earlobe) potentially activates somatosensory neurons in the dorsal horn of the upper cervical. It also may cause direct activation of NTS through ABVN afferents. The NTS may be activated in secondary order from somatosensory neurons. Initiation of neuronal firing in the NTS activation caused an activation of the CVLM, to inhibit the RVLM. In turn, central sympathetic activity discharge is reduced and lead to depressed vascular tone. The stimulation effects on cardiac vagal output is still unknown as no changes in the RSA after tragus stimulation, but decreased in earlobe stimulation. The full line style represents findings from current study while the dotted lines represent findings drawn from previous literature. The intensity of afferent terminals detected from current study represented by with different thickness. NTS- nucleus tractus solitarius, CVLM/RVLM- caudal/rostral ventro lateral medulla, DVN- dorsal vagal nucleus, NA- nucleus ambiguus, RSA- respiratory sinus arrhythmia.

**Table 6.1: Comparison on central projection of afferents from tragus, earlobe and other isolated nerves**

** This table is comparing results from the current and previous studies. This is different to Table 1.3 in the General Introduction which summarizes studies from the literature.

| Study | Author | Site of injection | Tracer | Species | NTS | | | | | | | Vagal | | | trigeminal | | | cervical | | |
|---|---|---|---|---|---|---|---|---|---|---|---|---|---|---|---|---|---|---|---|---|
| | | | | | l | dl | comm | m | d | i | v | DMVN | ap | Cu | Pa5 | SPV | SPVtr | C1 | C2 | C3 |
| Chapter 4 | | Tragus | CTB | Rats | + | | | + | + | | | | | + | + | + | | + | + | + |
| Chapter 5 | | Earlobe | CTB | Rats | + | | | | | | + | | | + | + | | | + | + | + |
| Isolated GAN | Liu and Hu (1988) | GAN root | HRP | Rabbit | | | | | | + | | | | + | | + | + | + | + | + |
| Isolated ABVN | Nomura and Mizuno (1984) | ABVN | HRP | Cats | | + | + | | + | | | + | | + | | + | + | + | + | + |

| | | | | | | | | | | | | | | | | | | |
|---|---|---|---|---|---|---|---|---|---|---|---|---|---|---|---|---|---|---|
| Vagus Nerve | Kalia and Sullivan (1982) | Cervical trunk | HRP | Rats | + | + | + | + | + | + | + | + | + | ■ | ■ | ■ | + | + | ■ |
| | Nomura and Mizuno (1983) | Cervical trunk | HRP | Cats | + | + | + | + | + | + | + | + | ■ | ■ | ■ | | + | + | ■ |

172

## 6.2   Further Experiments

These studies revealed that tragus and earlobe stimulation both evoked an inhibition of sympathetic nerve activity. Contrary to expectations, the major afferent pathways did not seem to include the NTS as a first order target. Some progress was made towards identifying the pathways as sectioning of the cervical nerves eliminated the stimulation-evoked sympathoinhibition. However, the role of the inputs to the Pa5 and the minor projections to the NTS were not explored. Furthermore, it is not clear how the excitatory afferent signals are translated into a sympathoinhibition. Contemporary neuronal tracing techniques using viruses and/or functional studies with optogenetics could be used to shed some light on the neuronal pathways mediating the effects of auricular stimulation.

### 6.2.1  Examining the pathway of upper cervical stimulation

The current anatomical and functional study suggests a possibility of a cervical pathway being activated from the ear stimulation. Only a few studies have stimulated the upper cervical nerves of rats in WHBP. Stimulating the spinal nerve at C2 level with glass suction electrode in rats caused a temporary cessation of phrenic nerve activity, increased the arterial pressure with little effect upon heart rate (Edwards *et al.*, 2015). The effect of upper cervical stimulation on the autonomic control in WHBP is still unknown. By adapting the stimulating electrodes into upper cervical stimulation (C1-C3), a direct recording from vagal efferent and sympathetic nerves would be possible. The spino-medullary activation pathway can further be tested by direct recording on the NTS or pharmacologically inhibiting the NTS. A previous WHBP study suggested the cardio-autonomic inhibition during nociception was mediated by an intrinsic GABAergic mechanism within the NTS (Boscan *et al.*, 2002). Thus, microinjection of reversible GABA receptor antagonists (e.g.:

bicuculline, flumazenil) into the NTS right before auricular stimulation might be useful.

Future studies on examining the effects of upper cervical stimulation could be performed *in vivo.* In this study, healthy adult rats would be implanted with an electrode system for spinal cord stimulation (SCS) on the upper cervical segments. The surgical procedure for the SCS has been explained in detail by Linderoth *et al.* (1993). Briefly, animals would be laminectomized at the C1 – C3 segments and intraspinal electrodes placed extradurally onto the dorsal aspect of the cord. A silver anode would be implanted in the paravertebral subcutaneous tissue. The SCS would be applied twice per day and the effects of stimulation could be measured on autonomic parameters such as HR, BP, and RSA which obtained from telemetry system. The autonomic indicator in the blood can be obtained and compared before and after the stimulation period. A microdialysis probe can be placed near to any interested regions in the brain (eg: NTS/Upper cervical) for measurement of endogenous molecules to assess the biochemical functions upon the SCS. Histological analysis can be examined after animals being sacrificed and the distribution of activated regions can be studied with cFos.

### 6.2.2 Combining anatomical and functional studies in optogenetics

Development of technologies which can regulate the specific type of cells using optical control provides a reliable method to stimulate or supressed neural activity, thus allows combination on anatomical and functional studies. This was made possible by artificial incorporation of light-sensitive proteins eg:Channelrhodopsin-2 (ChR2) into cell membranes (Fenno *et al.*, 2011). This method is known as optogenetics, where neural activation upon light activation at certain wavelength could be suitable to replace the current electrical stimulation to understand the ear stimulation circuitry.

The easiest strategy to investigate auricular stimulation would be through viral transduction with viral vectors to drive the channelrhodopsin expression. The use of rabies virus in rats has been shown to infect sensory neurons in the somatosensory system and could be used to introduce channelrhodopsins into the afferent nerve terminals by injection into either the tragus or the lobe. The fusion of ChR2 (a specific channelrhodopsin) with the fluorescent marker mCherry allows *post-hoc* identification and mapping of the ChR2-expressing cells for direct assessment of the specificity of expression (Cardin *et al.*, 2010) . Injection of the rabies viral vector RV-ChR2-mCherry into the tragus or lobe of the rats would result in ChR2 expression in the central terminations. The terminals in different areas (e.g. dorsal horn, Pa5, NTS) can then be specifically activated by illumination of light at appropriate wavelengths in each area. The effects of such specific afferent activation can be determined *in vivo* where the rats are equipped with telemetric devices to record heart rate and blood pressure. Further, this can also be applied in WHBP where the extracellular cellular activities of the autonomic neuronal regions (e.g.: NTS, Pa5) can be recorded upon light simulation on the afferent termination area using electrophysiology technique. Finally, acute slices could be utilised to study the synaptic activity of the afferent terminations. In all cases the associated mCherry could be used to confirm the termination sites of the afferents.

Further refinements of rabies viral labelling strategies could enable the mapping of second order neurons to be conducted with accuracy. Some rabies viruses have been modified to allow the transfer across a single synapse in either the anterograde or retrograde direction (Zampieri *et al.*, 2014). For these experiments, such viruses could be injected into the tragus or lobe and the location of the transsynaptically labelled target neurons identified. If conducted in transgenic reporter animals in which different cell types have become labelled (Tamamaki *et al.*, 2003) this would reveal the nature of the postsynaptic neurons.

## 6.2.3 Animal model in heart failure

There has been accumulating evidence on the application of auriculomedicine to alleviate HF symptoms in dogs (Yu *et al.*, 2011; Wang *et al.*, 2015; Zhou *et al.*, 2016). However, there is limited evidence on the application of electrical auricular stimulation on rat model of heart failure. In this particular interest, a rodent model that accurately produces heart failure pathology can be utilised. There are numerous transgenic rats that are spontaneously prone to the cardiovascular conditions and can be purchased from Charles River. One of which is a Spontaneously Hypertensive Heart Failure Rat (SHHF). The SHHF rats progressed from a spontaneously hypertensive and converted phenotype into overt, late-stage HF (Heyen *et al.*, 2002; Youcef *et al.*, 2014). This provides close approximations of humans HF pathophysiology which was associated with gradual onset of hypertension and also autonomic imbalance with ageing. The effects of ear stimulation on cardiac remodelling can be studied using either transgenic or induced HF animal model. In non-transgenic animals, common practice for HF was anterior interventricular coronary artery ligation causing myocardial infarction. The rapid onset of HF is, however, not accurate representative for human pathological heart development (Shaw *et al.*, 2001). Another widely used HF model in rats was the use of ascending aortic band that placed around the ascending aorta in weaned rats (3-4 week old). As these rats grow, hypertension develops gradually during aortic outflow is increasingly impeded. During 8 weeks of post-banding, the left ventricular exhibited signs of hypertrophy suggesting increased in left arterial pressure. After 18 weeks of post-banding, clear signs of HF became evident which include tachypnea, oedema, pleural effusion, and ascites (Shaw *et al.*, 2001). The development of HF can be monitored using echocardiogram where left ventricular hypertrophy is assessed. Ear stimulation also can be applied where the effects of stimulation is compared with the control groups. This gives an idea as to whether the effects of ear stimulation ameliorates the progression of HF *in vivo*.

## 6.3 Relation to human work

The current thesis project provides a basic physiological outcome of non-specific auricular stimulation causing sympathoinhibition. As described in the General Introduction (Section 1.3.7), auricular stimulation on the ABVN innervated areas has been shown to modulate autonomic changes in healthy humans (Haker *et al.*, 2000; Clancy *et al.*, 2014). The autonomic changes from the GAN sensory afferents activation may have been underestimated. As such, there is limited study to examine the autonomic effects of earlobe stimulation. The only available literature found online was published in Latvian and reading the article with Google translate assistance may affect the real meaning. Basically, this study examined the changes in cardiac autonomic function non-invasively using SDNN analysis of HRV derived from 60 minutes of ECG recording (Līcis *et al.*, 2015). Bilateral earlobe stimulation (20 minutes, 500 µA) in adult handball players marked increase in the parasympathetic tone in 60 minutes after the stimulation. With the current research finding, there is a possibility that both stimulation sites are activating a similar activation pathway to cause reduction in sympathetic nerve activity. If our proposed activation pathway is accurate, previous human work may require re-evaluation since the earlobe is commonly used as a point of sham control stimulation (Kraus *et al.*, 2013; Frangos *et al.*, 2015; Yakunina *et al.*, 2016).

## 6.4 Study limitations

One major limitation in this study was presumptive nerve distribution on the external auricle structure of the rats. This presumption was made based on cadaver examination where the tragus has a mixed of the GAN and ABVN, while the earlobe has total ABVN innervation (Peuker & Filler, 2002). It is unknown if peripheral distribution of the auricular nerves in humans is similar

to that in rats. Given that current evidence, anatomical and physiological, showed a degree of similarity between these two auricular regions, there is a possibility that a similar nerve is innervating these structures. We did not clarify if this nerve is either the GAN or the ABVN. Hence, throughout the entire thesis the stimulation was referred to as general auricular stimulation rather than specific auricular afferent stimulation.

Another major consideration in this study was the use of WHBP as a method to explore the vagal changes after ear stimulation. Given that the parasympathetic activity was indirectly measured with cardiac RSA in this preparation. The validity of cardiac RSA to measure autonomic activity has been debated in healthy young adults (Kollai & Mizsei, 1990). The cardiac parasympathetic activity was taken by changes in heart period from propranolol treatment while the RSA was quantified as difference between maximum and minimum heart periods in a given respiratory cycle. Regression analysis between the RSA and vagal control was found to be significant but weak (r=0.63), suggesting they are not necessarily reflective. With the WHBP, a direct measurement from the vagal tone measurement from the preparation can be measured directly from the cervical vagal nerve (Paton, 1996b) and that wasn't utilized in this study.

The afferent labelling may also be biased in this study. Double labelling between CTB and either IB4 or WGA into sciatic nerve of rats revealed the tendency of myelinated fibres labelling only (Shehab & Hughes, 2011). This may resulted inaccuracy of the result interpretation since the vagus nerve (our initial nerve of interest) in cats is composed of 20% unmyelinated and 80% of myelinated fibres (DuBois & Foley, 1936). However, the fibres composition of the GAN is unknown. An electrophysiological study on single afferent fibres recorded from the C3 (origin of the GAN) in cats suggested domination of low conduction velocity afferents (Abrahams *et al.*, 1984). The low conduction velocity commonly have a high threshold activation points and this is mainly in the unmyelinated neuronal fibres. Hence, different neuronal tracing should be considered in the future to address this limitation.

Similar to that labelling outcome, there is also a possibility of bias in activation of certain type of afferent fibres particularly the C fibres. The activation threshold of C fibres (unmyelinated) in dogs is usually greater than 4 mA (Yoo *et al.*, 2016), and cats is more than 2 mA that is higher than any other myelinated fibres (Blair & Erlanger, 1933). Extracellular recording on the vagal preganglionic neurones in the dorsal vagal motor nucleus of anaesthetized rats revealed to have majority of C fibre axons and this may play a role in autonomic control (Jones *et al.*, 1998). Alas, this may not be necessarily relevant to our current interpretation since the autonomic functions are potentially mediated by the GAN rather than the vagus nerve.

The WHBP can offer further advantages that were not conducted in this study. For example testing if stimulation can alter baroreceptor or chemoreceptor reflexes. Baroreceptor reflexes can be elicited by brief increases in pump pressure (Lall *et al.*, 2012). Similarly, injection of sodium cyanide (to activate chemoreceptors) into the perfusate of the preparation decreases HR and increase phrenic nerve discharge. Changes in sensitivity of these reflexes would be consistent with autonomic influences of auricular stimulation.

Another limitation of the current study is the relatively small number of the animals used for analysis of each experiment and so limits the power to detect some differences (e.g.: reduction in HR after earlobe stimulation). The average number of animals used for each experiments were 10. This may not be critical since previous literature of rodents physiological functions in WHBP has various number of replications ranging between 2 – 20 (Potts *et al.*, 2000; Lall *et al.*, 2012; Edwards *et al.*, 2015).

Attempts were made to look at the targets of labelled afferents that projected from the stimulation site (Chapter 4). Rare and infrequent co-localizations were found between the afferent terminals with the ChAT, Calb, ParV, GAD 67, and also NKR1 expressing cells, thus counting was not performed.

## 6.5   Conclusions

Autonomic function in WHBP of the rats following auricular electrical stimulation has been examined for the first time. To find a suitable animal model, the autonomic profile in rats WHBP from different circadian cycle was primarily characterized. Secondly, basal effects of tragus and earlobe stimulation caused central sympathoinhibition. Anatomical and physiological work in this theses proposed somatosensory pathway activation (presumably from the GAN) to upper cervical spinal, and potentially projects to autonomic modulation centre in the brainstem (e.g.: NTS). The significance of somatosensory activation from ear stimulation to cause autonomic changes became evident as central sympathoinhibition became absent in transected upper cervical preparation. This may explain a non-specific functional map in the ear as sympathoinhibition was seen in both tragus and earlobe stimulation. However, sensory nerve innervation in rats' auricular dermatome needed to be clarified prior to confirming the proposed activation pathway. The neurophysiological work covered in this thesis may clinically be applied as a non-surgical treatment for chronically elevated sympathetic activity and sympatho-vagal imbalance such as heart failure.

# List of References

Abraham PJ, Capobianco DJ & Cheshire WP. (2003). Facial pain as the presenting symptom of lung carcinoma with normal chest radiograph. *Headache: The Journal of Head and Face Pain* **43,** 499-504.

Abrahams V, Lynn B & Richmond F. (1984). Organization and sensory properties of small myelinated fibres in the dorsal cervical rami of the cat. *The Journal of physiology* **347,** 177.

Agarwal S, Gelsema A & Calaresu F. (1990). Inhibition of rostral VLM by baroreceptor activation is relayed through caudal VLM. *American Journal of Physiology-Regulatory, Integrative and Comparative Physiology* **258,** R1271-R1278.

Agnew WF & McCreery DB. (1990). Considerations for safety with chronically implanted nerve electrodes. *Epilepsia* **31,** S27-S32.

Amirhaeri S & Spencer D. (2010). Myocardial infarction with unusual presentation of otalgia: a case report. *International journal of emergency medicine* **3,** 459-460.

Andresen MC & Kunze DL. (1994). Nucleus tractus solitarius—gateway to neural circulatory control. *Annual review of physiology* **56,** 93-116.

Badoer E. (2000). Hypothalamic paraventricular nucleus and cardiovascular regulation. *Clinical and experimental pharmacology & physiology* **28,** 95-99.

Baekey DM, Dick TE & Paton JF. (2008). Pontomedullary transection attenuates central respiratory modulation of sympathetic discharge, heart rate and the baroreceptor reflex in the in situ rat preparation. *Experimental physiology* **93,** 803-816.

Baekey DM, Morris KF, Gestreau C, Li Z, Lindsey BG & Shannon R. (2001). Medullary respiratory neurones and control of laryngeal motoneurones during fictive eupnoea and cough in the cat. *The Journal of Physiology* **534,** 565-581.

Barman SM & Gebber GL. (1976). Basis for synchronization of sympathetic and phrenic nerve discharges. *Am J Physiol* **231,** 1601-1607.

Barone L, Colicchio G, Policicchio D, Di Clemente F, Di Monaco A, Meglio M, Lanza GA & Crea F. (2008). Effect of vagal nerve stimulation on systemic inflammation and cardiac autonomic function in patients with refractory epilepsy. *Neuroimmunomodulation* **14,** 331-336.

Baumgartner C, Lurger S & Leutmezer F. (2001). Autonomic symptoms during epileptic seizures. *Epileptic disorders: international epilepsy journal with videotape* **3,** 103-116.

Berilgen MS, Sari T, Bulut S & Mungen B. (2004). Effects of epilepsy on autonomic nervous system and respiratory function tests. *Epilepsy & Behavior* **5,** 513-516.

Berthoud H-R & Neuhuber WL. (2000). Functional and chemical anatomy of the afferent vagal system. *Autonomic Neuroscience* **85,** 1-17.

Bianchi AL & Gestreau C. (2009). The brainstem respiratory network: an overview of a half century of research. *Respiratory physiology & neurobiology* **168,** 4-12.

Bieger D & Hopkins DA. (1987). Viscerotopic representation of the upper alimentary tract in the medulla oblongata in the rat: the nucleus ambiguus. *Journal of Comparative Neurology* **262,** 546-562.

Billman GE. (2007). The LF/HF ratio does not accurately measure cardiac sympatho-vagal balance. *Heart Rate Variability: Clinical Applications and Interaction between HRV and Heart Rate,* 54.

Bindoff L & Heseltine D. (1988). Unilateral facial pain in patients with lung cancer: a referred pain via the vagus? *The Lancet* **331,** 812-815.

Blair E & Erlanger J. (1933). A comparison of the characteristics of axons through their individual electrical responses. *American Journal of Physiology--Legacy Content* **106,** 524-564.

Bodenlos JS, Schneider KL, Oleski J, Gordon K, Rothschild AJ & Pagoto SL. (2014). Vagus nerve stimulation and food intake: effect of body mass index. *Journal of diabetes science and technology* **8,** 590-595.

Bonaz B, Sinniger V, Hoffmann D, Clarençon D, Mathieu N, Dantzer C, Vercueil L, Picq C, Trocmé C & Faure P. (2016). Chronic vagus nerve stimulation in Crohn's disease: a 6-month follow-up pilot study. *Neurogastroenterology & Motility*.

Bonnemeier H, Wiegand UK, Brandes A, Kluge N, Katus HA, Richardt G & Potratz J. (2003). Circadian profile of cardiac autonomic nervous modulation in healthy subjects. *Journal of cardiovascular electrophysiology* **14,** 791-799.

Borst C, Van Brederode J, Wieling W, Van Montfrans G & Dunning A. (1984). Mechanisms of initial blood pressure response to postural change. *Clinical Science* **67,** 321-327.

Boscan P, Allen A & Paton J. (2001). Baroreflex inhibition of cardiac sympathetic outflow is attenuated by angiotensin II in the nucleus of the solitary tract. *Neuroscience* **103,** 153-160.

Boscan P, Pickering AE & Paton JF. (2002). The nucleus of the solitary tract: an integrating station for nociceptive and cardiorespiratory afferents. *Experimental physiology* **87,** 259-266.

Bradford FK. (1938). THE AURICULO-GENITAL REFLEX IN CATS. *Quarterly Journal of Experimental Physiology* **27,** 271-279.

Braga VA, Soriano RN, Braccialli AL, De Paula PM, Bonagamba LG, Paton JF & Machado BH. (2007). Involvement of l-glutamate and ATP in the neurotransmission of the sympathoexcitatory component of the chemoreflex in the commissural nucleus tractus solitarii of awake rats

and in the working heart–brainstem preparation. *The Journal of physiology* **581,** 1129-1145.

Brockhaus J, Ballanyi K, Smith JC & Richter DW. (1993). Microenvironment of respiratory neurons in the in vitro brainstem-spinal cord of neonatal rats. *J Physiol* **462,** 421-445.

Brophy S, Ford TW, Carey M & Jones JF. (1999). Activity of aortic chemoreceptors in the anaesthetized rat. *The Journal of Physiology* **514,** 821-828.

Brotman DJ, Davidson MB, Boumitri M & Vidt DG. (2008). Impaired diurnal blood pressure variation and all-cause mortality. *American journal of hypertension* **21,** 92-97.

Buijs RM, la Fleur SE, Wortel J, van Heyningen C, Zuiddam L, Mettenleiter TC, Kalsbeek A, Nagai K & Niijima A. (2003). The suprachiasmatic nucleus balances sympathetic and parasympathetic output to peripheral organs through separate preautonomic neurons. *Journal of comparative neurology* **464,** 36-48.

Buijs RM, Markman M, Nunes-Cardoso B, Hou YX & Shinn S. (1993). Projections of the suprachiasmatic nucleus to stress-related areas in the rat hypothalamus: A light and electron microscopic study. *Journal of comparative neurology* **335,** 42-54.

Cardin JA, Carlén M, Meletis K, Knoblich U, Zhang F, Deisseroth K, Tsai L-H & Moore CI. (2010). Targeted optogenetic stimulation and recording of neurons in vivo using cell-type-specific expression of Channelrhodopsin-2. *Nature protocols* **5,** 247-254.

Chen F. (2006). *Progress in Brain Mapping Research*. Nova Publishers.

Chen M, Yu L, Liu Q, Wang Z, Wang S, Jiang H & Zhou S. (2015). Low level tragus nerve stimulation is a non-invasive approach for anti-atrial fibrillation via preventing the loss of connexins. *International journal of cardiology* **179,** 144-145.

Cheng Z & Powley TL. (2000). Nucleus ambiguus projections to cardiac ganglia of rat atria: an anterograde tracing study. *Journal of Comparative Neurology* **424,** 588-606.

Cheng Z, Powley TL, Schwaber JS & Doyle FJ. (1999). Projections of the dorsal motor nucleus of the vagus to cardiac ganglia of rat atria: an anterograde tracing study. *Journal of Comparative Neurology* **410,** 320-341.

Chien C-H, Shieh J-Y, Ling E-A, Tan C-K & Wen C-Y. (1996). The composition and central projections of the internal auricular nerves of the dog. *Journal of anatomy* **189,** 349.

Christmas D & Matthews K. (2015). Neurosurgical Treatments for Patients with Chronic, Treatment-Refractory Depression: A Retrospective, Consecutive, Case Series Comparison of Anterior Capsulotomy, Anterior Cingulotomy and Vagus Nerve Stimulation. *Stereotactic and functional neurosurgery* **93,** 387-392.

Ciriello J. (1983). Brainstem projections of aortic baroreceptor afferent fibers in the rat. *Neuroscience letters* **36,** 37-42.

Ciriello J & Calaresu FR. (1981). Projections from buffer nerves to the nucleus of the solitary tract: an anatomical and electrophysiological study in the cat. *Journal of the autonomic nervous system* **3,** 299-310.

Ciriello J, Hrycyshyn AW & Calaresu FR. (1981). Horseradish peroxidase study of brain stem projections of carotid sinus and aortic depressor nerves in the cat. *Journal of the autonomic nervous system* **4,** 43-61.

Clancy JA, Deuchars SA & Deuchars J. (2013). The wonders of the Wanderer. *Experimental physiology* **98,** 38-45.

Clancy JA, Mary DA, Witte KK, Greenwood JP, Deuchars SA & Deuchars J. (2014). Non-invasive vagus nerve stimulation in healthy humans reduces sympathetic nerve activity. *Brain stimulation* **7,** 871-877.

Corning JL. (1884). *Electrization of the sympathetic and pneumogastric nerves, with simultaneous bilateral compression of the carotids.*

Dash D. (2014). Advanced Signal Processing Techniqes to Study Normal and Epileptic EEG. *arXiv preprint arXiv:14015791.*

De Boer S & Van der Gugten J. (1987). Daily variations in plasma noradrenaline, adrenaline and corticosterone concentrations in rats. *Physiology & behavior* **40,** 323-328.

De Couck M, Cserjesi R, Caers R, Zijlstra W, Widjaja D, Wolf N, Luminet O, Ellrich J & Gidron Y. (2017). Effects of short and prolonged transcutaneous vagus nerve stimulation on heart rate variability in healthy subjects. *Autonomic Neuroscience* **203,** 88-96.

De Ferrari GM, Crijns HJ, Borggrefe M, Milasinovic G, Smid J, Zabel M, Gavazzi A, Sanzo A, Dennert R & Kuschyk J. (2011). Chronic vagus nerve stimulation: a new and promising therapeutic approach for chronic heart failure. *European heart journal* **32,** 847-855.

De Ridder D, Vanneste S, Engineer ND & Kilgard MP. (2014). Safety and efficacy of vagus nerve stimulation paired with tones for the treatment of tinnitus: a case series. *Neuromodulation: Technology at the Neural Interface* **17,** 170-179.

De S, Ghose M & Sen A. (1960). Activities of bacteria-free preparations from Vibrio cholerae. *The Journal of pathology and bacteriology* **79,** 373-380.

DeGiorgio C, Schachter S, Handforth A, Salinsky M, Thompson J, Uthman B, Reed R, Collin S, Tecoma E & Morris G. (2000). Prospective long-term study of vagus nerve stimulation for the treatment of refractory seizures. *Epilepsia* **41,** 1195-1200.

Deuchars SA, Morrison SF & Gilbey MP. (1995a). Medullary-evoked EPSPs in neonatal rat sympathetic preganglionic neurones in vitro. *The Journal of physiology* **487,** 453.

Deuchars SA, Spyer KM, Brooks PA & Gilbey MP. (1995b). A study of sympathetic preganglionic neuronal activity in a neonatal rat brainstem-spinal cord preparation. *Journal of the autonomic nervous system* **52,** 51-63.

Deuchars SA, Spyer KM & Gilbey MP. (1997). Stimulation within the rostral ventrolateral medulla can evoke monosynaptic GABAergic IPSPs in sympathetic preganglionic neurons in vitro. *Journal of neurophysiology* **77,** 229-235.

Deuchars SA, Trippenbach T & Spyer KM. (2000). Dorsal column nuclei neurons recorded in a brain stem-spinal cord preparation: characteristics and their responses to dorsal root stimulation. *Journal of neurophysiology* **84,** 1361-1368.

Docherty R, Charlesworth G, Farrag K, Bhattacharjee A & Costa S. (2005). The use of the rat isolated vagus nerve for functional measurements of the effect of drugs in vitro. *Journal of pharmacological and toxicological methods* **51,** 235-242.

Dodt C, Breckling U, Derad I, Fehm HL & Born J. (1997). Plasma epinephrine and norepinephrine concentrations of healthy humans associated with nighttime sleep and morning arousal. *Hypertension (Dallas, Tex : 1979)* **30,** 71-76.

Dong X-W, Morin D & Feldman JL. (1996). Multiple actions of 1S, 3R-ACPD in modulating endogenous synaptic transmission to spinal respiratory motoneurons. *The Journal of neuroscience* **16,** 4971-4982.

Donoghue S, Felder R, Jordan D & Spyer K. (1984). The central projections of carotid baroreceptors and chemoreceptors in the cat: a neurophysiological study. *The Journal of Physiology* **347,** 397.

Driessen AK, Farrell MJ, Mazzone SB & McGovern AE. (2015). The Role of the Paratrigeminal Nucleus in Vagal Afferent Evoked Respiratory Reflexes: A Neuroanatomical and Functional Study in Guinea Pigs. *Frontiers in physiology* **6,** 378.

DuBois FS & Foley JO. (1936). Experimental studies on the vagus and spinal accessory nerves in the cat. *The Anatomical Record* **64,** 285-307.

Dutschmann M, Waki H, Manzke T, Simms A, Pickering A, Richter D & Paton J. (2009). The potency of different serotonergic agonists in counteracting opioid evoked cardiorespiratory disturbances. *Philosophical Transactions of the Royal Society of London B: Biological Sciences* **364,** 2611-2623.

Edwards IJ, Lall VK, Paton JF, Yanagawa Y, Szabo G, Deuchars SA & Deuchars J. (2015). Neck muscle afferents influence oromotor and cardiorespiratory brainstem neural circuits. *Brain structure & function* **220,** 1421-1436.

Engel D. (1979). The gastroauricular phenomenon and related vagus reflexes. *European Archives of Psychiatry and Clinical Neuroscience* **227,** 271-277.

Espinosa-Medina I, Saha O, Boismoreau F, Chettouh Z, Rossi F, Richardson W & Brunet J-F. (2016). The sacral autonomic outflow is sympathetic. *Science (New York, NY)* **354,** 893-897.

Fenno L, Yizhar O & Deisseroth K. (2011). The development and application of optogenetics. *Annual review of neuroscience* **34,** 389-412.

Folan-Curran J, Hickey K & Monkhouse W. (1994). Innervation of the rat external auditory meatus: a retrograde tracing study. *Somatosensory & motor research* **11,** 65-68.

Foley JO & DuBois FS. (1937). Quantitative studies of the vagus nerve in the cat. I. The ratio of sensory to motor fibers. *Journal of Comparative neurology* **67,** 49-67.

Fort P & Jouvet M. (1990). Iontophoretic application of unconjugated cholera toxin B subunit (CTb) combined with immunohistochemistry of neurochemical substances: a method for transmitter identification of retrogradely labeled neurons. *Brain research* **534,** 209-224.

Frangos E, Ellrich J & Komisaruk BR. (2015). Non-invasive Access to the Vagus Nerve Central Projections via Electrical Stimulation of the External Ear: fMRI Evidence in Humans. *Brain stimulation* **8,** 624-636.

Furlan R, Guzzetti S, Crivellaro W, Dassi S, Tinelli M, Baselli G, Cerutti S, Lombardi F, Pagani M & Malliani A. (1990). Continuous 24-hour assessment of the neural regulation of systemic arterial pressure and RR variabilities in ambulant subjects. *Circulation* **81,** 537-547.

Gamboa-Esteves FO, Tavares I, Almeida A, Batten TF, McWilliam PN & Lima D. (2001). Projection sites of superficial and deep spinal dorsal horn cells in the nucleus tractus solitarii of the rat. *Brain research* **921,** 195-205.

Gao X-Y, Zhang S-P, Zhu B & Zhang H-Q. (2008). Investigation of specificity of auricular acupuncture points in regulation of autonomic function in anesthetized rats. *Autonomic Neuroscience* **138,** 50-56.

Gao XY, Li YH, Liu K, Rong PJ, Ben H, Li L, Zhu B & Zhang SP. (2011). Acupuncture-like stimulation at auricular point Heart evokes cardiovascular inhibition via activating the cardiac-related neurons in the nucleus tractus solitarius. *Brain research* **1397,** 19-27.

Ginsberg LE & Eicher SA. (2000). Great auricular nerve: anatomy and imaging in a case of perineural tumor spread. *American journal of neuroradiology* **21,** 568-571.

Gold MR, Van Veldhuisen DJ, Hauptman PJ, Borggrefe M, Kubo SH, Lieberman RA, Milasinovic G, Berman BJ, Djordjevic S & Neelagaru S. (2016). Vagus nerve stimulation for the treatment of heart failure: the INOVATE-HF trial. *Journal of the American College of Cardiology* **68,** 149-158.

Gori L & Firenzuoli F. (2007). Ear acupuncture in European traditional medicine. *Evidence-Based Complementary and Alternative Medicine* **4,** 13-16.

Grassi G. (2009). Assessment of sympathetic cardiovascular drive in human hypertension. *Hypertension (Dallas, Tex : 1979)* **54,** 690-697.

Grélot L, Barillot J & Bianchi A. (1989). Central distributions of the efferent and afferent components of the pharyngeal branches of the vagus and glossopharyngeal nerves: an HRP study in the cat. *Experimental brain research* **78,** 327-335.

Gupta D, Verma S & Vishwakarma S. (1986). Anatomic basis of Arnold's ear-cough reflex. *Surgical and Radiologic Anatomy* **8,** 217-220.

Guyenet PG. (2006). The sympathetic control of blood pressure. *Nature Reviews Neuroscience* **7,** 335-346.

Guyenet PG. (2008). The 2008 Carl Ludwig Lecture: retrotrapezoid nucleus, CO2 homeostasis, and breathing automaticity. *Journal of applied physiology* **105,** 404-416.

Guyenet PG & Bayliss DA. (2015). Neural control of breathing and CO 2 homeostasis. *Neuron* **87,** 946-961.

Haker E, Egekvist H & Bjerring P. (2000). Effect of sensory stimulation (acupuncture) on sympathetic and parasympathetic activities in healthy subjects. *Journal of the autonomic nervous system* **79,** 52-59.

Hamann JJ, Ruble SB, Stolen C, Wang M, Gupta RC, Rastogi S & Sabbah HN. (2013). Vagus nerve stimulation improves left ventricular function in a canine model of chronic heart failure. *European journal of heart failure* **15,** 1319-1326.

Hashimoto M, Kuwahara M, Tsubone H & Sugano S. (1999). Diurnal variation of autonomic nervous activity in the rat: investigation by power spectral analysis of heart rate variability. *Journal of electrocardiology* **32,** 167-171.

Hayashi F, Jiang C & Lipski J. (1991). Intracellular recording from respiratory neurones in the perfused 'in situ'rat brain. *Journal of neuroscience methods* **36,** 63-70.

Hayashi F & Lipski J. (1992). The role of inhibitory amino acids in control of respiratory motor output in an arterially perfused rat. *Respir Physiol* **89,** 47-63.

He W, Jing X-H, Zhu B, Zhu X-L, Li L, Bai W-Z & Ben H. (2013). The auriculo-vagal afferent pathway and its role in seizure suppression in rats. *BMC neuroscience* **14,** 85.

He W, Wang X, Shi H, Shang H, Li L, Jing X & Zhu B. (2012). Auricular acupuncture and vagal regulation. *Evidence-Based Complementary and Alternative Medicine* **2012**.

Herichová I, Mravec B, Stebelová K, Jurkovičová D, Kvetňanský R & Zeman M. (2007). Rhythmic clock gene expression in heart, kidney and some

brain nuclei involved in blood pressure control in hypertensive TGR (mREN-2) 27 rats. *Molecular and cellular biochemistry* **296,** 25-34.

Heyen JR, Blasi ER, Nikula K, Rocha R, Daust HA, Frierdich G, Van Vleet JF, De Ciechi P, McMahon EG & Rudolph AE. (2002). Structural, functional, and molecular characterization of the SHHF model of heart failure. *American Journal of Physiology-Heart and Circulatory Physiology* **283,** H1775-H1784.

Hirooka Y, Polson J, Potts P & Dampney R. (1997). Hypoxia-induced Fos expression in neurons projecting to the pressor region in the rostral ventrolateral medulla. *Neuroscience* **80,** 1209-1224.

Horowitz S. (2013). Transcranial Magnetic Stimulation and Cranial Electrotherapy Stimulation: Treatments for Psychiatric and Neurologic Disorders. *Alternative and Complementary Therapies* **19,** 188-193.

Hosoya Y, Sugiura Y, Okado N, Loewy A & Kohno K. (1991). Descending input from the hypothalamic paraventricular nucleus to sympathetic preganglionic neurons in the rat. *Experimental brain research* **85,** 10-20.

Illert M & Gabriel M. (1972). Descending pathways in the cervical cord of cats affecting blood pressure and sympathetic activity. *Pflügers Archiv* **335,** 109-124.

Isojärvi JI, Ansakorpi H, Suominen K, Tolonen U, Repo M & Myllylä VV. (1998). Interictal cardiovascular autonomic responses in patients with epilepsy. *Epilepsia* **39,** 420-426.

Izzo PN, Deuchars J & Spyer KM. (1993). Localization of cardiac vagal preganglionic motoneurones in the rat: immunocytochemical evidence of synaptic inputs containing 5-hydroxytryptamine. *The Journal of comparative neurology* **327,** 572-583.

Jacquin MF, Semba K, Rhoades RW & Egger MD. (1982). Trigeminal primary afferents project bilaterally to dorsal horn and ipsilaterally to cerebellum, reticular formation, and cuneate, solitary, supratrigeminal and vagal nuclei. *Brain research* **246,** 285-291.

Jansen A & Loewy A. (1997). Neurons lying in the white matter of the upper cervical spinal cord project to the intermediolateral cell column. *Neuroscience* **77,** 889-898.

Janssen B, Tyssen C, Duindam H & Rietveld W. (1994). Suprachiasmatic lesions eliminate 24-h blood pressure variability in rats. *Physiology & Behavior* **55,** 307-311.

John WMS- & Paton JF. (2000). Characterizations of eupnea, apneusis and gasping in a perfused rat preparation. *Respiration physiology* **123,** 201-213.

Johnson AW, Hissen SL, Macefield VG, Brown R & Taylor CE. (2016). Magnitude of Morning Surge in Blood Pressure Is Associated with Sympathetic but Not Cardiac Baroreflex Sensitivity. *Frontiers in neuroscience* **10,** 412.

Johnson SM, Turner SM, Huxtable AG & Ben-Mabrouk F. (2012). Isolated in vitro brainstem-spinal cord preparations remain important tools in respiratory neurobiology. *Respiratory physiology & neurobiology* **180,** 1-7.

Jones JF, Wang Y & Jordan D. (1998). Activity of C fibre cardiac vagal efferents in anaesthetized cats and rats. *The Journal of Physiology* **507,** 869-880.

Joustra S, Reijntjes R, Pereira A, Lammers G, Biermasz N & Thijs R. (2016). The Role of the Suprachiasmatic Nucleus in Cardiac Autonomic Control during Sleep. *PloS one* **11,** e0152390.

Kalia M & Sullivan JM. (1982). Brainstem projections of sensory and motor components of the vagus nerve in the rat. *The Journal of comparative neurology* **211,** 248-265.

Kalmár Z, Kovács N, Balás I, Perlaki G, Plózer E, Orsi G, Altbacker A, Schwarcz A, Hejjel L & Komoly S. (2013). Effects of spinal cord stimulation on heart rate variability in patients with chronic pain. *IDEGGYÓYÁZATI SZEMLE/CLINICAL NEUROSCIENCE* **66,** 102-106.

Kelley GA & Kelley KS. (2000). Progressive resistance exercise and resting blood pressure. *Hypertension (Dallas, Tex : 1979)* **35,** 838-843.

Kitamura S, Ogata K, Nishiguchi T, Nagase Y & Shigenaga Y. (1991). Location of the motoneurons supplying the rabbit pharyngeal constrictor muscles and the peripheral course of their axons: a study using the retrograde HRP or fluorescent labeling technique. *The Anatomical Record* **229,** 399-406.

Kollai M & Mizsei G. (1990). Respiratory sinus arrhythmia is a limited measure of cardiac parasympathetic control in man. *The Journal of Physiology* **424,** 329.

Koo B, Ham SD, Sood S & Tarver B. (2001). Human vagus nerve electrophysiology: a guide to vagus nerve stimulation parameters. *Journal of clinical neurophysiology* **18,** 429-433.

Koshiya N & Guyenet P. (1996). NTS neurons with carotid chemoreceptor inputs arborize in the rostral ventrolateral medulla. *American Journal of Physiology-Regulatory, Integrative and Comparative Physiology* **270,** R1273-R1278.

Krahl SE & Clark KB. (2012). Vagus nerve stimulation for epilepsy: A review of central mechanisms. *Surgical neurology international* **3,** S255-259.

Krahl SE, Senanayake SS & Handforth A. (2001). Destruction of peripheral C-fibers does not alter subsequent vagus nerve stimulation-induced seizure suppression in rats. *Epilepsia* **42,** 586-589.

Krauchi K & Wirz-Justice A. (1994). Circadian rhythm of heat production, heart rate, and skin and core temperature under unmasking conditions in men. *American Journal of Physiology-Regulatory, Integrative and Comparative Physiology* **267,** R819-R829.

Kraus T, Kiess O, Hösl K, Terekhin P, Kornhuber J & Forster C. (2013). CNS BOLD fMRI effects of sham-controlled transcutaneous electrical nerve stimulation in the left outer auditory canal–a pilot study. *Brain stimulation* **6,** 798-804.

Lall VK, Dutschmann M, Deuchars J & Deuchars SA. (2012). The anti-malarial drug Mefloquine disrupts central autonomic and respiratory control in the working heart brainstem preparation of the rat. *Journal of biomedical science* **19,** 1.

Lambert EA, Chatzivlastou K, Schlaich M, Lambert G & Head GA. (2014). Morning surge in blood pressure is associated with reactivity of the sympathetic nervous system. *American journal of hypertension,* hpt273.

Lanska DJ. (2002). JL Corning and vagal nerve stimulation for seizures in the 1880s. *Neurology* **58,** 452-459.

Laubie M & Schmitt H. (1979). Destruction of the nucleus tractus solitarii in the dog: comparison with sinoaortic denervation. *American Journal of Physiology-Heart and Circulatory Physiology* **236,** H736-H743.

Law M, Morris J & Wald N. (2009). Use of blood pressure lowering drugs in the prevention of cardiovascular disease: meta-analysis of 147 randomised trials in the context of expectations from prospective epidemiological studies. *Bmj* **338,** b1665.

Leutmezer F, Schernthaner C, Lurger S, Pötzelberger K & Baumgartner C. (2003). Electrocardiographic changes at the onset of epileptic seizures. *Epilepsia* **44,** 348-354.

Li M, Zheng C, Sato T, Kawada T, Sugimachi M & Sunagawa K. (2004). Vagal nerve stimulation markedly improves long-term survival after chronic heart failure in rats. *Circulation* **109,** 120-124.

Līcis R, Molotanovs A & Žīdens J. (2015). Cranial Electrotherapy Stimulation and Influence of the Hart Rate Variability. In *SOCIETY INTEGRATION EDUCATION Proceedings of the International Scientific Conference*, pp. 318-326.

Linderoth B, Herregodts P & Meyerson BA. (1994). Sympathetic mediation of peripheral vasodilation induced by spinal cord stimulation: animal studies of the role of cholinergic and adrenergic receptor subtypes. *Neurosurgery* **35,** 711-719.

Linderoth B, Stiller C-O, O'Connor W, Hammarström G, Ungerstedt U & Brodin E. (1993). An animal model for the study of brain transmittor release in response to spinal cord stimulation in the awake, freely moving rat: preliminary results from the periaqueductal grey matter. In *Advances in Stereotactic and Functional Neurosurgery 10*, pp. 156-160. Springer.

Litscher G, Bahr F, Litscher D, Min L-Q & Rong P-J. (2015). A New Method in Auricular Medicine for the Investigation of the Nogier Reflex. *Integrative Medicine International* **1,** 205-210.

Liu D & Hu Y. (1988). The central projections of the great auricular nerve primary afferent fibers--an HRP transganglionic tracing method. *Brain Res* **445,** 205-210.

Loewy AD & Spyer KM. (1990). *Central regulation of autonomic functions*. Oxford University Press.

Lu F, Qin C, Foreman RD & Farber JP. (2004). Chemical activation of C1-C2 spinal neurons modulates intercostal and phrenic nerve activity in rats. *American Journal of Physiology-Regulatory, Integrative and Comparative Physiology* **286,** R1069-R1076.

Lumsden T. (1923). Observations on the respiratory centres in the cat. *The Journal of physiology* **57,** 153.

Luppi PH, Sakai K, Salvert D, Fort P & Jouvet M. (1987). Peptidergic hypothalamic afferents to the cat nucleus raphe pallidus as revealed by a double immunostaining technique using unconjugated cholera toxin as a retrograde tracer. *Brain Res* **402,** 339-345.

Malherbe W. (1958). Otalgia with oesophageal hiatus hernia. *The Lancet* **271,** 1368-1369.

Malpas SC & Purdie GL. (1990). Circadian variation of heart rate variability. *Cardiovascular research* **24,** 210-213.

Marrosu F, Serra A, Maleci A, Puligheddu M, Biggio G & Piga M. (2003). Correlation between GABA A receptor density and vagus nerve stimulation in individuals with drug-resistant partial epilepsy. *Epilepsy research* **55,** 59-70.

Martin-Fairey CA, Ramanathan C, Stowie A, Walaszczyk E, Smale L & Nunez AA. (2015). Plastic oscillators and fixed rhythms: Changes in the phase of clock-gene rhythms in the PVN are not reflected in the phase of the melatonin rhythm of grass rats. *Neuroscience* **288,** 178-186.

Martínez-Vargas D, Valdés-Cruz A, Magdaleno-Madrigal V, Fernández-Mas R & Almazán-Alvarado S. (2016). Effect of Electrical Stimulation of the Nucleus of the Solitary Tract on Electroencephalographic Spectral Power and the Sleep–Wake Cycle in Freely Moving Cats. *Brain stimulation*.

Massin MM, Maeyns K, Withofs N, Ravet F & Gérard P. (2000). Circadian rhythm of heart rate and heart rate variability. *Archives of Disease in Childhood* **83,** 179-182.

Masuda N, Terui N, Koshiya N & Kumada M. (1991). Neurons in the caudal ventrolateral medulla mediate the arterial baroreceptor reflex by inhibiting barosensitive reticulospinal neurons in the rostral ventrolateral medulla in rabbits. *Journal of the autonomic nervous system* **34,** 103-117.

McAllen R & Spyer K. (1978). Two types of vagal preganglionic motoneurones projecting to the heart and lungs. *The Journal of Physiology* **282,** 353-364.

McCorry LK. (2007). Physiology of the autonomic nervous system. *American journal of pharmaceutical education* **71,** 78.

McGovern AE, Driessen AK, Simmons DG, Powell J, Davis-Poynter N, Farrell MJ & Mazzone SB. (2015). Distinct brainstem and forebrain circuits receiving tracheal sensory neuron inputs revealed using a novel conditional anterograde transsynaptic viral tracing system. *The Journal of neuroscience : the official journal of the Society for Neuroscience* **35,** 7041-7055.

Meglio M, Cioni B, Rossi G, Sandric S & Santarelli P. (1987). Spinal cord stimulation affects the central mechanisms of regulation of heart rate. *Stereotactic and Functional Neurosurgery* **49,** 139-146.

Mei N, Condamin M & Boyer A. (1980). The composition of the vagus nerve of the cat. *Cell and tissue research* **209,** 423-431.

Mellen NM, Janczewski WA, Bocchiaro CM & Feldman JL. (2003). Opioid-induced quantal slowing reveals dual networks for respiratory rhythm generation. *Neuron* **37,** 821-826.

Merrill CA, Jonsson MA, Minthon L, Ejnell H, Hans C, Blennow K, Karlsson M, Nordlund A, Rolstad S & Warkentin S. (2006). Vagus nerve stimulation in patients with Alzheimer's disease: additional follow-up results of a pilot study through 1 year. *The Journal of clinical psychiatry* **67,** 1171-1178.

Merritt EA, Sarfaty S, Akker FVD, L'Hoir C, Martial JA & Hol WG. (1994). Crystal structure of cholera toxin B-pentamer bound to receptor GM1 pentasaccharide. *Protein Science* **3,** 166-175.

Millar-Craig M, Bishop C & Raftery E. (1978). Circadian variation of blood-pressure. *The Lancet* **311,** 795-797.

Mitchell G. (1954). The autonomic nerve supply of the throat, nose and ear. *The Journal of Laryngology & Otology* **68,** 495-516.

Moore RY & Lenn NJ. (1972). A retinohypothalamic projection in the rat. *The Journal of comparative neurology* **146,** 1-14.

Moorthy S, KRISHNA G & Elliott C. (1985). Is there an auriculovagal reflex producing cardiac dysrhythmias? *Archives of Otolaryngology* **111,** 631-631.

Motawei K, Pyner S, Ranson RN, Kamel M & Coote JH. (1999). Terminals of paraventricular spinal neurones are closely associated with adrenal medullary sympathetic preganglionic neurones: immunocytochemical evidence for vasopressin as a possible neurotransmitter in this pathway. *Experimental brain research* **126,** 68-76.

Müngen B, Berilgen MS & Arıkanoğlu A. (2010). Autonomic nervous system functions in interictal and postictal periods of nonepileptic psychogenic

seizures and its comparison with epileptic seizures. *Seizure* **19,** 269-273.

Murray AR, Atkinson L, Mahadi MK, Deuchars SA & Deuchars J. (2016). The strange case of the ear and the heart: The auricular vagus nerve and its influence on cardiac control. *Autonomic neuroscience : basic & clinical*.

Narkiewicz K, Winnicki M, Schroeder K, Phillips BG, Kato M, Cwalina E & Somers VK. (2002). Relationship between muscle sympathetic nerve activity and diurnal blood pressure profile. *Hypertension (Dallas, Tex : 1979)* **39,** 168-172.

Nathan MA & Reis DJ. (1977). Chronic labile hypertension produced by lesions of the nucleus tractus solitarii in the cat. *Circulation Research* **40,** 72-81.

NICE NIfHaCE. (2004). Vagus nerve stimulation for refractory epilepsy in children.

Niederbichler AD, Papst S, Claassen L, Jokuszies A, Ipaktchi K, Reimers K, Hirsch T, Steinstraesser L, Kraft T & Vogt PM. (2010). Burn-induced organ dysfunction: vagus nerve stimulation improves cardiac function. *Eplasty* **10,** e45.

Nogier R. (2014). How did Paul Nogier establish the map of the ear? *Medical Acupuncture* **26,** 76-83.

Nomura S & Mizuno N. (1983). Central distribution of efferent and afferent components of the cervical branches of the vagus nerve. *Anatomy and embryology* **166,** 1-18.

Nomura S & Mizuno N. (1984). Central distribution of primary afferent fibers in the Arnold's nerve (the auricular branch of the vagus nerve): a transganglionic HRP study in the cat. *Brain Res* **292,** 199-205.

Nozdrachev A. (2002). John Newport Langley and His Construction of the Autonomic (Vegetative) Nervous System. *Journal of Evolutionary Biochemistry and Physiology* **38,** 537-546.

O'Leary DM & Jones JF. (2003). Discharge patterns of preganglionic neurones with axons in a cardiac vagal branch in the rat. *Experimental physiology* **88,** 711-723.

Okada H, Iwase S, Mano T, Sugiyama Y & Watanabe T. (1991). Changes in muscle sympathetic nerve activity during sleep in humans. *Neurology* **41,** 1961-1961.

Okada Y, Muckenhoff K, Holtermann G, Acker H & Scheid P. (1993). Depth profiles of pH and PO2 in the isolated brain stem-spinal cord of the neonatal rat. *Respir Physiol* **93,** 315-326.

Palmieri A. (2006). Lung cancer presenting with unilateral facial pain: remission after laryngeal nerve palsy. *Headache: The Journal of Head and Face Pain* **46,** 813-815.

Panda S. (2016). Circadian physiology of metabolism. *Science (New York, NY)* **354,** 1008-1015.

Panza JA, Epstein SE & Quyyumi AA. (1991). Circadian variation in vascular tone and its relation to α-sympathetic vasoconstrictor activity. *New England Journal of Medicine* **325,** 986-990.

Patel N, Har-El G & Rosenfeld R. (2001). Quality of life after great auricular nerve sacrifice during parotidectomy. *Archives of Otolaryngology–Head & Neck Surgery* **127,** 884-888.

Paton JF. (1996a). The ventral medullary respiratory network of the mature mouse studied in a working heart-brainstem preparation. *J Physiol* **493 ( Pt 3),** 819-831.

Paton JF. (1996b). A working heart-brainstem preparation of the mouse. *J Neurosci Methods* **65,** 63-68.

Paton JF & Butcher JW. (1998). Cardiorespiratory reflexes in mice. *Journal of the autonomic nervous system* **68,** 115-124.

Peuker ET & Filler TJ. (2002). The nerve supply of the human auricle. *Clinical Anatomy* **15,** 35-37.

Phillipson EA, Duffin J & Cooper JD. (1981). Critical dependence of respiratory rhythmicity on metabolic CO2 load. *Journal of Applied Physiology* **50,** 45-54.

Pickering AE, Waki H, Headley PM & Paton JF. (2002). Investigation of systemic bupivacaine toxicity using the in situ perfused working heart-brainstem preparation of the rat. *The Journal of the American Society of Anesthesiologists* **97,** 1550-1556.

Pickering TG, Harshfield GA, Kleinert HD, Blank S & Laragh JH. (1982). Blood pressure during normal daily activities, sleep, and exercise: comparison of values in normal and hypertensive subjects. *Jama* **247,** 992-996.

Pintea B, Hampel K, Boström J, Surges R, Vatter H, Lendvai IS & Kinfe TM. (2016). Extended Long-Term Effects of Cervical Vagal Nerve Stimulation on Headache Intensity/Frequency and Affective/Cognitive Headache Perception in Drug Resistant Complex-Partial Seizure Patients. *Neuromodulation: Technology at the Neural Interface*.

Piskuric NA & Nurse CA. (2013). Expanding role of ATP as a versatile messenger at carotid and aortic body chemoreceptors. *The Journal of physiology* **591,** 415-422.

Popov SV, Afanasiev SA, Kurlov IO & Pisklova A. (2013). Drug-free correction of the tone of the autonomic nervous system in the management of cardiac arrhythmia in coronary artery disease. *Int J Biomed* **3,** 74.

Potts JT, Lee SM & Anguelov PI. (2002). Tracing of projection neurons from the cervical dorsal horn to the medulla with the anterograde tracer biotinylated dextran amine. *Autonomic Neuroscience* **98,** 64-69.

Potts JT, Spyer KM & Paton JF. (2000). Somatosympathetic reflex in a working heart-brainstem preparation of the rat. *Brain Res Bull* **53,** 59-67.

Prabhakar NR & Semenza GL. (2015). Oxygen sensing and homeostasis. *Physiology* **30,** 340-348.

Premchand RK, Sharma K, Mittal S, Monteiro R, Dixit S, Libbus I, DiCarlo LA, Ardell JL, Rector TS & Amurthur B. (2016). Extended follow-up of patients with heart failure receiving autonomic regulation therapy in the ANTHEM-HF study. *Journal of cardiac failure* **22,** 639-642.

Richter D. (1982). Generation and maintenance of the respiratory rhythm. *Journal of Experimental Biology* **100,** 93-107.

Richter DW. (2003). Commentary on eupneic breathing patterns and gasping. *Respiratory physiology & neurobiology* **139,** 121-130.

Ronkainen E, Korpelainen JT, Heikkinen E, Myllylä VV, Huikuri HV & Isojärvi JI. (2006). Cardiac Autonomic Control in Patients with Refractory Epilepsy before and during Vagus Nerve Stimulation Treatment: A One-Year Follow-up Study. *Epilepsia* **47,** 556-562.

Rothwell P. (1993). Angina and myocardial infarction presenting with pain confined to the ear. *Postgraduate medical journal* **69,** 300-301.

Ruffoli R, Giorgi FS, Pizzanelli C, Murri L, Paparelli A & Fornai F. (2011). The chemical neuroanatomy of vagus nerve stimulation. *Journal of chemical neuroanatomy* **42,** 288-296.

Rutecki P. (1990). Anatomical, physiological, and theoretical basis for the antiepileptic effect of vagus nerve stimulation. *Epilepsia* **31,** S1-S6.

Ryan WR & Fee WE. (2006). Great auricular nerve morbidity after nerve sacrifice during parotidectomy. *Archives of Otolaryngology–Head & Neck Surgery* **132,** 642-649.

Ryan WR & Fee WE. (2009). Long-term great auricular nerve morbidity after sacrifice during parotidectomy. *The Laryngoscope* **119,** 1140-1146.

Sagher O & Huang D-L. (2000). Effects of cervical spinal cord stimulation on cerebral blood flow in the rat. *Journal of Neurosurgery: Spine* **93,** 71-76.

Saito Y, Shimizu T, Takahashi Y, Mishima K, Takahashi K-i, Ogawa Y, Kogawa S & Hishikawa Y. (1996). Effect of bright light exposure on muscle sympathetic nerve activity in human. *Neuroscience letters* **219,** 135-137.

Santoso P, Nakata M, Ueta Y & Yada T. (2017). Suprachiasmatic Vasopressin to Paraventricular Oxytocin Neurocircuit in the Hypothalamus Relays Light Reception to Inhibition of Feeding Behavior. *American Journal of Physiology-Endocrinology and Metabolism***,** ajpendo. 00338.02016.

Sato MA, Menani JV, Lopes OU & Colombari E. (1999). Commissural NTS Lesions and Cardiovascular Responses in Aortic Baroreceptor–Denervated Rats. *Hypertension (Dallas, Tex : 1979)* **34,** 739-743.

Satomi H & Takahashi K. (1990). Distribution of the cells of primary afferent fibers to the cat auricle in relation to the innervated region. *Anatomischer Anzeiger* **173,** 107-112.

Schomer AC, Nearing BD, Schachter SC & Verrier RL. (2014). Vagus nerve stimulation reduces cardiac electrical instability assessed by quantitative T-wave alternans analysis in patients with drug-resistant focal epilepsy. *Epilepsia* **55,** 1996-2002.

Schwartz PJ, De Ferrari GM, Sanzo A, Landolina M, Rordorf R, Raineri C, Campana C, Revera M, Ajmone-Marsan N & Tavazzi L. (2008). Long term vagal stimulation in patients with advanced heart failure First experience in man. *European journal of heart failure* **10,** 884-891.

Seifert EL & Mortola JP. (2002). The circadian pattern of breathing in conscious adult rats. *Respiration physiology* **129,** 297-305.

Selekler M, Kutlu A, Uçar S & Almaç A. (2009). Immediate response to greater auricular nerve blockade in red ear syndrome. *Cephalalgia* **29,** 478-479.

Shaffer F, McCraty R & Zerr CL. (2014). A healthy heart is not a metronome: an integrative review of the heart's anatomy and heart rate variability. *Frontiers in psychology* **5,** 1040.

Shaw JA, Chin-Dusting JP, Kingwell BA & Dart AM. (2001). Diurnal variation in endothelium-dependent vasodilatation is not apparent in coronary artery disease. *Circulation* **103,** 806-812.

Shehab SA & Hughes DI. (2011). Simultaneous identification of unmyelinated and myelinated primary somatic afferents by co-injection of isolectin B4 and Cholera toxin subunit B into the sciatic nerve of the rat. *Journal of neuroscience methods* **198,** 213-221.

Sherwood L. (2008). *Human Physiology: From Cells to Systems*. Cengage Learning, London.

Shibata S, Oomura Y, Kita H & Hattori K. (1982). Circadian rhythmic changes of neuronal activity in the suprachiasmatic nucleus of the rat hypothalamic slice. *Brain research* **247,** 154-158.

Smith JC, Ellenberger HH, Ballanyi K, Richter DW & Feldman JL. (1991). Pre-Botzinger complex: a brainstem region that may generate respiratory rhythm in mammals. *Science (New York, NY)* **254,** 726-729.

Smith JC & Feldman JL. (1987). In vitro brainstem-spinal cord preparations for study of motor systems for mammalian respiration and locomotion. *Journal of neuroscience methods* **21,** 321-333.

Smith JE, Paton JF & Andrews PL. (2001). Cardiorespiratory reflexes in a working heart-brainstem preparation of the house musk shrew, Suncus murinus. *Autonomic neuroscience : basic & clinical* **89,** 54-59.

Smyth MD, Tubbs RS, Bebin EM, Grabb PA & Blount JP. (2003). Complications of chronic vagus nerve stimulation for epilepsy in children. *Journal of neurosurgery* **99,** 500-503.

Sobocki J, Herman RM & Fraczek M. (2013). Occipital C1–C2 Neuromodulation Decreases Body Mass and Fat Stores and Modifies Activity of the Autonomic Nervous System in Morbidly Obese Patients—a Pilot Study. *Obesity surgery* **23,** 693-697.

Somers VK, Dyken ME, Mark AL & Abboud FM. (1993). Sympathetic-nerve activity during sleep in normal subjects. *New England Journal of Medicine* **328,** 303-307.

Sonnino S, Mauri L, Chigorno V & Prinetti A. (2007). Gangliosides as components of lipid membrane domains. *Glycobiology* **17,** 1R-13R.

Sousa L & Lindsey CJ. (2009). Cardiovascular and baroreceptor functions of the paratrigeminal nucleus for pressor effects in non-anaesthetized rats. *Autonomic Neuroscience* **147,** 27-32.

Spuck S, Tronnier V, Orosz I, Schönweiler R, Sepehrnia A, Nowak G & Sperner J. (2010). Operative and technical complications of vagus nerve stimulator implantation. *Neurosurgery* **67,** ons489-ons494.

Spyer K. (1994). Annual review prize lecture. Central nervous mechanisms contributing to cardiovascular control. *The Journal of Physiology* **474,** 1.

St-John WM & Leiter JC. (2003). High-frequency oscillations of phrenic activity in eupnea and gasping of in situ rat: influence of temperature. *American journal of physiology Regulatory, integrative and comparative physiology* **285,** R404-412.

St-John WM & Paton J. (2003). Defining eupnea. *Respiratory physiology & neurobiology* **139,** 97-103.

St-John WM & Paton JF. (2002). Neurogenesis of gasping does not require inhibitory transmission using GABA(A) or glycine receptors. *Respiratory physiology & neurobiology* **132,** 265-277.

St John WM & Bartlett D, Jr. (1985). Comparison of phrenic motoneuron activity in eupnea and apneusis. *Respir Physiol* **60,** 347-355.

St John WM & Knuth KV. (1981). A characterization of the respiratory pattern of gasping. *J Appl Physiol Respir Environ Exerc Physiol* **50,** 984-993.

Stavrakis S, Humphrey MB, Scherlag BJ, Hu Y, Jackman WM, Nakagawa H, Lockwood D, Lazzara R & Po SS. (2015). Low-level transcutaneous electrical vagus nerve stimulation suppresses atrial fibrillation. *Journal of the American College of Cardiology* **65,** 867-875.

Stemper B, Devinsky O, Haendl T, Welsch G & Hilz M. (2008). Effects of vagus nerve stimulation on cardiovascular regulation in patients with epilepsy. *Acta Neurologica Scandinavica* **117,** 231-236.

Stephan FK & Zucker I. (1972). Circadian rhythms in drinking behavior and locomotor activity of rats are eliminated by hypothalamic lesions. *Proceedings of the National Academy of Sciences* **69,** 1583-1586.

Stephenson R, Liao KS, Hamrahi H & Horner RL. (2001). Circadian rhythms and sleep have additive effects on respiration in the rat. *The Journal of physiology* **536,** 225-235.

Stoeckel K, Schwab M & Thoenen H. (1977). Role of gangliosides in the uptake and retrograde axonal transport of cholera and tetanus toxin as compared to nerve growth factor and wheat germ agglutinin. *Brain research* **132,** 273-285.

Suzue T. (1984). Respiratory rhythm generation in the in vitro brain stem-spinal cord preparation of the neonatal rat. *J Physiol* **354,** 173-183.

Takemura M, Sugimoto T & Sakai A. (1987). Topographic organization of central terminal region of different sensory branches of the rat mandibular nerve. *Experimental neurology* **96,** 540-557.

Tamamaki N, Yanagawa Y, Tomioka R, Miyazaki JI, Obata K & Kaneko T. (2003). Green fluorescent protein expression and colocalization with calretinin, parvalbumin, and somatostatin in the GAD67-GFP knock-in mouse. *Journal of Comparative Neurology* **467,** 60-79.

Teclemariam-Mesbah R, Kalsbeek A, Pevet P & Buijs RM. (1997). Direct vasoactive intestinal polypeptide-containing projection from the suprachiasmatic nucleus to spinal projecting hypothalamic paraventricular neurons. *Brain research* **748,** 71-76.

Tekdemir I, Aslan A & Elhan A. (1998). A clinico-anatomic study of the auricular branch of the vagus nerve and Arnold's ear-cough reflex. *Surgical and Radiologic Anatomy* **20,** 253-257.

Terui N, Masuda N, Saeki Y & Kumada M. (1990). Activity of barosensitive neurons in the caudal ventrolateral medulla that send axonal projections to the rostral ventrolateral medulla in rabbits. *Neuroscience letters* **118,** 211-214.

Thakar A, Deepak K & Kumar SS. (2008). Auricular syncope. *The Journal of Laryngology & Otology* **122,** 1115-1117.

Thallaj A, Marhofer P, Moriggl B, Delvi B, Kettner S & Almajed M. (2010). Great auricular nerve blockade using high resolution ultrasound: a volunteer study. *Anaesthesia* **65,** 836-840.

Thiagarajah JR & Verkman AS. (2005). New drug targets for cholera therapy. *Trends Pharmacol Sci* **26,** 172-175.

Todd AJ. (2010). Neuronal circuitry for pain processing in the dorsal horn. *Nature reviews Neuroscience* **11,** 823-836.

Tsutsumi T, Ide T, Yamato M, Kudou W, Andou M, Hirooka Y, Utsumi H, Tsutsui H & Sunagawa K. (2007). Modulation of the myocardial redox state by vagal nerve stimulation after experimental myocardial infarction. *Cardiovascular research*.

Van Den Buuse M. (1994). Circadian rhythms of blood pressure, heart rate, and locomotor activity in spontaneously hypertensive rats as measured with radio-telemetry. *Physiology & Behavior* **55,** 783-787.

Vanoli E, De Ferrari GM, Stramba-Badiale M, Hull SS, Foreman RD & Schwartz PJ. (1991). Vagal stimulation and prevention of sudden death in conscious dogs with a healed myocardial infarction. *Circulation research* **68,** 1471-1481.

Vrang N, Mikkelsen JD & Larsen PJ. (1997). Direct link from the suprachiasmatic nucleus to hypothalamic neurons projecting to the spinal cord: a combined tracing study using cholera toxin subunit B and Phaseolus vulgaris-leucoagglutinin. *Brain research bulletin* **44,** 671-680.

Walker BR, Easton A & Gale K. (1999). Regulation of limbic motor seizures by GABA and glutamate transmission in nucleus tractus solitarius. *Epilepsia* **40,** 1051-1057.

Wang W, Fung M-L, Darnall RA & St John WM. (1996). Characterizations and comparisons of eupnoea and gasping in neonatal rats. *The Journal of Physiology* **490,** 277.

Wang Z, Yu L, Wang S, Huang B, Liao K, Saren G, Tan T & Jiang H. (2014). Chronic intermittent low-level transcutaneous electrical stimulation of auricular branch of vagus nerve improves left ventricular remodeling in conscious dogs with healed myocardial infarction. *Circulation Heart failure* **7,** 1014-1021.

Wang Z, Zhou X, Sheng X, Yu L & Jiang H. (2015). Unilateral low-level transcutaneous electrical vagus nerve stimulation: A novel noninvasive treatment for myocardial infarction. *International journal of cardiology* **190,** 9-10.

Weddell G, Pallie W & Palmer E. (1955a). Studies on the innervation of skin: I. The origin, course and number of sensory nerves supplying the rabbit ear. *Journal of anatomy* **89,** 162.

Weddell G, Taylor D & Williams C. (1955b). Studies on the innervation of skin: III. The patterned arrangement of the spinal sensory nerves to the rabbit ear. *Journal of anatomy* **89,** 317.

Wehrwein EA & Joyner MJ. (2013). Regulation of blood pressure by the arterial baroreflex and autonomic nervous system. *Handb Clin Neurol* **117,** 89-102.

Weijnen J, Surink S, Verstralen M, Moerkerken A, De Bree G & Bleys R. (2000). Main trajectories of nerves that traverse and surround the tympanic cavity in the rat. *Journal of anatomy* **197,** 247-262.

WHO WHO. (2017). Epilepsy Fact Sheet.

Wilson RJ, Remmers JE & Paton JF. (2001). Brain stem PO(2) and pH of the working heart-brain stem preparation during vascular perfusion with aqueous medium. *American journal of physiology Regulatory, integrative and comparative physiology* **281,** R528-538.

Woodbury DM & Woodbury JW. (1990). Effects of vagal stimulation on experimentally induced seizures in rats. *Epilepsia* **31,** S7-S19.

Wurtman RJ & Axelrod J. (1966). A 24-hour rhythm in the content of norepinephrine in the pineal and salivary glands of the rat. *Life sciences* **5,** 665-669.

Yakunina N, Kim SS & Nam EC. (2016). Optimization of Transcutaneous Vagus Nerve Stimulation Using Functional MRI. *Neuromodulation: Technology at the Neural Interface.*

Yoo PB, Liu H, Hincapie JG, Ruble SB, Hamann JJ & Grill WM. (2016). Modulation of heart rate by temporally patterned vagus nerve stimulation in the anesthetized dog. *Physiological reports* **4,** e12689.

Youcef G, Olivier A, L'Huillier CP, Labat C, Fay R, Tabcheh L, Toupance S, Rodriguez-Guéant R-M, Bergerot D & Jaisser F. (2014). Simultaneous characterization of metabolic, cardiac, vascular and renal phenotypes of lean and obese SHHF rats. *PloS one* **9,** e96452.

Yu L, Scherlag BJ, Li S, Fan Y, Dyer J, Male S, Varma V, Sha Y, Stavrakis S & Po SS. (2013). Low-level transcutaneous electrical stimulation of the auricular branch of the vagus nerve: a noninvasive approach to treat the initial phase of atrial fibrillation. *Heart rhythm : the official journal of the Heart Rhythm Society* **10,** 428-435.

Yu L, Scherlag BJ, Li S, Sheng X, Lu Z, Nakagawa H, Zhang Y, Jackman WM, Lazzara R & Jiang H. (2011). Low-level vagosympathetic nerve stimulation inhibits atrial fibrillation inducibility: direct evidence by neural recordings from intrinsic cardiac ganglia. *Journal of cardiovascular electrophysiology* **22,** 455-463.

Yu L, Scherlag BJ, Sha Y, Li S, Sharma T, Nakagawa H, Jackman WM, Lazzara R, Jiang H & Po SS. (2012). Interactions between atrial electrical remodeling and autonomic remodeling: how to break the vicious cycle. *Heart rhythm : the official journal of the Heart Rhythm Society* **9,** 804-809.

Yu Y-G & Lindsey CJ. (2003). Baroreceptor-sensitive neurons in the rat paratrigeminal nucleus. *Autonomic Neuroscience* **105,** 25-34.

Zamotrinsky A, Afanasiev S, Karpov RS & Cherniavsky A. (1997). Effects of electrostimulation of the vagus afferent endings in patients with coronary artery disease. *Coronary artery disease* **8,** 551-558.

Zamotrinsky A, Kondratiev B & de Jong JW. (2001). Vagal neurostimulation in patients with coronary artery disease. *Autonomic Neuroscience* **88,** 109-116.

Zampieri N, Jessell TM & Murray AJ. (2014). Mapping sensory circuits by anterograde transsynaptic transfer of recombinant rabies virus. *Neuron* **81,** 766-778.

Zannad F, De Ferrari GM, Tuinenburg AE, Wright D, Brugada J, Butter C, Klein H, Stolen C, Meyer S & Stein KM. (2015). Chronic vagal stimulation for the treatment of low ejection fraction heart failure: results

of the NEural Cardiac TherApy foR Heart Failure (NECTAR-HF) randomized controlled trial. *European heart journal* **36,** 425-433.

Zhou X, Zhou L, Wang S, Yu L, Wang Z, Huang B, Chen M, Wan J & Jiang H. (2016). The Use of Noninvasive Vagal Nerve Stimulation to Inhibit Sympathetically Induced Sinus Node Acceleration: A Potential Therapeutic Approach for Inappropriate Sinus Tachycardia. *Journal of cardiovascular electrophysiology* **27,** 217-223.

Zoccal DB, Simms AE, Bonagamba LG, Braga VA, Pickering AE, Paton JF & Machado BH. (2008). Increased sympathetic outflow in juvenile rats submitted to chronic intermittent hypoxia correlates with enhanced expiratory activity. *The Journal of physiology* **586,** 3253-3265.